DISSERTATION

Non-stationarity as a central aspect of financial markets

Von der Fakultät für Physik
der Universität Duisburg-Essen
genehmigte Dissertation
zur Erlangung des Grades
Dr. rer. nat.
von

Dipl.-Phys. Thilo Albrecht Schmitt
aus Mülheim an der Ruhr

Tag der Disputation: 1. Dezember 2014
Referent: Prof. Dr. Thomas Guhr
Korreferent: Prof. Dr. Andreas Schadschneider

Hiermit versichere ich, die vorliegende Dissertation selbstständig, ohne fremde Hilfe und ohne Benutzung anderer als den angegebenen Quellen angefertigt zu haben. Alle aus fremden Werken direkt oder indirekt übernommenen Stellen sind als solche gekennzeichnet. Die vorliegende Dissertation wurde in keinem anderen Promotionsverfahren eingereicht. Mit dieser Arbeit strebe ich die Erlangung des akademischen Grades “Doktor der Naturwissenschaften” (Dr. rer. nat.) an.

Datum	Thilo A. Schmitt

Teile dieser Dissertation sind in die folgenden Veröffentlichungen und Manuskripte eingegangen:

[1] T.A. Schmitt, D. Chetalova, R. Schäfer and T. Guhr, *Non-Stationarity in Financial Time Series and Generic Features*, Europhysics Letters 103, 58003 (2013)

[2] T.A. Schmitt, D. Chetalova, R. Schäfer and T. Guhr, *Credit risk and the instability of the financial system: An ensemble approach*, Europhysics Letters 105, 38004 (2014)

[3] D. Chetalova, T.A. Schmitt, R. Schäfer and T. Guhr, *Portfolio return distributions: Sample statistics with non-stationary correlations*, arXiv:1308.3961, submitted to International Journal of Theoretical and Applied Finance in Mar 2014

[4] T.A. Schmitt, R. Schäfer, D. Wied and T. Guhr, *Spatial Dependence in Stock Returns - Local Normalization and VaR Forecasts*, SSRN.com/abstract=2320675, re-submitted to Empirical Economics in Jun 2014

[5] T.A. Schmitt, R. Schäfer and T. Guhr, *Credit risk: Taking fluctuating asset correlations into account*, in preparation (2014)

[6] T.A. Schmitt, R. Schäfer, H. Dette and T. Guhr, *Quantile correlations: Uncovering temporal dependencies in financial time series*, submitted to International Journal of Theoretical and Applied Finance in Aug 2014

Die folgenden Veröffentlichungen und Manuskripte sind während der Promotion entstanden und nicht Teil dieser Dissertation:

[7] T.A. Schmitt, R. Schäfer, M.C. Münnix and T. Guhr, *Microscopic understanding of heavy-tailed return distributions in an agent-based model*, Europhysics Letters 100, 38005 (2012)

[8] D.C. Wagner, T.A. Schmitt, R. Schäfer, T. Guhr and D.E. Wolf, *Analysis of a decision model in the context of equilibrium pricing and order book pricing*, arXiv:1102.3900, accepted for publication in Physica A in Aug 2014

Author contributions

Here, I lay out my contributions to the publications and manuscripts mentioned above:

[1] The letter introduces the correlation-averaged multivariate normal distribution, which is the starting point for further studies [2, 3, 5]. Under supervision of R. Schäfer and T. Guhr and in collaboration with D. Chetalova, I calculated this distribution analytically for the general case. In addition I contributed the data analysis. The text was mainly written by T. Guhr with contributions from D. Chetalova, R. Schäfer and me.

[2] The correlation-averaged multivariate normal distribution is used in the context of credit risk. I calculated the average loss distribution for arbitrary correlation levels and contributed the data analysis. The initial text was written by me and later edited by D. Chetalova, R. Schäfer and T. Guhr.

[3] I provided the correlation-averaged multivariate normal distribution. The application to portfolio returns and the data analysis was carried out by D. Chetalova. The text was primarily written by D. Chetalova. The project was supervised by R. Schäfer and T. Guhr.

[4] The portfolio optimization and application of the various refinement methods was carried out by me. All authors contributed ideas for the selection of the refinement methods. The text was mainly written by me. The project was mainly supervised by R. Schäfer.

[5] The paper extends reference [2] with a larger empirical study and numerical simulations which I contributed. The text was mainly written by me.

[6] The empirical study was carried out by me. R. Schäfer and I equally contributed to the interpretation of the results in the context of financial time series. The text was mainly written by me with contributions from H. Dette and T. Guhr. The project was initiated by T. Guhr and was mainly supervised by R. Schäfer.

Acknowledgements

I want to express my gratitude to my supervisor Thomas Guhr for creating an outstanding environment to conduct research in the interdisciplinary field of econophysics. His support and guidance broadened my knowledge in physics and economics. My appreciation also goes to my second advisor Rudi Schäfer for his unbroken persistence in educating and discussing all kinds of topics.

Special thanks go to Dominik Wied for insightful discussions about covariance estimation techniques and portfolio benchmarks and to Holger Dette for bringing the quantile-based correlation to our attention.

I thank all members of the group, especially Maram Akila, Alexander Becker, Desislava Chetalova, Lukas Gathmann, Frederik Meudt, Michael Münnix, Tobias Nitschke, Peter Raiser, Joachim Sicking, Yuriy Stepanov, Martin Theissen, Daniel Wagner, Daniel Waltner, Shanshan Wang, Tim Wirtz and Marcel Wollschläger for fruitful and extensive discussions. You have been great colleagues during the last three years.

In addition, I would like to thank John Norrie for proofreading this work.

Finally, I want to say special thanks to my parents and friends who have supported me during my studies.

Abstract

We leverage methods from statistical physics to study problems in economics, particularly financial markets. While there are some examples in history where physicists contributed to problems in economics, both sciences developed independently. The interdisciplinary field of econophysics has been formed during the last twenty years to facilitate the transfer of methods.

We start by investigating the influence of the non-stationarity in financial time series on portfolio optimization and assess different methods designed to suppress the negative effects on the covariance estimation. The study compares different models to estimate the covariance matrix and how combinations of refinements can improve on them. The effectiveness of the refinements depends on the covariance estimators and they are essential to receive good results for portfolio optimization.

The temporal dependencies inherent in financial time series are investigated with a recently introduced quantile-based correlation function. The results provide a much broader overview of the time series' features compared to the classic method of studying the autocorrelation of the absolute or squared returns. In addition, we study how well different common stochastic processes capture the features of empirical time series and find striking differences.

To model the influence of the non-stationarity, we use an ensemble approach to construct a multivariate correlation-averaged normal distribution, which addresses the non-stationarity of the covariance matrix. We carry out an extensive empirical study to validate the approach.

The correlation-averaged normal distribution is then used as a realistic distribution for the asset values in the Merton model. We calculate the average loss distribution which takes the non-stationarity into account. This approach yields a quantitative understanding of why the benefits of diversification are limited. As practitioner-oriented risk measures we investigate the Value at Risk and Expected Tail Loss for credit portfolios.

Zusammenfassung

Wir nutzen Methoden der statistischen Physik, um wirtschaftswissenschaftliche Fragestellungen mit dem Schwerpunkt Finanzmärkte zu studieren. Obwohl es in der Geschichte Beispiele dafür gibt, dass Physiker Beiträge zu wirtschaftswissenschaftlichen Problemstellungen geleistet haben, entwickelten sich beide Wissenschaften unabhängig voneinander. Die interdisziplinäre Wirtschaftsphysik entstand in den letzten zwanzig Jahren, um den Austausch von Methoden zu fördern.

Zunächst studieren wir den Einfluss der Nichtstationarität von Finanzzeitreihen auf Portfoliooptimierung und evaluieren verschiedene Methoden, welche die negativen Folgen für die Schätzung der Kovarianzmatrix minimieren. Die Studie vergleicht verschiedene Ansätze zur Schätzung von Kovarianzmatrizen und untersucht, wie Kombinationen von Methoden sie verbessern können. Die Auswirkungen der Verbesserungen sind stark von den verwendeten Schätzern abhängig und die Verbesserungen sind essentiell, um gute Ergebnisse bei der Portfoliooptimierung zu erreichen.

Die zeitlichen Abhängigkeiten in Finanzzeitreihen werden mit Hilfe der kürzlich eingeführten quantilbasierten Korrelationsfunktion untersucht. Die Ergebnisse liefern ein deutlich umfangreicheres Bild von den Eigenschaften der Zeitreihe im Vergleich zum üblichen Vorgehen, die Autokorrelation der betragsmäßigen oder der quadrierten Renditen zu betrachten. Außerdem vergleichen wir gebräuchliche stochastische Prozesse mit den empirischen Daten und finden beachtliche Unterschiede.

Um den Einfluss der Nichtstationarität zu modellieren, benutzen wir einen Ensembleansatz. Wir konstruieren eine multivariate korrelationsgemittelte Normalverteilung, welche die Nichtstationarität der Kovarianzmatrix beschreiben kann. Wir führen eine umfassende empirische Studie durch, um diesen Ansatz zu validieren.

Die so gefundene Verteilung nutzen wir anschließend als realistische Verteilung der Vermögenswerte von Unternehmen im Mertonmodell zur Beschreibung von Ausfallrisiken bei Krediten. Wir berechnen die gemittelte Verlustverteilung, welche die Nichtstationarität der Finanzmärkte berücksichtigt. Mit Hilfe dieses Ansatzes erhalten wir ein quantitatives Verständnis, weshalb die Vorteile der Diversifizierung im Falle von Kreditportfolios sehr begrenzt sind. Zum Schluss betrachten wir zwei praxisrelevante Risikomaße, den Value at Risk und Expected Tail Loss von Kreditportfolios.

Contents

Chapter 1

Introduction

1.1 Econophysics

Econophysics is a rather young interdisciplinary research field. The term econophysics was coined by H. Eugene Stanley in 1995 at a conference about statistical physics and first used in a publication in 1996 [9]. The general idea is to apply methods from physics, especially statistical physics, to problems from economics. Here, we focus on the non-stationarity of financial time series and its consequences.

It is a little bit peculiar that the field of econophysics only formed recently with its own identity. There are many examples through history where scientists with a mathematics or physics background have contributed to the economic sciences. One of the earliest examples traces back to the mathematician and physicist Daniel Bernoulli, who is among physicists probably known best for Bernoulli's principle published in his book "Hydrodynamica" [10]. However, he also contributed to probability and decision theory related to economics problems. Bernoulli proposed a solution to the Saint Petersburg paradox, which was described first by his cousin Nicolas Bernoulli in a private letter to Pierre Raymond de Montmort in 1713. Imagine, we meet a stranger on a bridge who offers to play a game of chance for a stake. The pot starts with one dollar. Every round a fair coin is tossed. If head shows up the pot is doubled. Otherwise the game ends and the player gets the money from the pot. For three heads in a row the pot would contain four dollars and the chance of winning is 1/8. Now, the question is: How much should we pay (our stake) to play the game and why is it a paradox? Most people are not willing to pay more than a few dollars to participate in the game [11, 12]. However, those who are familiar with probability theory will quickly notice that the value for the expected win diverges to infinity, if we can play the game any number of times. Therefore, we should pay any price to participate in the game if we can play multiple times. It is called a paradox, because for most people the perceived value of playing the game differs greatly form the expectation value. Daniel Bernoulli introduced the concept of utility and marginal utility to better describe the behavior of the players in 1738. He proposes that the fair price to play the game depends on the current wealth of

the player and the expected wealth after playing the game [13]. This laid the ground work for the theory of utility in economics. The solution of the Saint Petersburg paradox is still subject to discussion [14]. In a recent study Peters argues that the problem is non-ergodic and therefore an expectation value has no meaning [15].

The Saint Petersburg paradox spawned an ongoing interdisciplinary discussion for over 300 years. This is not a singular event and history shows that economic and physical problems often overlap. We briefly outline some further examples:

In 1905 Albert Einstein published a paper [16] to describe the phenomenon of an erratically moving particle in a fluid observed by Robert Brown [17]. He used a stochastic process to model the movement, which now is named after Brown. However, the stochastic process was already used five years earlier by the mathematician Louis Bachelier in his thesis to describe the motion of stock prices [18]. Einstein developed the mathematical framework to model Brownian motion independently and certainly was not aware of Bachelier's work, which did not receive widespread acclaim at the time. Today, the geometric Brownian motion is a standard tool among others to describe stock prices.

The work of Benoît Mandelbrot on fractals was at first motivated by his studies on stock prices [19], but quickly grew to a much more general relevance describing many forms observed in nature, *e.g.*, the shape of mountains or coast lines [20].

In 1973 Black and Scholes presented their theory of option pricing [21], which has become a standard tool in quantitative risk management. The price of options is described by a partial differential equation which can be solved by mapping it to a diffusion problem. Fischer Black held a bachelors degree in physics and a Ph.D. in applied mathematics.

These examples show that the educational background of physicists enables them to contribute new ideas and concepts to problems in economics and how science can benefit as a whole from interdisciplinary approaches.

1.2 Financial markets

Ever since the crisis in 2008 financial markets and the products traded there are omnipresent in the news. The structural problems in the financial sector became visible to the public with the collapse of the investment bank Lehman Brothers on September 15, 2008 [22]. The following depression destroyed many jobs and the unemployment rate in most industrialized countries is still above the pre-crisis level as of 2014 [23].

Financial markets are viewed by many people with suspicion, especially in Germany. This view may stem from bad experiences with investments, biased news coverage or a lack of knowledge about the inner workings of financial markets and its associated risks. Before we proceed, we discuss how financial

markets work and define important technical terms. We start with a typical textbook definition [24] of financial markets

> "Markets in which funds are transferred from people who have a surplus of available funds to people who have a shortage of available funds."

The definition states that people in a financial market trade funds with each other in contrast to commodity markets where goods are traded. In every market driven economy the price of the traded fund is driven by supply and demand. Fund is a very general term and we need to specify it in the following in more detail. To describe all financial products (financial securities) which are traded on financial markets is beyond the scope of this introduction. We limit ourselves to the most common and basic types. If a government or a company needs money to support their activities they can issue a bond and sell it to people who have an excess of funds. The entity which buys the bond, *i.e.*, lends the funds is called creditor. The issuer of the bond is obliged to pay back the principal, *i.e.*, the amount of money borrowed, at a predefined maturity time and in general also has to pay interest (coupons) at fixed time points. The broad textbook definition from reference [24] is

> "A debt security that promises to make payments periodically for a specified period of time."

If the lender (the entity which issued the bond) is not able to pay back the creditor at maturity the lender goes bankrupt. In this case the creditor may lose a part or all of his invested money. Bonds are standardized contracts and therefore can be easily traded on bond markets. The new owner of the bond is then entitled to receive the periodical coupon payments. Being able to sell the bond makes it more flexible compared to a time deposit at a bank. However, depending on who issues the bond, the chance of losing the invested money can be substantially higher compared to a deposit at a bank. A recent example are bonds issued by the Greek government. As a result of the debt crisis the principal value of privately held short term bonds, *i.e.*, the amount which will be payed back at maturity, was cut by 53.5% in 2012 [25]. Bonds will play an important role in chapter 5 where we apply the concept of ensemble average to credit risk estimation. The most prominent financial security is stock, which represents ownership in a company. According to the textbook [24] it is defined as

> "A security that is a claim on the earnings and assets of a company."

In contrast to bonds there is no maturity time. The contract runs indefinitely and the stock owner may get a share of the earnings in form of a dividend. Due to the more open nature of stocks, *e.g.*, the dividend payments can change over time, they are more prone to speculation, *i.e.*, the hope of a higher stock

price in the future. This leads straight to the motivation of people to sell or buy stocks. They try to earn a profit with their surplus of money which exceeds the interest rate paid by a bank and are willing to take a higher risk to achieve this goal. The profit can be earned by speculation, by receiving dividends and/or by interest payments from bonds. However, bonds from very solid countries or companies are often considered risk-free and therefore have very low interest rates. A curious example is the negative interest rate for German government bonds during the European debt crisis. Investors had to pay "interest" to the German government for securely storing their money. The Wall Street Journal [26] summarized the anomalous situation with

> "Investors agreed to pay the German government for the privilege of lending it money."

Each market participant has his own strategies and expectations for the future development of different financial securities. The expectations can differ quite substantially between the market participants. Obviously, the thoughts and strategies of all participants are not accessible for scientific study. On

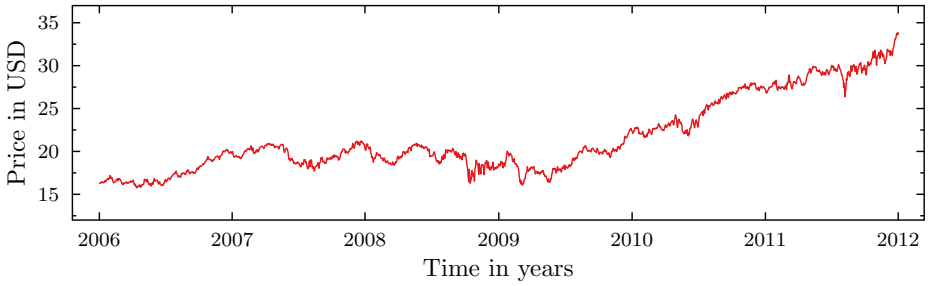

(a) Time evolution of Wisconsin Energy Corp. from 2006 to 2012.

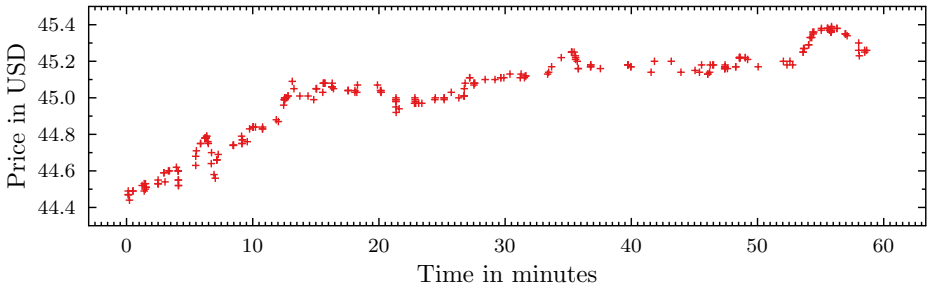

(b) Price for each trade between 10:00 AM and 11:00 AM, September 15, 2008

Figure 1.1: The chart for Wisconsin Energy Corp. on different time scales.

a much smaller scale, barely comparable to a real market, studies with a limited number of participants are the subject of behavioral economics [27]. On financial markets the most important accessible observable is the traded

price, *i.e.*, the price on which two participants agree to exchange financial securities. A formal mechanism exists to assist participants in agreeing on a price, which we discuss in section 1.4. For now it is only important to know that each time two participants agree on a price a trade takes place and the price will be recorded. The visual representation of the time evolution of the price is called chart. Figure 1.1 shows the chart for Wisconsin Energy Corp. (WEC) from January 2006 to December 2011 (top) and for one hour between 10:00 AM and 11:00 AM on September 15, 2008. For the one hour time horizon each trade which took place is shown as a cross. We notice as a remark that price time series are often considered to be invariant under rescaling [19]. In addition to the price, the traded volume, *i.e.*, the number of securities traded, is known for each transaction. Hence, the actions of a large number of diverse participants are culminated in two observables: price and volume.

This is reminiscent of a physical system we already mentioned earlier, namely Brownian motion. A particle is suspended in a fluid and moves seemingly at random in it. The movement of the particle is the result of the collision with the many quickly moving atoms or molecules of the fluid. Here, the observable is the position of the particle. Therefore, it is no surprise that both Einstein and Bachelier came up with a stochastic process of Brownian motion. On a small scale with a limited number of atoms or molecules we can simulate the collisions with the particle, for example, with molecular dynamics simulations, see reference [28–30] for an overview. While such simulations yield a microscopic understanding they are computationally hard and often not analytically tractable. The stochastic process provides a description of the macroscopic outcome without any knowledge of the inner microscopic workings of the system.

Facing the financial crisis of 2008 and its consequences, the reader might ask if we should get rid of financial markets. Despite the risks, we should not overlook the positive effects of strong financial markets. Young innovative companies need the ability to collect risk capital by going public to expand their business. Recent examples are Google (GOOG), Amazon (AMZN) or Facebook (FB) who have changed how we find information, buy things or communicate. In some countries, *e.g.*, USA or Sweden, pension funds hold long term investments in stocks to participate in the general long term trend of growing economic productivity and rising stock prices, as well as dividends. The strong dependency of all developed countries on financial markets shows how important it is to study financial systems and gain a deeper understanding of its inner mechanics. Concepts from theoretical physics can help to achieve this goal. Here, we transfer the concept of ensemble average to describe financial markets to model the probability of losses for credit portfolios in chapter 5.

1.3 Option pricing

We explore a new class of securities called derivatives in this section. This will allow us to gain a deep understanding of the underlying model for credit risk in chapter 5. In a very broad sense we can distinguish two classes of

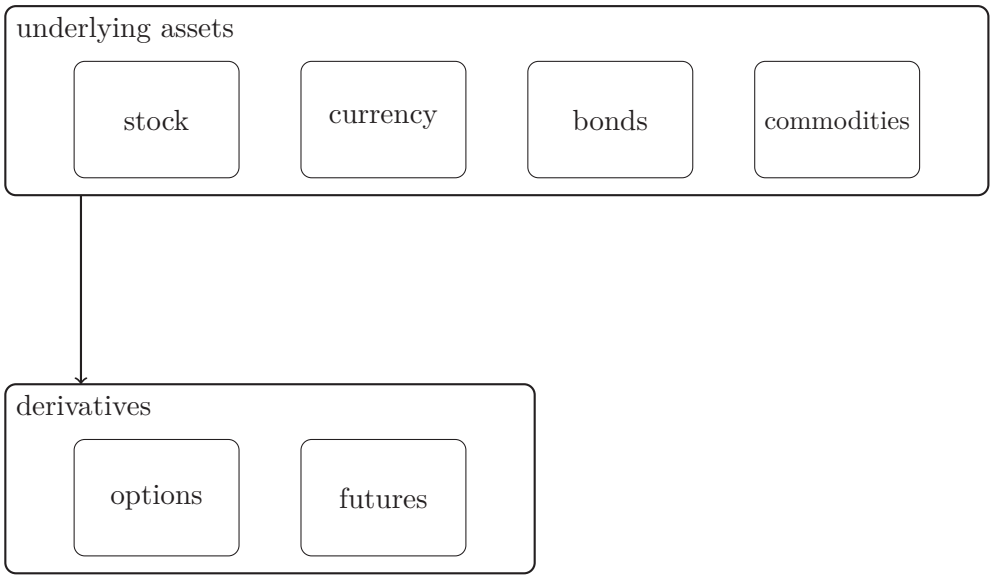

Figure 1.2: Non-exhaustive overview of financial products.

financial products, see figure 1.2. However, we have to accept that a comprehensive overview is not possible due to the vast number of different financial products. We start with the second category which includes all derivatives. Derivatives are financial contracts whose value is determined from the value of an underlying asset. The first category includes these underlying assets. A typical requirement for an underlying asset is that its price is easily obtainable, *e.g.*, it is continuously traded at a stock exchange. Popular assets are stocks, currency and bonds, which we already know from the previous section. We notice that money, *i.e.*, currency, is an asset which can be traded for foreign currencies for example. The exchange rate between Euro and US dollar, for instance, is the result of this trading process. From such underlying assets clever bankers construct derived products called derivatives. The price of a derivative is determined from the underlying asset by a fixed set of conditions and rules. Sometimes these rules only describe the price of the derivative at a specified time in the future. Then, it is up to the traders to estimate the price during normal trading. This involves complex pricing formulas which can become so difficult to understand that the actual trader uses the derivative without deeper knowledge of the consequences. The derivatives shown

in figure 1.2 are options and futures. An option is the right to sell or buy a specified asset at a predefined price at some point in the future. The characteristic of the option is the asymmetry of the rights. If the owner of the option executes his right to sell or buy the counter party must buy or sell at the negotiated price. In contrast, a future does not have this asymmetry, *i.e.*, it is a contract which sets a fixed price for an asset in the future. Both parties have to trade at the price negotiated in the contract.

Here, we will have a short discussion how the pricing of options works. The model of option pricing was developed by Black and Scholes [21] and Merton [31] in 1973. However, the model is normally referred to as "Black and Scholes model". In 1997, Schole's and Merton's contribution to quantitative risk management was honored with the Nobel Prize in Economics. Black died in 1995 and therefore was not eligible for the prize.

The model makes several assumptions on the assets and market, which we should keep in mind:

- An asset with a constant risk-free interest rate is available, *e.g.*, bonds.
- The log returns follow a geometric Brownian motion with constant drift and volatility.
- No dividend payments.
- Arbitrage free markets.
- Unlimited credit opportunities for money at the risk free interest rate.
- Unlimited amount of available stock, short selling allowed.
- No transaction fees.

Arbitrage free means that it is not possible to buy an asset at market A and immediately sell it at market B for a profit. This assumption is justified, because if it were possible traders would immediately exploit the opportunity, which will annihilate the arbitrage opportunity by balance of supply and demand. Short selling allows us to sell stock which we do not own. We borrow shares from our broker and sell them at price $S(0)$. At a predefined time in the future T we have to return the shares. Therefore, we buy the shares at price $S(T)$ at the stock market and return them to our broker. If $S(T) < S(0)$ we earn a profit. Otherwise we lose money. Short selling makes it possible to earn money by speculating on falling stock prices. As always the broker will not lend us the shares for free, so in reality we have to take a fee into account while calculating the profit. Under the above assumptions, imagine a derivative which is traded on this market. Again, the possibilities to construct derivatives are limitless. Here, we discuss two common options, for which the Black and Scholes model yields closed analytic solutions, European call and

put options. A European option gives the right to buy (call) or sell (put) the underlying asset at a predefined strike price E (exercise price) at a fixed time T in the future. The right may or may not be exercised at time T, but neither before nor after. Options which allow to exercise the right before the time T are called American-style options. The relevant question is now: What happens at time T? Imagine, at time $t = 0$, we got a call option to buy the underlying asset at a strike or exercise price of $E = 100$ USD one year from now in the future. We have to buy the option, *e.g.*, for $C = 10$ USD, which is the service fee the issuer of the option takes. Three possible outcomes exist at time T. The value of the underlying is greater than 110 USD. In this case our profit is the amount of money which exceeds the strike price plus the option price. If the value of the underlying is below 100 USD, we will not exercise the right to buy the underlying, but we only lose the 10 USD from the option price. In the region from 100 to 110 we exercise the right to buy to reduce our losses, inflicted by the price of the option. For example, if the value of the underlying is 105 USD, we earn 5 USD from selling the underlying, but still have a loss of 5 USD because of the 10 USD option price. The payoff $V(S,T)$ for the call and put option is

$$\begin{aligned} V_C(S,T) &= \max(S-E,0) \\ V_P(S,T) &= \max(E-S,0) \quad , \end{aligned} \tag{1.1}$$

and does not take the price C of the option into account, therefore the profit is the payoff minus the option price.

Given the assumptions, which we discussed in this section, the price $V(S,t)$ of an option according to the Black and Scholes model is described by the partial differential equation

$$\frac{\partial V}{\partial t} + \frac{1}{2}\sigma^2 S^2 \frac{\partial^2 V}{\partial S^2} + rS\frac{\partial V}{\partial S} - rV = 0 \quad , \tag{1.2}$$

where $S(t)$ is the price of the underlying asset and σ the constant volatility of the underlying. To simplify the notation we omit the dependencies of S and V in the equations. The risk free interest rate is denoted as r. For a full derivation of the Black and Scholes equation, see reference [32]. To get the functional form for the option price $V(S,t)$, we have to solve equation (1.2) for a boundary condition, which describes the kind of option, *e.g.*, European call or put option (1.1). The solution of equation (1.2) yields the famous Black and Scholes formula for European call options

$$V_C(S,t) = S\,N(d_+) - E\,N(d_-)\,\mathrm{e}^{-r(T-t)} \quad , \tag{1.3}$$

where $N(d)$ is the cumulative standard normal distribution

$$N(d) = \frac{1}{\sqrt{2\pi}} \int_{-\infty}^{d} \mathrm{d}z \, \exp\left(-\frac{z^2}{2}\right) \quad . \tag{1.4}$$

with the dimensionless quantities d_+ and d_-

$$d_\pm = \frac{1}{\sigma\sqrt{T-t}} \left(\ln \frac{S}{E} + \left(r \pm \frac{\sigma^2}{2} \right) (T-t) \right) \quad . \tag{1.5}$$

For the price of a put option $V_P(S,t)$ Black and Scholes find

$$V_P(S,t) = E\, N(-d_-)\, \mathrm{e}^{-r(T-t)} - S\, N(-d_+) \quad . \tag{1.6}$$

The great importance of the Black and Scholes model lies in its implications for quantitative risk management. Assume, we construct a portfolio in the following way

$$\hat{V}(S,t) = V_C(S,t) - \Delta(S,t) S \quad , \tag{1.7}$$

where we buy a call option and sell a certain amount $\Delta(S,t)$ of the underlying asset. If we now cleverly choose the amount of underlying assets we sell, according to

$$\Delta(S,t) = \frac{\partial V_C}{\partial S}(S,t) = N(d_+) \quad , \tag{1.8}$$

the stochastic parts of the option and the underlying will annihilate and our portfolio yields the risk free interest rate r. Again, for a comprehensive description and derivation see reference [32]. We recall, that we use the geometric Brownian motion as a stochastic process to describe the motion of the underlying. Due to the assumption of no arbitrage a risk free investment must yield the risk free interest rate.

An investor will probably never build his portfolio according to equation (1.8), because the point of investing money on a stock market is to take a risk and earn a higher profit compared to a risk free investment. However, the result of Black and Scholes gives a benchmark to the investor. The investor chooses a different $\Delta(S,t)$ in a controlled way to take more risk and then decides whether it was worth the risk or not.

The concept of options will play a general role in chapter 5 in the context of credit risk. It was Merton's idea to view a credit contract (from the point of the creditor) as a call option of the total value of the company.

1.4 Order book trading

After the general discussion on financial markets in section 1.2 we want to understand how trading is organized and what exactly happens when a trade is executed. The trading of financial products is done via an exchange. The exchange provides an environment where the participants meet and perform the trade. Examples are the New York Stock Exchange (NYSE) by NYSE Euronext, Frankfurt Stock Exchange by Deutsche Börse or the Tokyo Stock Exchange (東京証券取引所) by Japan Exchange Group. The most common mechanism to organize the trading of financial securities is called order book [33, 34]. For each product which can be traded there exists a separate order book. There are two actions a trader wants to perform: buy or sell. In addition, the trader might have an expectation how much he is willing to pay to buy a security or how much he wants to earn by selling it. In such a case the trader can submit a limit order. The limit order to buy states the highest price the trader is willing to pay for a certain number of shares. Accordingly, the limit order to sell states the lowest price at which the trader is willing to sell. The limit orders of all traders are written in the order book. Figure 1.3 shows the content of an order book before and after a buy order. The left

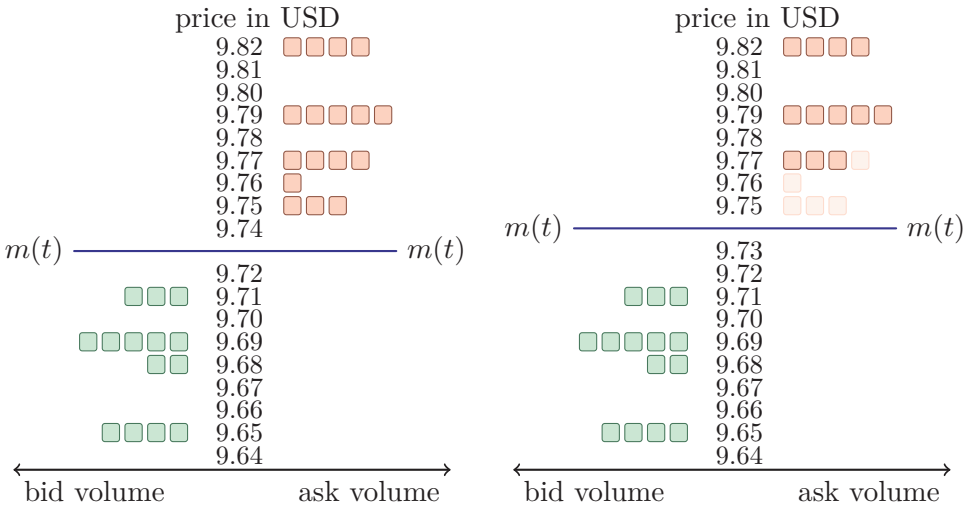

(a) Order book at time t

(b) Order book at time $t+1$

Figure 1.3: Snap shot of the order book before and after a limit buy order with volume 5 is executed. We notice how the midpoint moves up as a result.

side shows a state where no trade will happen, because no buyer is willing to pay the price for the cheapest offer at 9.75 USD. The cheapest offer is called

the *best ask* $a(t)$. On the other hand, no seller is willing to sell as low as the highest bid at 9.71 USD, which is called the *best bid* $b(t)$. The arithmetic mean of the best ask and bid is called the *midpoint*

$$m(t) = \frac{a(t) + b(t)}{2} \quad . \tag{1.9}$$

The midpoint is the second best guess for the current price if no last traded price is available. The difference $a(t) - b(t)$ is called the spread and is an indicator for the liquidity of the stock. A small spread is characteristic for high liquidity while larger spreads happen during periods of low liquidity. Let us return to our example order book in figure 1.3. Now a trader decides to buy five shares and is willing to pay up to 9.78 USD. He will receive three shares at 9.75 USD, one at 9.76 USD and 9.77 USD. The trader pays a total of $3 \cdot 9.75 + 9.76 + 9.77 = 48.78$ USD. The last traded price is 9.77 USD. We notice how the midpoint moves up. If the trader is willing to sell or buy at any price he can submit a market order instead of a limit order. Then he will get the best available price in the order book. Each time a trade happens the last traded price and the volume are recorded by the exchange. In addition, the best ask and bid prices are stored. We note that the best ask and bid can also change if a limit order at the best price is cancelled or a new order is placed in the spread. The occurrence of a trade is not necessary. This data can then be bought from the exchange. Given enough money, it is also possible to buy the entire order book information. The next section discusses the available data and its use in this thesis in detail.

1.5 Financial time series

In section 1.2, we discussed the importance of the time evolution of prices as an observable. Historically, the traders met on the trading floor provided by an exchange and trades were performed by open outcry. This method uses shouting and hand signals to propagate information between traders and perform sell or buy orders. All transactions had to be recorded by hand. In the late 1980s a move started to make electronic trading via networked computers possible. Since then electronic trading has become the dominant method. For example, the trading floor of the Frankfurt Stock Exchange ceased operation in March 2011. The advantage of electronic trading from a researcher's point of view is that a large quantity of accurate price data is available.

We have a dataset from the New York Stock Exchange (NYSE) covering the years 2007 and 2008. It contains all trades that took place at nine different stock exchanges including the NYSE.

A typical excerpt from this data for trades looks like this:

```
2008-09-15 10:00:08 44.49 100 0 0 F
2008-09-15 10:00:08 44.47 100 0 0 F
2008-09-15 10:00:09 44.47 100 0 0 F
2008-09-15 10:00:10 44.47 200 0 0 @
2008-09-15 10:00:14 44.44 100 0 0 @
```

It shows the first five trades between 10:00 AM and 11:00 AM for Wisconsin Energy Corp. (WEC), see figure 1.1. Besides the date, the data contains the time accurate to the second, the price and volume. The last three columns contain regulatory information, a correction indicator and a sale condition, which are not important at the moment. For more details see appendix A. Due to the time resolution of one second we have to merge all trades which occur during one second. We use the price of the last trade in this second and sum up the volume of all regular trades during the second. At least for the NYSE data set it is not possible to know from which trader the order came.

Besides the prices the database contains the quotes for all traded stocks. In section 1.4 we learned about the best ask and best bid. Stating the best ask and best bid price at a given time is called a quote. The according excerpt for WEC looks like this:

```
2008-09-15 10:00:02 44.3900 44.5200 5 3 12
2008-09-15 10:00:02 44.3800 44.5200 5 8 12
2008-09-15 10:00:02 44.3800 44.5100 2 8 12
2008-09-15 10:00:02 44.3900 44.5100 2 2 12
2008-09-15 10:00:02 44.3800 44.5100 2 6 12
```

It contains the date and time in the first two columns. The next two columns state the best bid and best ask followed by their accordingly available volume in multiplies of 100. The last column is the quote condition, where 12 shows that it is a regular quote. More details are shown in appendix A.

In the excerpts we notice that not at every second a trade happens or a quote is given. This poses a problem if we want to calculate price differences between fixed time intervals. The problem and its solution are illustrated in figure 1.4. We assume that the last traded price is the best estimate for the current price. Then we can fill the seconds which have no price with the price from the previous second and get prices on a equidistant time lattice.

For now we discussed intraday data, *i.e.*, the data which stems from the continuous trading process during the day. The advantage of this data is that it gives a complete picture of all trading activities. Disadvantages are that it is not freely available, *i.e*, it must be bought from the NYSE, and processing the data takes a lot of time. The full data set for 2007 and 2008 takes 4.2TB of storage. The other commonly used method is to take daily data. This data is sampled on a daily basis and takes only the opening price when trading starts

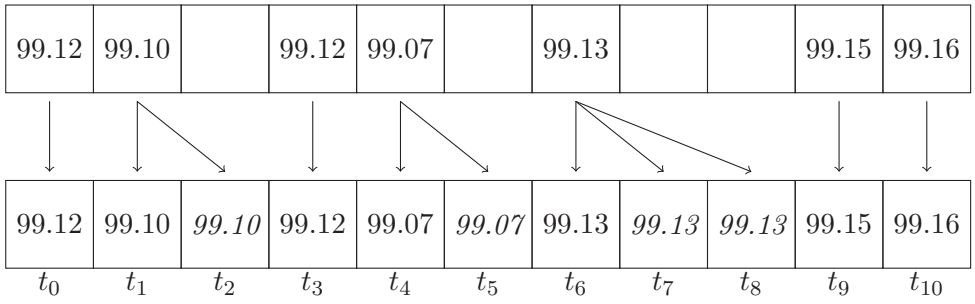

Figure 1.4: Processing the empirical data from stock exchanges. Where no data is available the previous last traded price is used.

and the closing price when trading concludes at the end of the day. Sometimes the highest and lowest price during the day is recorded. This information is freely available on the internet [35]. It is very fast to process and allows us to study larger time horizons up to decades in a manageable fashion. Selecting the right data source depends on the availability of the data and the question asked. We will use daily data in chapter 2 and 5, because of the long time horizons in question. In chapter 3 we use the NYSE intraday data to study the temporal dependencies in financial time series on short time scales of minutes up to one hour.

1.6 Returns and volatility

Figure 1.5 shows the price chart for three different stocks, Citigroup, Microsoft and Goldman Sachs, from 2001 to 2012. We notice that the absolute prices between the three stocks differ quite substantially. There are also strong local up and down trends for each stock. It is intuitively clear that the absolute prices $S_k(t)$ of the k-th stock are not suitable for statistical analysis, especially if we want to work with multiple stocks. A better way is to use relative price changes, where we divide the absolute price change

$$\Delta S_k(t) = S_k(t + \Delta t) - S_k(t) \tag{1.10}$$

by the price $S_k(t)$,

$$r_k(t) = \frac{\Delta S_k(t)}{S_k(t)} = \frac{S_k(t + \Delta t) - S_k(t)}{S_k(t)} \quad . \tag{1.11}$$

This quantity is called return, where Δt is the return interval. The distribution of returns shows a remarkable pattern of behavior. For small return intervals up to days the distribution has heavy tails, significantly deviating from a nor-

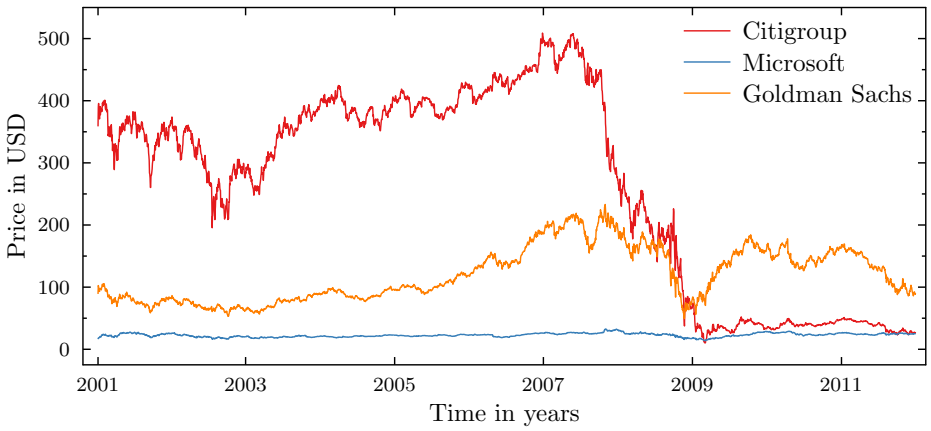

Figure 1.5: The chart for Citigroup, Microsoft and Goldman Sachs from 2001 to 20012.

mal distribution. For larger return intervals the distribution becomes normally distributed. This behavior reached a wider audience in 1963 through Mandelbrot's work "On the variation of certain speculative prices" [19]. However, as Mandelbrot notes it was first discussed by Wesley C. Mitchell [36] in 1915 and proof was given by Maurice Oliver [37] in 1926 and Frederick Mills [38] in 1927. In the following years the explanation of the effect started a controversial discussion [39–47]. Even the functional description of the return distribution, *i.e.*, the shape of the distribution, is an ongoing topic [19, 48–52]. The tails of the distribution can be described by a power-law at least for small return intervals of up to one day [53, 54]. It might be impossible to find a definite answer, because from empirical data there is no safe way to distinguish between power-laws and stretched exponentials [55].

A widespread opinion is that large order volumes cause large price shifts [56–58]. Gabaix *et al.* present a model where large funds with their big order volumes cause the heavy tails [46]. Another proposition by Farmer *et al.* [59] finds in a careful empirical investigation that gaps between the limit orders in the order book are responsible for the heavy tails. This view is supported by my own research [7] in the framework of an agent-based model.

If we look at the development of the stock market in the last 150 years we notice an exponential growth. Figure 1.6 shows the Dow Jones Industrial Average index which consists of the 30 largest companies in the USA. The exponential growth motivates the use of logarithmic returns

$$G_k(t) = \ln S_k(t + \Delta t) - \ln S_k(t) = \ln \frac{S_k(t + \Delta t)}{S_k(t)} \quad . \tag{1.12}$$

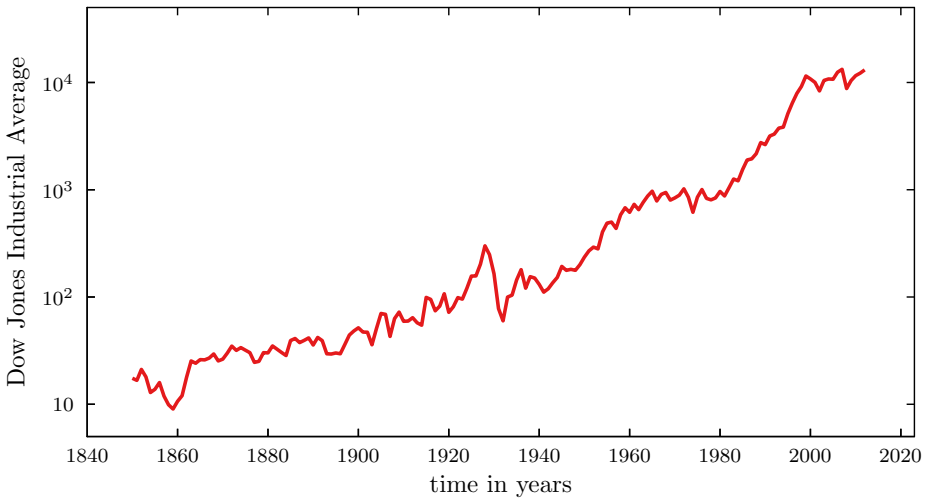

Figure 1.6: Logarithmic plot of the Dow Jones Industrial Average index. An exponential growth is observable.

For small return intervals Δt, where $\Delta S_k(t)/S_k(t) < 1$ holds we can expand the logarithm

$$G_k(t) = \ln\left(1 + \frac{\Delta S_k(t)}{S_k(t)}\right) \approx \frac{\Delta S_k(t)}{S_k(t)} = r_k(t) \tag{1.13}$$

and notice that the result equals the return $r_k(t)$.

An important measure for the risk of a stock k is the standard deviation of its returns

$$\sigma_k = \sqrt{\langle r_k^2(t)\rangle - \langle r_k(t)\rangle^2} \quad , \tag{1.14}$$

which is called volatility in economics. In practice, we will not use the expectation value, but the mean value

$$\langle r_k(t)\rangle_T = \frac{1}{T}\sum_{t=1}^{T} r_k(t) \tag{1.15}$$

if we work with sampled time series. This has some important implications. First, the volatility depends to some degree on the return interval Δt. Second, and more important, the volatility depends on the estimation horizon T. This would pose no major problem if the volatility is stationary, but empirical data shows that volatility is a highly fluctuating quantity [60, 61]. In addition, the absolute returns $|r_k(t)|$ or squared returns $r_k^2(t)$ show a slowly decaying autocorrelation [62]. This means that in phases of large returns, positive

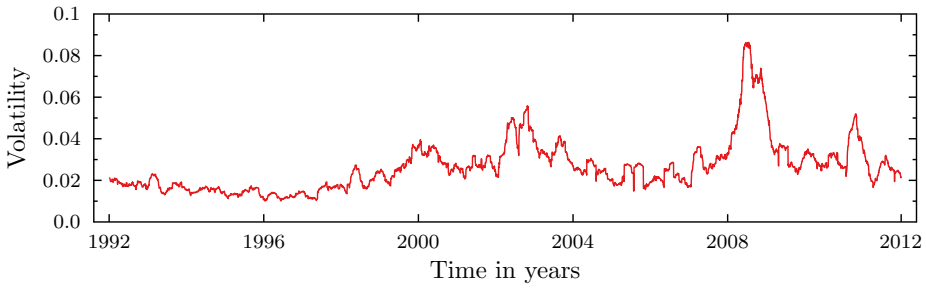

Figure 1.7: Time evolution for the volatility of Goodyear from 1992 to 2012.

and negative, the probability is elevated that the next return is also large. The same applies to small absolute returns. Therefore, the volatilities are clustered and also show a slowly decaying autocorrelation. Figure 1.7 shows the fluctuating volatility for Goodyear from 1992 to 2012. The volatility is estimated from daily returns on a moving time window of $T = 60$ trading days.

1.7 Risk

The discussion of financial markets in section 1.2 shows that the market participants face a certain risk of losing their money. In economics the financial risk can be divided roughly into four categories [63]: market risks, liquidity risks, credit risks and operational risks.

Market risks emerge from the unexpected movement of prices or changes in volatility. Liquidity risks arise from a lack of available volume. For example, if we want to sell a large number of shares at once, more than current buyers are willing to take, we may not be able to sell everything or have to accept lower prices. A recent example of a liquidity shortage that gained public attention was the rise of the Volkswagen stock from 200 to 1000€ on October 27, 2008. Due to the takeover attempt by Porsche only 6% of the Volkswagen shares were freely available to trade [64]. In addition, many investors speculated that the price of Volkswagen would decline and were selling the stock short, see section 1.3. To limit their losses the investors tried to cover their positions and bought the Volkswagen shares thus further increasing the price. This effect is called *short squeeze*.

A credit is a contract between two parties, where one party provides something, which is not immediately paid by the other party. The payment is deferred to a later point in time. The first party is called *creditor* and for example lends money (loan) to the second party which is called *debtor* or *obligor*. If the obligor cannot fulfill the contractually required payment a *default* occurs. Credit risks stem from the possibility that obligors are not able to fully

or partially pay back their loans, *i.e.*, default. Credit risk will play a major role in chapter 5.

Operational risks include losses from human error or fraud and through external events. This also includes legal risks if one party tries to reverse a trade, which created losses, in court. Operational risk can be minimized by improved internal processes, the four eye principle and legally well written contracts. Here, we consider market and credit risks, which can be described quantitatively. This is also true for liquidity risks, see reference [63]. Controlling these risks is essential for many companies, especially banks, to stay in business long-term. A first step to control risk is to quantify it.

Measuring the risk of investments is the task of quantitative risk management. In 1952, Harry M. Markowitz published "Portfolio Selection" [65], where he presented a method to optimize the return of a portfolio given a certain risk tolerance. Under normal circumstances we have to take a higher risk to have the chance of a higher return in the future. The Markowitz approach uses the correlations between stocks to minimize the variance of the portfolio. The portfolio variance is the most basic risk measure. We will use Markowitz portfolio optimization in chapter 2 and discuss it there in greater detail.

The importance of risk management led to the development of more advanced risk measures, for example Value at Risk (VaR) or Expected Tail Loss (ETL). Figure 1.8 shows a theoretical profit-loss distribution for a portfolio

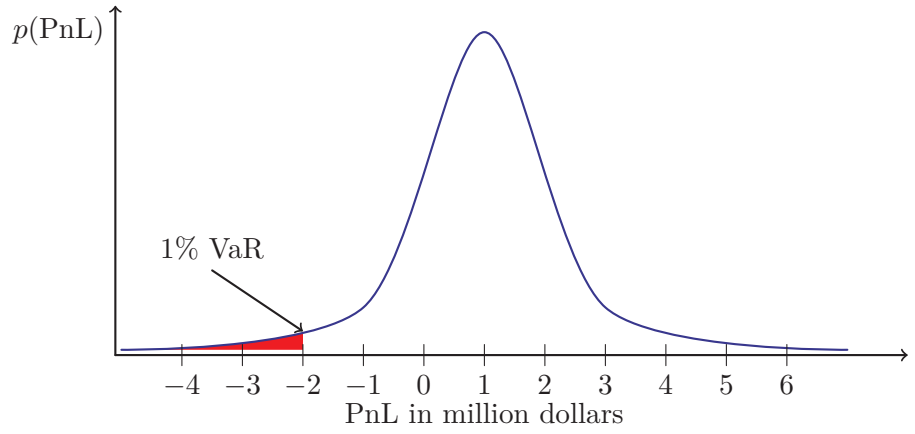

Figure 1.8: Hypothetical profit and loss (PnL) distribution for a portfolio of assets. The profit and loss is shown in multitudes of one million dollars. The tails of the loss distribution are more pronounced compared to a normal distribution.

of stocks. In principle, the Value at Risk is the value of the quantile of the profit and loss distribution at a freely chooseable probability level. It is always stated on a given time horizon. For example, if the 1% VaR is at −2 million

dollars for a day there is a one percent chance that the portfolio will lose 2 million or more dollars at the end of the day. In other words: On average the portfolio will have a loss of 2 million dollars or more in one of a hundred days. It is very important to understand that the VaR is only as good as the underlying distribution. In particular, this means that the VaR cannot capture the rare extreme events, for example Black Friday or the financial crisis. These so called *black swan* events happen so infrequently that they are impossible to predict from a statistical point of view [66]. Nonetheless, the Value at Risk is an important risk measure in daily life and is the preferred method in the Basel II guidelines for market risk [67]. Basel III adds recommendations to calculate the VaR of bank portfolios assuming stressed market conditions [68].

The Expected Tail Loss also known as Expected Shortfall (ES) is a risk measure which has a higher emphasis on the tail of the distribution. Risk wise it is a more conservative approach compared to the Value at Risk and reacts more strongly on the shape of the tail. The Expected Tail Loss is the average

$$\mathrm{ETL}_\alpha = \frac{1}{\alpha}\int_0^\alpha \mathrm{d}\gamma\, \mathrm{VaR}_\gamma \tag{1.16}$$

over all Values at Risk up to the α probability level. The Value at Risk will be used in chapters 2 and 5 to characterize the risk of stock and credit portfolios. For the credit portfolios we also study the Expected Tail Loss.

1.8 Correlation and covariance of stocks

Figure 1.9 shows the price development of three stocks, Google, Apple and Nokia, normalized to their starting prices. From just looking at the chart we get the impression that the stock prices of the three companies move in a similar fashion on some time horizons. Starting at 2009 the Nokia stock starts to stagnate while Apple and Google thrive.

A quantitative way to determine the connection between stocks is the Pearson correlation coefficient. However, it does not make sense to calculate the correlation coefficient directly from the prices due to their absolute nature. Therefore, the correlation coefficient should always be calculated from return time series. First, we have to normalize the return time series $r_k(t)$ of each stock k

$$M_k(t) = \frac{r_k(t) - \mu_k}{\sigma_k} \quad , \tag{1.17}$$

to standard deviation (volatility) one and zero mean. We notice that the mean μ_k and volatility σ_k have to be calculated on a finite time interval T, the length

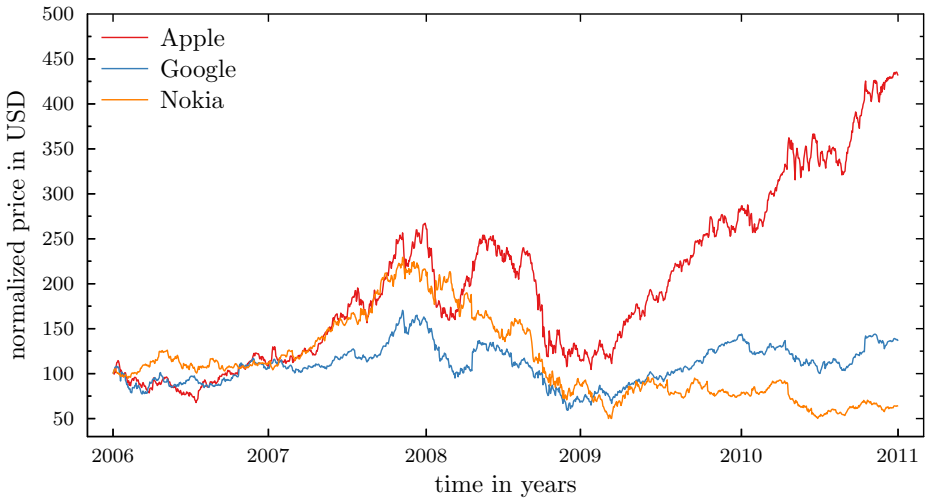

Figure 1.9: Price evolution of Apple, Google and Nokia normalized to a starting price of 100 USD.

of the return time series

$$\mu_k = \frac{1}{T}\sum_{t=1}^{T} r_k(t)$$
$$\sigma_k^2 = \frac{1}{T-1}\sum_{t=1}^{T}(r_k(t)-\mu_k)^2 \quad , \tag{1.18}$$

for empirical data. For the standard deviation we use the unbiased estimator with $1/(T-1)$. The Pearson correlation coefficient for two stocks k and l is defined as

$$C_{kl} = \frac{1}{T}\sum_{t=1}^{T} M_k(t)M_l(t) \quad . \tag{1.19}$$

Due to the normalization of the return time series in equation (1.17) the values of the correlation coefficient lie between minus one and plus one. For minus one the time series are perfectly anti-correlated and for plus one perfectly correlated, *i.e.*, identical. If the correlation coefficient is zero, the time series are uncorrelated.

Calculating the correlation coefficient for each pair out of K stocks yields a $K \times K$ correlation matrix. The correlation matrix contains a lot of information about the stock market. If we sort the stocks according to their industrial sectors, the inner sector correlations are clearly visible in the block structure of the correlation matrix. Figure 1.10 shows the correlation matrix for 306

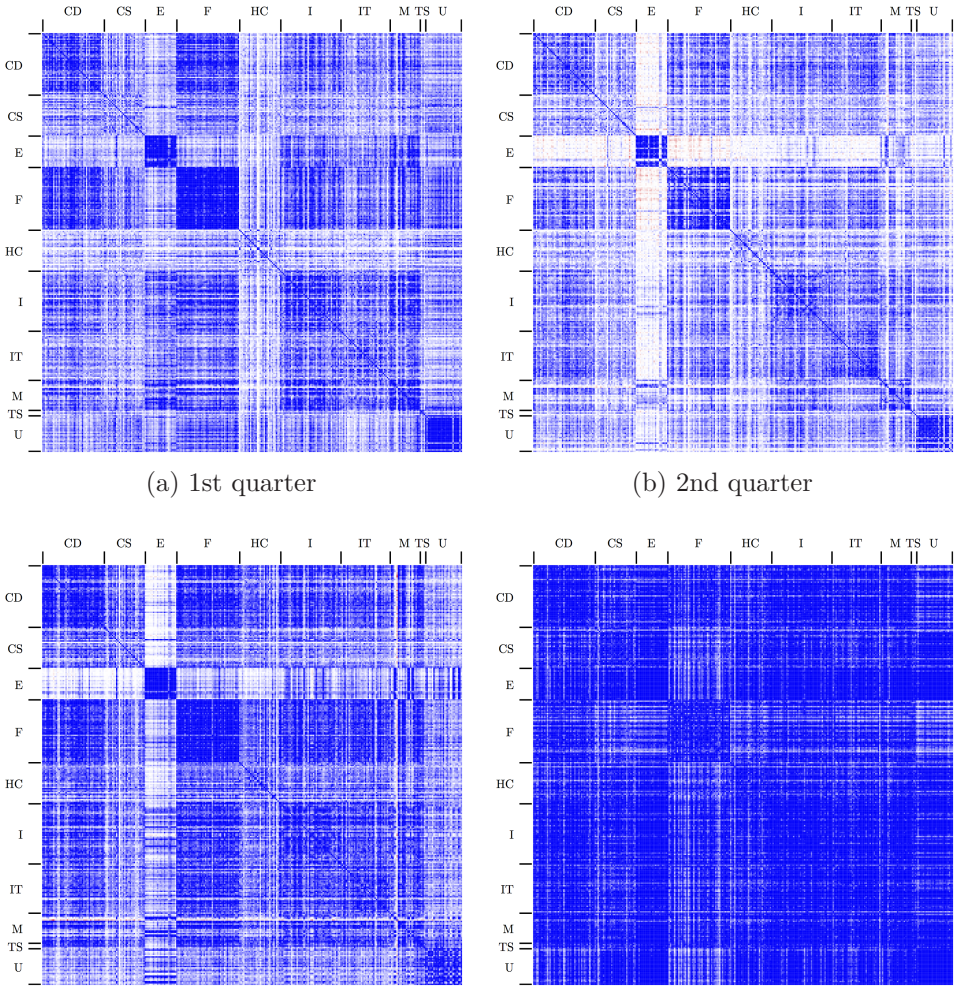

(a) 1st quarter (b) 2nd quarter

(c) 3rd quarter (d) 4th quarter

Figure 1.10: Correlation matrices for 306 stocks from the S&P 500 index for each quarter of 2008. Blue denotes positive correlation, while red indicates anti-correlation.

stocks from the S&P 500 index for four different quarters of 2008. The industrial sectors are classified according to the following branches: **C**onsumer **D**iscretionary, **C**onsumer **S**taples, **E**nergy, **F**inancials, **H**ealth **C**are, **I**ndustrials, **I**nformation **T**echnology, **M**aterials, **T**elecommunications **S**ervices and **U**tilities. We observe that the correlation matrix significantly changes over time. This is intuitively clear, because the relations between companies change over time. Therefore, we might be tempted to reduce the length of the time series T to better capture the current state of the market. However, reducing

the length of the time series leads to more measurement noise in the correlation matrix [69]. Choosing a length for the return time series is therefore always a compromise and different approaches exist to improve the estimation of the correlation matrix [70, 71].

Often the covariance matrix is used instead of the correlation matrix. The difference is that the covariance matrix is not normalized to variance one and still includes the volatilities. As usual, we use the definition for the sample covariance matrix

$$\Sigma_{kl} = \frac{1}{T-1}\sum_{t=1}^{T}(r_k(t) - \mu_k)(r_l(t) - \mu_l) \quad , \tag{1.20}$$

where the sample mean is defined according to equation (1.18). The simple relation

$$\Sigma_{kl} = \frac{C_{kl}}{\sigma_k \sigma_l} \tag{1.21}$$

allows us to swap the covariance matrix for the correlation matrix and vice versa.

1.9 Guide to the thesis

At this point we have established a basic understanding of the properties of financial markets. In the process of competing against each other, companies may change the scope of their business. Maybe they stop competing against former rivals and start new areas of operations and compete against other companies. These constantly changing relationships are taken into account by the market participants to form their market expectation. The actions of the market participants are for example culminated in the non-stationarity of the correlation and covariance matrix.

In chapter 2 we study from an empirical point of view the effects of non-stationarity on the covariance estimation methods and to what extent they can be improved. A deeper look at the temporal dependencies in intraday time series uncovers the limits of certain stochastic processes to fully characterize the empirically observed time series in chapter 3.

Financial markets can be considered as complex systems in the sense of systems with many degrees of freedom. In physics, we know similar systems. Consider a thermodynamic system, *e.g.*, a gas in a room. Here, we also have a large number of particles with one cubic centimeter containing roughly $\sim 10^{23}$ particles. In principal, we could write down the equations of motion for the system of particles. However, it would be an impossible task to measure the initial conditions for each particle. Equally, we cannot measure the thoughts of the market participants. Statistical physics circumvents the problem by

characterizing the system by a small set of macroscopic observables, *e.g.*, temperature, number of particles and volume. This is achieved by an ensemble average over the states of all particles in the system. We do not want to overstretch the similarities, but it seems not too far fetched that an ensemble approach might work to describe financial markets.

In chapter 4, we construct a correlation-averaged multivariate normal distribution by averaging the multivariate normal distribution over an ensemble of correlation matrices. This approach addresses the non-stationarity of the correlation matrix and allows us to contribute a realistic distribution of asset prices. From this distribution we can construct the distribution of asset values assuming a geometric Brownian motion in chapter 5. A realistic distribution for the asset values is essential to calculate the loss distribution for a portfolio of credit contracts using the Merton model. This will allow us to develop a quantitative understanding for the risk of such portfolios. We summarize our findings in chapter 6.

Chapter 2

The impact of non-stationarity on covariance estimation

2.1 Introduction

The non-stationarity inherent in financial time series poses serious challenges to the estimation of covariance matrices, which are the main input for portfolio optimization techniques. Section 1.7 points out the importance of portfolio optimization by Markowitz for quantitative risk management, see reference [72] for a comprehensive introduction. A portfolio is a selection of K risk elements, *e.g.*, stocks. The total value of our portfolio is

$$\hat{V}(t) = \sum_{k=1}^{K} u_k(t) S_k(t) \quad , \tag{2.1}$$

where $u_k(t)$ is the number of shares we are holding for the k-th stock with price $S_k(t)$ at time t. For our purposes it comes in handy to use fractional portfolio weights $\omega_k(t)$ with the normalization

$$\sum_{k=1}^{K} \omega_k(t) = 1 \tag{2.2}$$

instead of the absolute number of shares. We notice that the portfolio weights are allowed to be negative if short-selling is allowed, see section 1.3. In addition, we need a risk measure to quantitatively describe the risk of our portfolio. Markowitz used the variance of the portfolio returns $\hat{\sigma}^2$, see equation (1.18). The seminal idea of Markowitz was to find a set of portfolio weights which minimizes the risk (portfolio variance) given a desired portfolio return. This optimization problem can be expressed as an Euler-Lagrange problem [72] with three boundary conditions: First, for the risk

$$\hat{\sigma}^2 = \sum_{k=1}^{K} \sum_{l=1}^{K} \omega_k \omega_l C_{kl}, \quad , \tag{2.3}$$

with the correlation coefficient C_{kl} according to equation (1.19). We drop the time dependence to simplify the notation. Second, the portfolio return

$$\hat{G} = \sum_{k=1}^{K} \omega_k G_k \quad , \tag{2.4}$$

with the return G_k of the k-th stock, see equation (1.11). Third, we use the normalization of the portfolio weights (2.2) as a boundary condition. The resulting Euler-Lagrange equation is

$$L = \sum_{k=1}^{K} \sum_{l=1}^{K} \omega_k \omega_l \sigma_k \sigma_l C_{kl} + \lambda_1 \left(\hat{r} - \sum_{k=1}^{K} \omega_k r_k \right) + \lambda_2 \left(1 - \sum_{k=1}^{K} \omega_k \right) \quad , \tag{2.5}$$

with the Lagrange multipliers λ_1 and λ_2. If short selling is allowed, we can find an analytic solution by calculating the partial derivatives

$$\frac{\partial L}{\partial \omega_k} = 0 \quad , \quad \frac{\partial L}{\partial \lambda_1} = 0 \quad , \quad \frac{\partial L}{\partial \lambda_2} = 0 \quad , \tag{2.6}$$

and solving the system of $K + 2$ equations. The portfolio weights for the minimum variance portfolio, *i.e.*, the portfolio with the highest possible return given the lowest possible risk, are

$$\omega_k^{(\mathrm{MV})} = \frac{1}{Z} \sum_{l=1}^{K} C_{kl}^{-1} \quad \text{with} \quad Z = \sum_{k,l=1}^{K} C_{kl}^{-1} \quad . \tag{2.7}$$

The general solution to the problem is a hyperbola, which is called the efficient frontier, see figure 2.1. The hyperbola describes all portfolios with the best expected return for a given risk level in the return-risk space. The space above the hyperbola contains the impossible portfolios, *i.e.*, it is not possible to construct a portfolio with a higher return at a given risk. Under the hyperbola we find the inefficient portfolios, which yield a lower return for a given risk compared the efficient portfolio.

The optimization process for a portfolio consisting of K stocks requires the correlation coefficients C_{kl} and the according volatilities σ_k and σ_l, *i.e.*, a $K \times K$ covariance matrix Σ, see section 1.8. The covariance matrix can be expressed as $\Sigma = \sigma C \sigma$ with $\sigma = \mathrm{diag}(\sigma_1, \ldots, \sigma_K)$ and the $K \times K$ correlation matrix C, compare equation (1.21). In the last case we have the freedom to estimate the volatilities separately. This can include the use of a different method to estimate the volatilities than was used to calculate the correlation matrix.

The quality of the portfolio optimization solely depends on the estimation of the covariance matrix. At first glance this might look like a minor problem.

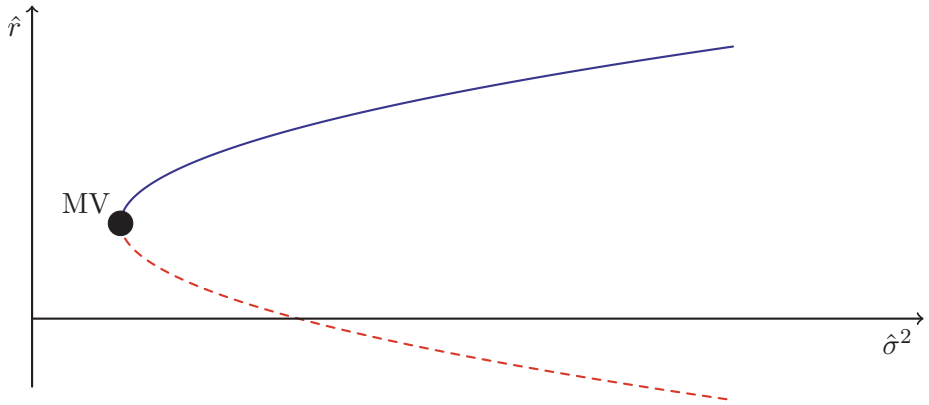

Figure 2.1: The portfolios with the highest expected return for a given risk level lie on the efficient frontier (solid line). The negative branch of the hyperbola (dashed line) plays no role. The minimum variance portfolio (MV) is denoted by a black dot.

According to equation (1.20) we can calculate the sample covariance matrix from the time series of K stocks. However, the expectation value of the covariance matrix is only equal to the sample covariance matrix for $T \to \infty$. Typical time series for stock returns are in general rather short. Daily data has roughly 250 prices per year. We could increase the length of the time series by taking 10 or 20 years into account. In particular in emerging markets, the total length of the available time series may be the limiting factor. Nevertheless, this has shortcomings, too. We recall, if we predict the future portfolio variance from the past, the chance that the historical data is a good predictor for the future shrinks the longer we go back in time. The economy as a whole is a constantly changing system [73–75] and assuming stationarity is asking for trouble [76, 77]. The non-stationarity of the correlation structure between stocks forbids the use of long time series. Since the sample covariance matrix for K assets requires $K(K+1)/2$ parameters to be estimated, the finiteness of the time series leads to a considerable amount of measurement noise [53, 69, 78, 79]. As pointed out by, *e.g.*, Pafka *et al.* [80, 81], this has dire consequences for portfolio optimization, but can be mitigated to a large extent by noise reduction techniques. We use a noise reduction method which is called power mapping to reduce noise in the correlation matrix [82, 83].

Reducing the noise inherent in sample covariance matrices is one approach. Another idea is to use a model covariance matrix. The purpose of the model is to reduce the number of parameters which have to be estimated and thus decrease measurement noise. A comparative analysis of such models is given in reference [84]. First, we consider a one-factor model [85], where $2K+1$ parameters have to be estimated. This is one of the simplest approaches. Second,

we study a more complex spatial autoregressive model for stock returns [86]. It requires $K + 3$ parameters, 3 for the spatial dependence and K parameters describing the individual volatilities. The model is able to give reliable Value at Risk (VaR) forecasts due to its reliance on a small set of parameters.

The non-stationarity of the times series leads to artifacts in the estimation of correlations due to abrupt changes of the volatility. This also affects the estimation of the spatial dependence parameters. We investigate whether local normalization [87] can suppress these artifacts or not.

In econometrics, the GARCH model [88, 89] is extremely popular to describe return time series with non-stationary volatilities. It is a generalization of the ARCH process proposed by Engle [90] in 1982.

In general a GARCH(1,1) is sufficient to capture the governing features of the return time series [91]. The study carried out in chapter 3 will reveal some shortcomings of selected GARCH type processes. We use a GARCH(1,1) process to remove fluctuating volatilities from the return time series and to predict future volatilities. Fitting the GARCH model to the data requires a rather long history of past returns, around 500 days. The shorter the time series, the smaller the probability that the fit will converge. Motivated by this restriction we suggest using local normalization in combination with a prediction of the individual volatilities from short-term historic data (last 14 trading days).

We study the influence of these refinements on each of the covariance estimation methods. Using the improved covariance matrices, we perform a portfolio optimization on stocks of the Euro Stoxx 50. This index includes a selection of large companies in the eurozone.

The quality of each method is evaluated by back-testing the predicted variances with the realized out-of-sample variances of the portfolio. In addition, we discuss how the VaR forecast compares to the predicted and realized variances. The comparison of different models regarding their VaR forecast capabilities is a common approach in the literature, see for example reference [92].

We focus on a narrow selection of common methods to keep the presentation clear. The results in this chapter are available as a working paper, see reference [4].

The chapter is structured as follows: Section 2.2 presents the above mentioned methods for estimating the covariance matrix of stock returns. In section 2.3 we discuss the refinements to these methods, which aim at removing changes in local trends and volatilities, improving the quality of volatility predictions, and reducing estimation noise. Section 2.4 details the portfolio optimization technique and the data set under consideration. In section 2.6 we discuss the results of the covariance estimation and VaR forecasts, and we summarize our findings in section 2.7.

2.2 Covariance estimation

"Garbage in, garbage out" is a common joke in computer science. If we feed erroneous or unintended data into a computer, the program will produce wrong and unexpected results. The same applies to portfolio optimization, which is only as good as the input we provide.

We use a sample covariance matrix calculated from the return time series as a basis, see equation (1.20), for the comparison with the refined covariance matrices and the model versions. The sample covariance matrix requires the estimation of $K(K+1)/2$ parameters.

The non-stationarity of financial markets, especially of the volatilities, makes the estimation of the covariance matrix a non-trivial task. If the covariance matrix is calculated on a short time horizon it contains a great degree of noise. For larger time horizons the predictive power of the covariance matrix decreases as the market constantly changes.

In sections 2.2.1 and 2.2.2 we discuss two models which go beyond the sample covariance matrix. These models produce covariance matrices which require fewer parameters to be estimated.

2.2.1 One-factor model

The one-factor model was proposed by Sharpe in 1963 [85]. The basic idea is that the price evolution of the assets can be modeled by a single factor only, *e.g.*, a market index. A detailed description of the model is given in reference [63]. Under this assumption the stock returns can be described by

$$G(t) = \alpha + \beta G_{\mathrm{m}}(t) + \eta(t) \quad , \tag{2.8}$$

where the K dimensional vector $G(t)$ is comprised of the logarithmic returns for each stock $1 \dots K$ at time t. The market return $G_{\mathrm{m}}(t)$, which is just a scalar, can be calculated from a stock index. We use the daily logarithmic returns of the Euro Stoxx 50 index. If we calculate $G_{\mathrm{m}}(t)$ from a market index, the vector $\beta = (\beta_1, \dots, \beta_K)$ is known as systematic risk. The vector of fixed intercepts α plays no role for the estimation of risk, because it contains no random information. Each value of β has to be estimated separately for each stock using a linear fit (ordinary least squares-estimator), for example. The error terms of the fit are included in the vector $\eta(t)$. The model requires the following assumptions to calculate the covariance matrix

$$\begin{aligned} \langle \eta_k(t) \rangle &= 0 \\ \langle \eta_k(t) G_{\mathrm{m}}(t) \rangle &= 0 \\ \langle \eta_k(t) \eta_l(t) \rangle &= 0 \qquad \text{for} \quad k \neq l \quad . \end{aligned} \tag{2.9}$$

First, the elements of the error vector have an expectation value of zero. Second, the single errors are uncorrelated to the market factor. Third, the elements of the error vector are uncorrelated to each other. Then, the variance for each stock k is defined as

$$\sigma_k^2 = \left\langle (G_k(t) - \langle G_k(t) \rangle)^2 \right\rangle \tag{2.10}$$

and the variance of the market is

$$\sigma_{\mathrm{m}}^2 = \left\langle (G_{\mathrm{m}}(t) - \langle G_{\mathrm{m}}(t) \rangle)^2 \right\rangle \quad . \tag{2.11}$$

According to equation (2.8) the variance σ_k^2 of stock k can be written as

$$\begin{aligned} \sigma_k^2 &= \left\langle (\beta_k G_{\mathrm{m}}(t) - \langle \beta_k G_{\mathrm{m}}(t) \rangle + \eta_k(t) - \langle \eta_k(t) \rangle)^2 \right\rangle \\ &= \beta_k^2 \left\langle (G_{\mathrm{m}}(t) - \langle G_{\mathrm{m}}(t) \rangle)^2 \right\rangle + 2\,\mathrm{covar}(\beta_k G_{\mathrm{m}}(t), \eta_k(t)) + \left\langle \eta_k^2(t) \right\rangle \\ &= \beta_k^2 \sigma_{\mathrm{m}}^2 + \langle \eta_k(t)^2 \rangle \quad , \end{aligned} \tag{2.12}$$

because the return $G_k(t)$ is modeled by $\beta G_m(t) + \eta(t)$. The covariance between stocks k and l is

$$\begin{aligned} \sigma_{kl} &= \mathrm{covar}(\beta_k G_{\mathrm{m}}(t) + \eta_k(t), \beta_l G_{\mathrm{m}}(t) + \eta_l(t)) \\ &= \beta_k \beta_l \sigma_{\mathrm{m}}^2 \quad , \end{aligned} \tag{2.13}$$

due to the assumptions in equation (2.9). We now know the diagonal and off-diagonal elements of the covariance matrix. Comparing equation (2.12) and equation (2.13) yields

$$\Sigma = \beta \beta' \sigma_{\mathrm{m}}^2 + \mathrm{diag}\left(\left\langle \eta_1^2(t) \right\rangle, \ldots, \left\langle \eta_K^2(t) \right\rangle \right) \tag{2.14}$$

for the covariance matrix in the one-factor model. We denote the transpose of a vector or matrix with a prime. The model requires the estimation of K entries for the β vector, K variances for the error terms, plus one for the market volatility σ_{m}. Using the model reduces the required number of parameters from $K(K+1)/2$ in the case of the sample covariance matrix to $2K+1$ parameters.

2.2.2 Spatial dependence model

The spatial dependence model for stock returns was introduced by Arnold *et al.* [86] in 2010. The basic idea of the model is to capture the correlations between stocks with three parameters. The first parameter captures the general dependence, which is quite similar to the market factor in Sharpe's one-factor model. The second parameter describes the dependence within industrial sec-

tors and the third parameter the dependence based on the geographic location. For an overview of spatial dependence modeling, even beyond financial applications, see [93–95].

The formal definition of the spatial autoregressive model reads

$$G(t) = \rho_{\mathrm{g}} W_{\mathrm{g}} G(t) + \rho_{\mathrm{b}} W_{\mathrm{b}} G(t) + \rho_{\mathrm{l}} W_{\mathrm{l}} G(t) + \eta(t) \ , \quad t = 1, \ldots, T \quad (2.15)$$

with three scalar parameters ρ_{g}, ρ_{b}, ρ_{l} for the general dependence, the dependence within branches and the local (geographic) dependence. The $K \times K$ matrices W_{g}, W_{b} and W_{l} are spatial weighting matrices. The K dimensional vector $\eta(t)$ of errors introduces a stochastic component to the model. As with the one-factor model some assumptions are required.

1. The return time series must have zero mean.

2. The off-diagonal elements of the weighting matrices are equal or greater than zero and the diagonal elements are zero.

3. Each row of the weighting matrices is normalized to unity.

4. The spatial parameters fulfill the condition $|\rho_{\mathrm{g}}| + |\rho_{\mathrm{b}}| + |\rho_{\mathrm{l}}| < 1$.

5. The covariance of the error terms is $\Omega \equiv \operatorname{covar} \eta(t) = \operatorname{diag}(\sigma_1^2, \ldots, \sigma_K^2)$.

The weighting matrices are constructed in the following way: For the general weighting matrix the off-diagonal elements for each row are set to the normalized market capitalization of each stock. This ensures that the spatial parameter for the general dependence takes the size of the companies into account. This is based on the assumption that companies with a higher market capitalization are more important. The local and branch weighting matrices have non-zero off-diagonal elements k, l if stock k and l are in the same country or branch. Again, we set the non-zero elements to the market capitalization and normalize the rows.

In principle, the spatial parameters can be estimated using a maximum likelihood function. However, Arnold *et al.* [86] point out that such an approach is computationally inefficient, especially for large K. They propose a two step estimation procedure, which estimates the spatial parameters first and in a second step use these to estimate the variances. Basically it is based on a generalized method of moments (GMM) approach [96, 97]. We have to minimize

the expression

$$\left\| \begin{bmatrix} A_{11} & A_{12} & A_{13} & B_{14} & B_{15} & B_{16} & C_1 & D_1 & E_1 \\ A_{21} & A_{22} & A_{23} & B_{24} & B_{25} & B_{26} & C_2 & D_2 & E_2 \\ A_{31} & A_{32} & A_{33} & B_{34} & B_{35} & B_{36} & C_3 & D_3 & E_3 \end{bmatrix} \begin{bmatrix} \rho_{\mathrm{g}} \\ \rho_{\mathrm{b}} \\ \rho_{\mathrm{l}} \\ \rho_{\mathrm{g}}^2 \\ \rho_{\mathrm{b}}^2 \\ \rho_{\mathrm{l}}^2 \\ \rho_{\mathrm{g}}\rho_{\mathrm{b}} \\ \rho_{\mathrm{g}}\rho_{\mathrm{l}} \\ \rho_{\mathrm{b}}\rho_{\mathrm{l}} \end{bmatrix} + \begin{bmatrix} \langle G'(t) W_{\mathrm{g}} G(t) \rangle \\ \langle G'(t) W_{\mathrm{b}} G(t) \rangle \\ \langle G'(t) W_{\mathrm{l}} G(t) \rangle \end{bmatrix} \right\| \tag{2.16}$$

with regard to the spatial parameters ρ_{g}, ρ_{b} and ρ_{l}. The elements of the first matrix are given by

$$\begin{aligned} A_{ij} &:= \langle -G'(t)(W_i + W_i')W_j G(t) \rangle \\ B_{ij} &:= \langle G'(t)W_j' + W_i' W_j G(t) \rangle \\ C_i &:= \langle -G'(t)W_{\mathrm{g}}'(W_i + W_i')W_{\mathrm{b}} G(t) \rangle \\ D_i &:= \langle G'(t)W_{\mathrm{g}}'(W_i + W_i')W_{\mathrm{l}} G(t) \rangle \\ E_i &:= \langle G'(t)W_{\mathrm{b}}'(W_i + W_i')W_{\mathrm{l}} G(t) \rangle \quad . \end{aligned} \tag{2.17}$$

Note that this minimization is done on a moving time horizon T. If we have the spatial parameters the variances for each stock k can be estimated from

$$\begin{aligned} \sigma_k^2 = & \frac{1}{T} \sum_{t=1}^{T} \mathrm{e}_k'(I_K - \rho_{\mathrm{g}} W_{\mathrm{g}} - \rho_{\mathrm{b}} W_{\mathrm{b}} - \rho_{\mathrm{l}} W_{\mathrm{l}}) G(t) \\ & \times G'(t)(I_K - \rho_{\mathrm{g}} W_{\mathrm{g}}' - \rho_{\mathrm{b}} W_{\mathrm{b}}' - \rho_{\mathrm{l}} W_{\mathrm{l}}') e_k \quad , \end{aligned} \tag{2.18}$$

where e_k denotes the i-th unit vector and I_K is an identity matrix with dimension $K \times K$. With this knowledge we can calculate the covariance matrix of the vector $G(t)$

$$\Sigma = (I_K - \rho_{\mathrm{g}} W_{\mathrm{g}} - \rho_{\mathrm{b}} W_{\mathrm{b}} - \rho_{\mathrm{l}} W_{\mathrm{l}})^{-1} \Omega (I_K - \rho_{\mathrm{g}} W_{\mathrm{g}}' - \rho_{\mathrm{b}} W_{\mathrm{b}}' - \rho_{\mathrm{l}} W_{\mathrm{l}}')^{-1} \quad . \tag{2.19}$$

The matrix Ω is the covariance matrix of the error terms from the estimation procedure, compare assumption 5 and equation (2.18). The error terms are assumed to be uncorrelated, so all off-diagonal elements of Ω are zero. The model requires the estimation of $K + 3$ parameters, K variances and three spatial parameters.

2.3 Refined methods of covariance estimation

We compare three methods to estimate the covariance matrix. The sample covariance matrix, which is calculated directly from return time series. In addition, we study two model approaches, which reduce the number of parameters by making assumptions about what factors the returns depend on.

There are two principle approaches to refine the estimation procedure. First, we can try to improve the return time series before estimating the covariance matrix. Second, we try to refine the covariance matrix directly. Certainly, both approaches can be used simultaneously.

The GARCH residuals (section 2.3.1) and local normalization (section 2.3.2) belong to the first category. They aim at removing the empirically observed non-stationarity of the volatilities in the return time series. The power mapping method discussed in section 2.3.3 is applied to a correlation matrix and reduces the noise. In section 2.3.4 we explore additional methods to estimate the volatilities of the individual stocks and replace them in the covariance matrix.

2.3.1 GARCH residuals

The equations for the return and variance in the GARCH(1,1)-model are

$$\begin{aligned} G(t) =& \sigma(t)\varepsilon(t) \\ \sigma^2(t) =& \omega + \alpha_1 G^2(t-1) + \beta_1 \sigma^2(t-1) \quad , \end{aligned} \tag{2.20}$$

where ω, α_1 and β_1 are parameters that have to be estimated by fitting the GARCH model to historical data. The GARCH residuals $\varepsilon(t)$ follow a strong white noise process and have zero mean $\langle \varepsilon(t) \rangle = 0$ and unit variance $\langle \varepsilon^2(t) \rangle = 1$. The GARCH process is designed to describe volatility clustering, *i.e.*, the non-stationarity of the volatility. Depending on the goodness of fit the volatility clustering is captured more or less in the conditional variances $\sigma^2(t)$. Therefore, it is not surprising that the GARCH residuals

$$\varepsilon(t) = \frac{G(t)}{\sigma(t)} \tag{2.21}$$

can be viewed as return time series where the non-stationarity is removed. We use these time series as an alternative to address the non-stationarity.

For the GARCH fit one particular *caveat* exists, which can be a drawback in practical applications. The fit requires a comparable long time horizon to converge. On our data set we had to select a moving time horizon of $T_{\mathrm{GARCH}} = 1000$ trading days to estimate the GARCH parameters. The problem of non-converging GARCH fits is known in the literature, see *e.g.*, references [98, 99]. For the evaluation of the models and methods in section 2.6, we use a moving

window of $T = 100$ trading days to estimate model parameters or calculate the sample covariance matrix. We emphasize that the larger window of 1000 trading days is only used to estimate the GARCH parameters.

2.3.2 Local normalization

Local normalization, introduced by Schäfer *et al.* [87], uses a local average to remove local trends and fluctuations in volatility. However, it does not impair the cross-correlations between different time series. In contrast to the GARCH fit it requires a very short time horizon of only 13 trading days.

The local average of a function is defined as

$$\langle f(t)\rangle_n = \frac{1}{n}\sum_{j=0}^{n-1} f(t - j\Delta t) \quad , \tag{2.22}$$

where Δt is the return interval. Then the locally normalized returns are given by

$$\rho_n(t) = \frac{G(t) - \langle G(t)\rangle_n}{\sqrt{\langle G^2(t)\rangle_n - \langle G(t)\rangle_n^2}} \quad , \tag{2.23}$$

where we subtract the local mean value $\langle G(t)\rangle_n$ from the return $G(t)$ and then divide by the local volatility. As shown in reference [87] a value of $n = 13$ yields optimal results for daily stock returns.

2.3.3 Power mapping

Correlation matrices calculated from financial return time series include a notable amount of noise. It has been shown that the eigenvalue density of a correlation matrix and a random matrix are similar to each other for small eigenvalues [69]. They only differ beyond the bulk part of the eigenvalue density. The correlation matrix has a series of larger eigenvalues, which are not observed in a random matrix. These large eigenvalues can be traced back to the industrial branches of the stocks. The largest eigenvalue is assumed to show the global trend of the whole market [78]. The noise becomes more pronounced the shorter the return time series are. Increasing the length of the time series has the disadvantage that the dependences between the companies are continuously changing. Companies start competing on new markets or discontinue their activities in a given domain. Many approaches have been proposed in the past to reduce the noise [70, 71].

We use the power mapping method introduced by Guhr *et al.* [82] to reduce the noise in a correlation matrix. Power mapping can only be applied directly to correlation matrices, because the diagonal of the matrix must contain ones as elements. This poses no problem, if we recall the relation $\Sigma = \sigma C \sigma$ with

$\sigma = \mathrm{diag}(\sigma_1, \ldots, \sigma_K)$. We can convert a covariance matrix Σ to a correlation matrix

$$C_{kl} = \frac{\Sigma_{kl}}{\sigma_k \sigma_l} \tag{2.24}$$

by dividing each element by its respective volatilities σ_k and σ_l.

To calculate the power mapped correlation matrix $C^{(q)}$, we apply

$$C_{kl}^{(q)} = \mathrm{sign}(C_{kl}) \, |C_{kl}|^q \tag{2.25}$$

to each element of the correlation matrix C. From this definition we immediately see why it must be a correlation matrix. The correlation for a stock with itself, *i.e.*, the diagonal elements, is only preserved in the case of a correlation matrix. Power mapping has one parameter q, which in principle depends on the length of the time series from which the correlation matrix is calculated. Therefore, the choice of the parameter depends on the degree of noise. However, power mapping is a robust method with regard to the parameter q and yields good results for a wide variety of q values around the optimal one [83]. We use $q = 1.5$ during this study.

2.3.4 Volatility forecast

Equation (2.24) shows a possibility to swap the original volatilities σ with volatilities $\sigma^{(n)}$ estimated from other methods. The covariance matrix $\Sigma^{(n)}$ includes the new volatilities if we apply

$$\Sigma_{kl}^{(n)} = \frac{\Sigma_{kl}}{\sigma_k \sigma_l} \sigma_k^{(n)} \sigma_l^{(n)} \tag{2.26}$$

to each element. For the original volatilities we use the standard deviations estimated on the time horizon $T = 100$ trading days in the case of the sample covariance matrix. For the two covariance models we take the volatilities from the model, see equation (2.14) and (2.19), respectively.

A vast collection of volatility forecast methods exists in the literature, a review is given in reference [100]. We study two common methods for volatility forecasting. First, we use the original returns to calculate the volatilities on a shorter moving time horizon $T_{\mathrm{vol}} = 14$ trading days. This assumes that the average over this short time horizon of the past three weeks is a superior predictor for the future volatilities compared to the full time horizon of 100 trading days. Second, the volatility for the next trading day can be predicted from the GARCH process presented in section 2.3.1, see equation (2.20).

2.4 The data set

The Euro Stoxx 50 index includes 50 large companies from the eurozone. The companies can be classified into eight industrial branches, see table 2.1. This information is used to build the W_{b} weighting matrix for the spatial dependence model. A requirement of the spatial dependence model is that each group consists of at least two members. Single stock groups cause singularities. Therefore, we group companies from Belgium, Netherlands and Luxembourg into the Benelux group, see table 2.2. In addition, we have to place Nokia from Finland and CRH from Ireland into the "others" group. We have to omit GDF Suez from the stock selection, because the available data is incomplete due to a merger in 2008. The data spans a time horizon of 11 years from January 2001 to December 2011. However, the actual covariance estimation is performed on a smaller time horizon from May 2005 to December 2011. The first four years ($\sim$ 1000 trading days) are needed to calculate the GARCH fit.

We calculate the logarithmic returns from the adjusted close prices of the 49 stocks. The data set is taken from Thomson Reuters Datastream.

Industrial sector	Stock
Automobile	BMW, Daimler, VW
Basic industry	Arcelor Mittal, CRH, Saint-Gobain, Vinci
Consumer electronics	Nokia, Philips, SAP, Schneider, Siemens
Consumer Retail	Anheuser Busch, Carrefour, Danone, Inditex, L'Oreal, LVMH, Unilever
Energy	E.ON, ENEL, ENI, Iberdrola, RWE, Repsol, Total
Finance	AXA, Allianz, BNP, Banco Bilbao, Banco Santander, Deutsche Bank, Deutsche Börse, Generali, ING, Intesa, Münchener Rück, Société Générale, Unicredit, Unibail-rodamco
Pharma and chemicals	Air Liquide, BASF, Bayer, Sanofi
Telecom and media	Deutsche Telekom, France Telecom, Telecom Italia, Telefonica, Vivendi

Table 2.1: The Euro Stoxx 50 stocks by their industrial sector.

2.5 Portfolio optimization

We use the Markowitz portfolio optimization [65, 72, 101] to benchmark the effectiveness of the covariance estimation methods from section 2.2 and refinements from section 2.3. Based on each covariance matrix we perform a portfolio optimization to determine the minimum variance portfolio. This is

Industrial sector	Geographical region
Benelux	Arcelor Mittal, Philips, Anheuser Busch, Unilever, ING
Germany	BMW, Daimler, VW, SAP, Siemens, E.ON, RWE, Allianz, Deutsche Bank, Deutsche Börse, Münchener Rück, BASF, Bayer, Deutsche Telekom
France	Saint-Gobain, Vinci, Schneider, Carrefour, Danone, L'Oreal, LVMH, Total, AXA, BNP, Société Générale, Unibail-rodamco, Air Liquide, Sanofi, France Telecom ,Vivendi
Italy	ENEL, ENI, Generali, Intesa, Unicredit, Telecom Italia
Spain	Inditex, Iberdrola, Repsol, Banco Bilbao, Banco Santander
Others	CRH, Nokia

Table 2.2: The Euro Stoxx 50 stocks by their geographical region.

done on a moving window of $T = 100$ trading days over the time period from January 2001 to May 2012. The predicted portfolio variance

$$\hat{\sigma}^2 = \left(\tau' \Sigma^{-1} \tau\right)^{-1} . \tag{2.27}$$

can then be compared to the realized out-of-sample portfolio variance. The vector τ contains ones in all elements.

The predicted portfolio variances are then used to calculate a Gaussian Value at Risk (VaR) for a given α-quantile u_α

$$\widehat{\mathrm{VaR}}_\alpha = u_\alpha \sqrt{\hat{\sigma}^2} . \tag{2.28}$$

The VaR is evaluated for each day and then compared to the out-of-sample realized portfolio returns.

2.6 Results

We study the results under three aspects. In section 2.6.1 we study how the estimation of parameters is influenced by the non-stationarity of financial time series. The effect on portfolio variances and the VaR forecast is discussed in section 2.6.2 and section 2.6.3, respectively.

2.6.1 Non-stationarity in the parameter estimation

The spatial dependence and one factor model require the estimation of model dependent parameters. In the case of the spatial dependence model the three spatial parameters have to be estimated. For the one-factor model only one

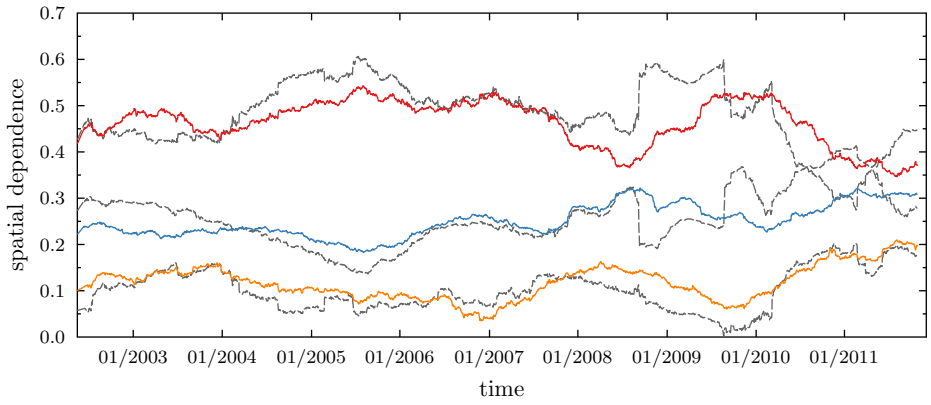

(a) Local normalization

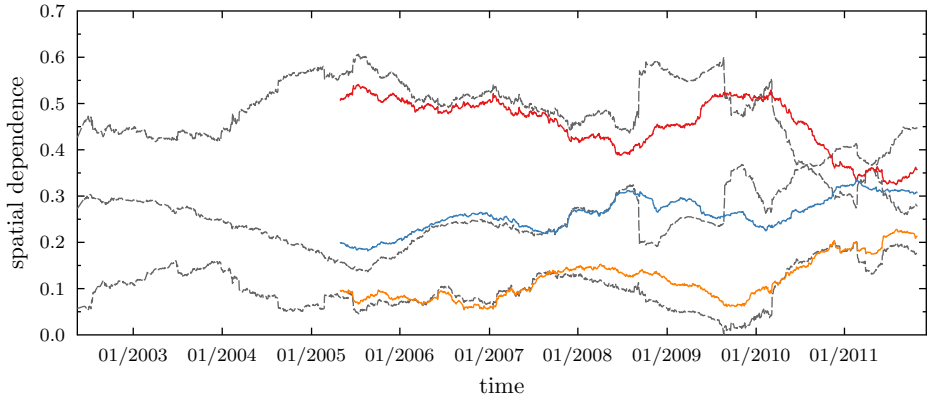

(b) GARCH residuals

Figure 2.2: The parameters ρ_{g}, ρ_{b} and ρ_{l} are shown from top to bottom estimated at each trading day for an interval of 250 days. The solid lines are with local normalization applied to the returns (top) and GARCH residuals (bottom), while the dotted lines are estimated from the unaltered returns.

parameter per stock needs to be estimated to describe the dependence on the market factor. Here, we study to which degree the non-stationarity, especially of the volatilities, influences the estimation of these parameters. Figure 2.2 shows the influence of local normalization and GARCH residuals on the parameter estimation for the spatial dependence model. The parameters are

estimated for a moving time window of $T = 250$ days. The figures show the time evolution of the spatial parameters ρ_{g}, ρ_{b} and ρ_{l} from top to bottom. The dashed black lines are from the estimation without applying local normalization or use of GARCH residuals as returns. We can clearly identify a sudden jump in the spatial parameters ρ_{g} and ρ_{b} during the financial crisis in 2008. During this time frame a stark rise in volatilities occurred. The plateaus observed have a width of 250 trading days, which underlines that it is an estimation artifact. Using locally normalized return time series the artifacts vanish. The same applies to the GARCH residuals. However, we can only show the spatial parameters starting from May 2005, because 1000 trading days are needed for the GARCH fit to converge. We note that local normalization and GARCH residuals are capable of improving the estimation of model parameters. In practice, local normalization has clear advantages over the GARCH residuals: it requires only a short period of historical data (13 days vs. 1000 days), is much faster to calculate and poses no convergence problems.

2.6.2 Portfolio variances

We examine the impact of each individual refinement method, see section 2.3, on the realized portfolio variances in the first part of this section. In the second part, we discuss how combinations of the methods affect the portfolio risk. The realized portfolio variances are given in table 2.3. The table is structured as follows: The second column states which returns were used. We can use the original returns, the GARCH residuals or the locally normalized returns. The volatility forecast method is specified in the third column. The fourth column indicates whether or not power mapping was used to suppress the estimation noise. The last three columns show the results of the realized portfolio variances for the spatial dependence model, the one-factor model and the sample covariance matrix.

Taking the GARCH residuals (row 2) instead of the returns or applying local normalization (row 3) to the return time series has almost identical effects on all three models. In the case of the spatial model this comes with no surprise after the discussion of the spatial parameters in section 2.6.1. Both methods lead to similarly improved estimations of the spatial parameters. The portfolio variances are improved for the spatial model, but get much worse for the one-factor model. A significant effect on the sample covariance matrix is not observable. Power mapping greatly improves the sample covariance matrix as expected and decreases the variance to one of the lowest. The one-factor model shows a slightly lower portfolio variance, while the spatial dependence model gets marginally worse. However, the one-factor model yields a quite impressive portfolio variance right from the start (row 1). Last but not least, the predicted volatilities from the GARCH process (row 7) are able to substantially reduce

	returns	volatility forecast	power mapping	realized portfolio variances sdep	1-factor	sample
1	original	hist	no	0.000241	0.000093	0.000121
2	GARCH	hist	no	0.000171	0.000171	0.000115
3	normalized	hist	no	0.000172	0.000148	0.000127
4	original	hist	yes	0.000256	0.000087	0.000086
5	GARCH	hist	yes	0.000133	0.000207	0.000086
6	normalized	hist	yes	0.000135	0.000190	0.000093
7	original	GARCH	no	0.000100	0.000087	0.000126
8	GARCH	GARCH	no	0.000087	0.000142	0.000119
9	normalized	GARCH	no	0.000087	0.000121	0.000132
10	original	GARCH	yes	0.000097	0.000086	0.000098
11	GARCH	GARCH	yes	0.000084	0.000160	0.000095
12	normalized	GARCH	yes	0.000084	0.000143	0.000101
13	original	hist†	no	0.000101	0.000086	0.000116
14	GARCH	hist†	no	0.000091	0.000138	0.000119
15	normalized	hist†	no	0.000088	0.000119	0.000120
16	original	hist†	yes	0.000099	0.000084	0.000092
17	GARCH	hist†	yes	0.000085	0.000156	0.000093
18	normalized	hist†	yes	0.000086	0.000139	0.000097

Table 2.3: Realized portfolio variances

the portfolio variance of the spatial model. There is a slightly positive effect for the one-factor model and a tiny negative impact on the sample covariance matrix.

Next, we take a deeper look at what happens if methods are used together. This can further decrease the portfolio variance. Using the GARCH predicted volatilities with GARCH residuals or local normalization(row 8,12 and 9,11) has a big effect on the spatial model. Combing these two methods catapults the spatial dependence model to the region of a power mapped sample covariance matrix. The results of the one-factor model get much worse and the sample covariance matrix yields only smaller variances if power mapping is applied (row 11,12). However, power mapping shows only a neglectable effect for the spatial dependence model.

The one-factor model works best in combination with the original returns (row 10, 13) and other refinements. In every other case GARCH residuals or local normalization have a negative effect on the one-factor model. The spatial dependence model substantially benefits from improved volatility forecasting (row 8-12 and 14-18) methods in combination with local normalization or GARCH residuals. However, the largest improvement stems from the better forecasting (row 7, 13). Local normalization or the GARCH residuals improve

the spatial dependence model (row 5,6), but not to the same extent as a better volatility forecast (row 7-12 and 13-18).

Using a short time horizon to predict the volatilities has a comparable effect to GARCH predicted volatilities (row 13-18 and 7-12). Importantly, it shows that local normalization with a short forecasting window for the volatilities can match the results of GARCH residuals and predicted volatilities (row 12, 18). However, local normalization and the short forecasting window require a roughly seventy times smaller window of historic data.

	returns	volatility forecast	power mapping	$\frac{\text{realized}-\text{predicted}}{\text{predicted}}$ in % sdep	1-factor	sample
1	original	hist	no	57	203	426
2	GARCH	hist	no	64	45	362
3	normalized	hist	no	73	53	397
4	original	hist	yes	80	195	180
5	GARCH	hist	yes	32	206	174
6	normalized	hist	yes	39	234	184
7	original	GARCH	no	137	256	581
8	GARCH	GARCH	no	141	847	515
9	normalized	GARCH	no	144	452	564
10	original	GARCH	yes	108	260	283
11	GARCH	GARCH	yes	119	1330	267
12	normalized	GARCH	yes	121	755	276
13	original	hist†	no	323	401	903
14	GARCH	hist†	no	297	953	877
15	normalized	hist†	no	233	480	727
16	original	hist†	yes	186	319	353
17	normalized	hist†	yes	187	765	359
18	GARCH	hist†	yes	183	1345	350

Table 2.4: Relative predicted portfolio variances in percent

After the evaluation of 18 combinations of refinements with regard to their effect on the realized portfolio variances we can conclude that the spatial dependence model gains the most from methods that improve the volatility forecasting, *i.e.*, GARCH predicted volatilities and or local normalization with short term predicted volatilities. The one-factor model yields low realized variances from the start and degrades massively if not used with the original returns. It shows a slight improvement if used with power mapping. For the sample covariance matrix it seems that power mapping is sufficient to realize the lowest variances.

Table 2.4 shows the relative predicted portfolio variances in percent. The sample covariance matrix alone is quite bad to predict the portfolio variances.

Power mapping greatly improves the prediction. On average the one-factor has the worst prediction capabilities. In most cases the spatial dependence model is the best predictor for the realized portfolio variances.

2.6.3 VaR forecast

Figure 2.3 shows the probability that the realized portfolio return $\hat{G}$ is smaller than the Value at Risk forecast $\widehat{\mathrm{VaR}}_\alpha$. We determine the $\widehat{\mathrm{VaR}}_\alpha$ forecast as stated in Equation (2.28) for $\alpha \in (0, 0.5]$ at each trading day. The probability $P(\hat{G} < \widehat{\mathrm{VaR}}_\alpha)$ is the average over all trading days. For a perfect prediction the probability $P(\hat{G} < \widehat{\mathrm{VaR}}_\alpha)$ is equal to α, which is indicated by a straight line.

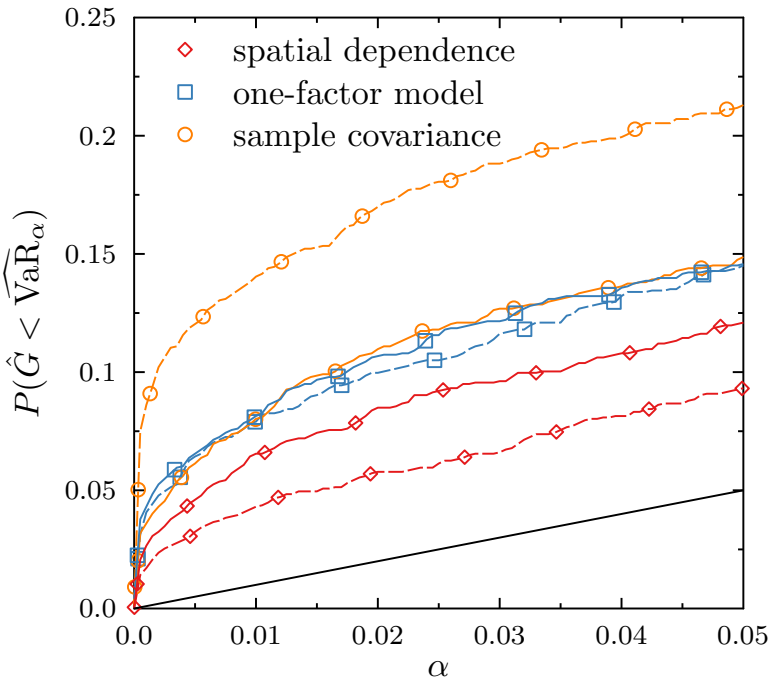

Figure 2.3: The probability of a portfolio return being smaller than the Value at Risk given a fixed probability of α. The dashed lines show the results without any refinements for the spatial dependence model (diamond), the one-factor model (square) and the sample covariance matrix (circle). The solid lines show the effect of improved covariance estimation methods (see text for details).

We only present one combination of refinements per model and do not show results for each row in table 2.3 to keep the presentation clear. For each model we select the set of refinements where the realized portfolio variances are lowest

and the prediction error is smallest. For the spatial dependence model (diamond) we present the VaR forecast with GARCH residuals, GARCH-predicted volatilities and applied power mapping. The one-factor model (squares) uses a combination of original returns, historic volatilities and power mapping, while the sample covariance matrix (circle) uses GARCH residuals instead, historic volatilities and power mapping. The dashed lines show the original models without any refinements while the solid lines show the refined cases.

The spatial dependence model yields the best VaR forecast in the period studied without any refinements applied. The sample covariance matrix gives the worst VaR forecast and the one-factor model lies in between. In the case of the spatial model using the refined methods decreases the VaR forecast capabilities. The reason for this behavior is the vast improvement in the realized portfolio variances. The one-factor model shows a non significant increase for the worse. On the other hand, the sample covariance matrix gains better realized variances by applying power mapping and using GARCH residuals but also improves the VaR forecast capabilities. Either way, the sample covariance matrix and the one-factor model are not able to match the VaR forecast capabilities of the spatial dependence model.

2.7 Conclusion

We evaluated three approaches to estimate the covariance matrix of return time series. First, the sample covariance matrix requires the estimation of $K(K+1)/2$ parameters. Second, a simple one-factor model, with $2K+1$ parameters. Third, the spatial dependence model tries to capture the global, branch and geographical dependences with a reduced set of $K+3$ parameters. To determine the goodness of the covariance estimation we perform a Markowitz portfolio optimization and carefully examine the out-of-sample realized portfolio variances and prediction errors. Furthermore, we studied five methods to refine the three approaches. The GARCH residuals and local normalization are able to address the non-stationary volatilities in the return time series. This is especially visible in the spatial parameters, where artifacts which are introduced by the fluctuating volatilities vanish.

The future volatilities for the individual stocks are better predicted by estimating them on a short-term historical time horizon. The reason lies in the slowly decaying autocorrelation of empirical volatilities [62]. Equally powerful are the GARCH predicted volatilities with the *caveat* of non-converging GARCH fits on time intervals smaller than 1000 trading days.

The sample covariance matrix shows a significant amount of noise if the time horizon for the estimation is short compared to the number of parameters, *i.e.*, $K(K+1)/2$. Noise reduction methods, such as power mapping, can effectively reduce such measurement errors.

The spatial dependence model is able to capture the correlation between as-

sets very well. Therefore, noise reduction techniques have no significant impact on the realized portfolio variances. However, the model has severe problems to correctly predict future volatilities. This problem can be eradicated by implementing better forecast methods for the volatilities. The realized portfolio variances can be reduced to the level of competing models by using better methods for volatility forecasting and locally normalized returns for the regression. The one-factor model yields low realized portfolio variances out of the box. It should only be used with the original returns and gets worse with GARCH residuals or locally normalized returns. Improvements from better volatility forecast methods or noise reduction are very small. With applied noise reduction the sample covariance matrix has no need to hide behind other models and can match their results.

With the right choice of refinements all three approaches are capable of producing equally good realized portfolio variances, though the spatial dependence model provides the smallest prediction error for portfolio variances and VaR forecasts.

Chapter 3

Uncovering temporal dependencies in financial time series

3.1 Introduction

We have seen the effects of non-stationarity for portfolio optimization in chapter 2. Financial time series display several non-trivial properties. As discussed in section 1.7 the analysis of financial time series revolves around the returns. The univariate distribution of returns for single stocks shows non-normality, *i.e.*, the tails of the distribution are much heavier than the tails of a normal distribution [19, 37, 38]. The empirical observation dates back to 1915 [36]. The heavier tails in principle can be modeled by a random walk if we draw the random numbers for the stochastic part from a distribution which has heavy tails. However, choosing an arbitrary distribution with heavy tails is unsatisfactory as it does not extend the underlying understanding. Stochastic volatility models address this problem by combining the normal distribution with a distribution for the variances. The resulting distribution of returns then exhibits non-normality [39, 102]. However, such an approach is not able to describe the non-stationarity of volatilities. Drawing the volatilities independently from a distribution does not replicate the empirically observed clustering of volatilities. To achieve this goal, returns and volatilities have to be modeled by a stochastic process. The ARCH process [90] started an endless stream of stochastic processes to model financial time series and their properties, *e.g.*, the glossary to ARCH lists over 50 different processes [103].

While it is fairly easy to write down a new stochastic process, it is far more complicated to correctly model all the features of empirical time series. The problem is to get an as accurate as possible description of the features for the empirical time series. Often the autocorrelation of the return time series is studied, which is essentially zero [104]. However, the autocorrelation of the absolute or squared returns is non-zero and slowly decays to zero for larger lags [62, 105, 106]. This effect arises due to the clustering of volatilities [19]. In high volatility phases the probability that a large (absolute) return is followed by another large return is higher than normal. The same holds true for phases of small volatility, where small returns are followed by small returns with higher probability. Another important observation is called the “leverage

effect", which states that returns and future volatilities are negatively correlated. The effect was first described by Black [60] in 1976 and attributed to the fact that stocks with falling prices are riskier and therefore have a higher volatility. The reduced market capitalization relative to the debt of the company makes it more leveraged, hence the name. This explanation is subject to controversial discussion [107–109]. The analysis of these effects typically focuses on the autocorrelation of return time series or cross correlations between returns and historical or implied volatilities.

In recent years, a growing interest evolved around advanced methods to analyze the temporal dependencies in time series with the help of periodograms, *i.e.*, the Fourier transform of the autocorrelation. However, the ordinary periodogram is not a good estimator for the spectrum and therefore improved estimators are required. Laplace periodograms, an extension to the ordinary periodogram, give an improved estimation and are used to study heart rate variability [110] in the frequency domain. The application of quantile regression [111] allows new quantile-based periodograms, which are for example used to investigate sun spot time series [112].

It is our aim to show that the quantile-based correlation of filtered time series [113, 114] in the time domain is a much more powerful tool to study financial time series and to uncover differences to stochastic processes. In section 3.2 we explain how the quantile-based correlation is calculated. Then we carry out an empirical study on intraday data on stocks taken from the Standard & Poor's 500 index (S&P 500) during the years 2007 and 2008 in section 3.3.1. We show the capabilities to uncover differences between empirical data and stochastic processes in section 3.3.2 for three important GARCH-type processes, the original GARCH [88], EGARCH [115] and GJR-GARCH [116] processes. The results presented in this chapter are available as a working paper [6].

3.2 Quantile-based correlation

We calculate the quantile-based correlation for a time series $x = (x_1, x_2, \ldots, x_T)$ of length T in the following way. Let $\alpha \in (0,1)$ and $\beta \in (0,1)$ be probability levels and q_α the value at the α-quantile for the time series x. We map the time series x to a filtered time series $\xi^{(\alpha)}$ as specified by the filter rule

$$\xi_t^{(\alpha)} = \begin{cases} 1 & , \quad x_t \leq q_\alpha \\ 0 & , \quad \text{otherwise} \end{cases} \quad . \tag{3.1}$$

Suppose as an example the time series

$$x = (1, -5, 10, 0, -6, -2, -2, 2, 0, 2) \quad . \tag{3.2}$$

The filtered time series for the 0.5-quantile is then

$$\xi^{(0.5)} = (0, 1, 0, 1, 1, 1, 1, 0, 1, 0) \quad . \tag{3.3}$$

For this time series, $q_{0.5}$ is zero. In exactly the same way, we set up an additional filtered time series $\xi^{(\beta)}$ for a second β-quantile. From the filtered time series $\xi^{(\alpha)}$ and $\xi^{(\beta)}$, we calculate the lagged cross-correlation for each lag $l \in (-T/2, T/2)$

$$\mathrm{qcf}_l(\xi^{(\alpha)}, \xi^{(\beta)}) = \frac{1}{T} \sum_{t=1}^{T-l} \frac{(\xi_t^{(\alpha)} - \bar{\xi}^{(\alpha)})(\xi_{t+l}^{(\beta)} - \bar{\xi}^{(\beta)})}{\sigma^{(\alpha)}\sigma^{(\beta)}} \tag{3.4}$$

where $\bar{\xi}^{(\alpha)}$ is the mean value of the filtered time series $\xi^{(\alpha)}$. We denote the according standard deviation of the filtered time series by $\sigma^{(\alpha)}$. The general idea to study filtered binary time series of a time series was first discussed in the literature by Kedem [113]. Dette *et al.* [114] extend this to correlating filtered time series of different quantiles and provide an estimator for the quantile-based correlation in the frequency domain using a quantile regression approach.

By its construction the quantile correlation function yields the autocorrelation of the filtered time series for equal probabilities $\alpha = \beta$, compare equation (3.4). Therefore, the quantile correlation function inherits the properties of the autocorrelation for equal probabilities and is symmetric around lag zero, *i.e.*, $\mathrm{qcf}_l(\xi^{(\alpha)}, \xi^{(\alpha)}) = \mathrm{qcf}_{-l}(\xi^{(\alpha)}, \xi^{(\alpha)})$. For different probabilities $\alpha \neq \beta$ the quantile correlation function is not necessarily symmetric.

In preparation for the empirical study we should discuss how to interpret different combinations of the probabilities α and β. From now on we denote the probabilities chosen for the quantile correlation function with (α, β). We start with the $(0.05, 0.05)$ quantiles. In this case both filtered time series will each contain 5% ones. These ones correspond to the smallest 5% of values in the time series x, compare equation (3.1). As a result, we are only correlating the smallest values of the time series, see equation (3.4). On the other hand, let us take a look at the $(0.95, 0.95)$ quantiles. In this scenario, we are correlating the smallest 95% of the values of the time series x. Typically, it is more interesting to know how the largest 5% of values of the time series are correlated and in fact the $(0.95, 0.95)$ quantiles also include this information. If we exchange the less-than or equal to sign in equation (3.1) for both filtered time series $\xi^{(\alpha)}$ and $\xi^{(\beta)}$ we immediately see that we receive the complement of the filtered time series, *i.e.*, ones become zeroes and zeroes become ones. Readers with a background in computer science will notice that this is equivalent to a binary NOT operation on each filtered time series. This operation does not change the sign of the quantile correlation function as long as it is performed on both time series, see equation (3.4).

The next logical step is the interesting case where we want to figure out how the smallest 5% values are correlated to the largest 5%. We select the $(0.05, 0.95)$ quantiles and effectively correlate the smallest 5% of the values with the smallest 95%. The solution to the question is to alter the lesser-than or equal to sign only for the second filtered time series $\xi^{(0.95)}$. The sign of the quantile-correlation function will change. Imagine we observe a negative correlation for the $(0.05, 0.95)$ quantiles. This means that the smallest 5% and 95% of the time series are negatively correlated. At the same time it implies that the smallest 5% and the largest 5% of the time series are positively correlated. To keep the notation simple, we will always calculate the filtered time series according to equation (3.1) and mention how to interpret the quantile correlation function in the given context.

We provide 95% confidence intervals (red, dotted) for the quantile correlation functions. Multiplying the standard deviation of the fluctuations of the $(0.5, 0.5)$ quantiles around zero with the standard score 1.96 corresponding to a 0.95 probability yields the confidence band. Here, we do not use the standard approach for cross-correlation confidence bands, *i.e.*, 1.96 divided by the square root of the sample size, because the elements of the financial time series are clearly not independent and identically distributed (*i.i.d*).

3.3 Empirical study

We carry out an empirical study by examining intraday data from the New York Stock Exchange (NYSE) from 2007 and 2008, compare section 1.5 for a detailed description. The selection of stocks is limited to companies listed in the S&P 500 index. The S&P 500 index includes the largest corporations mostly in the USA. This ensures that the stocks are traded frequently enough to deliver meaningful statistics. The time resolution of the data is accurate to the second. We discard the first and last ten minutes of each trading day to make sure that the time series is the result of the continuous double auction order book trading, see section 1.4. We end up with a time series of 22200 seconds per day. If for a given second no price is available we use the last previous price instead for this second.

We prepare the NYSE data set as described in section 1.5 and take only days for a given stock into account where at least 800 trades have taken place. Otherwise we discard the day. The quantile-based correlation function is always calculated on the intraday time series of 22200 seconds. This is necessary because of the intraday gap that may arise between trading days. If new information, which is important to the price of the stock becomes available while the stock exchange is closed, the closing price of the previous day may significantly differ from the opening price of the next day. Trading stocks over the counter is possible the whole day and is not limited to the trading hours of a stock exchange. Therefore, the evolution of the price continues outside of

the trading hours. We average the quantile correlation function of all trading days, roughly 250, for each year. From the price time series $S_k(t)$ of each stock k, we calculate the return time series

$$r_k(t) = \frac{S_k(t + \Delta t) - S_k(t)}{S_k(t)} \tag{3.5}$$

for one-minute intervals $\Delta t = 60$s. We always calculate the quantile-based correlation function from the return times series.

3.3.1 Results for stock data

We show the quantile-based correlation for six different quantile pairs (α, β). The quantile-based correlation function for Abercrombie & Fitch Co. (ANF) is depicted in figure 3.1. The $(0.05, 0.05)$ quantiles correlate only the largest

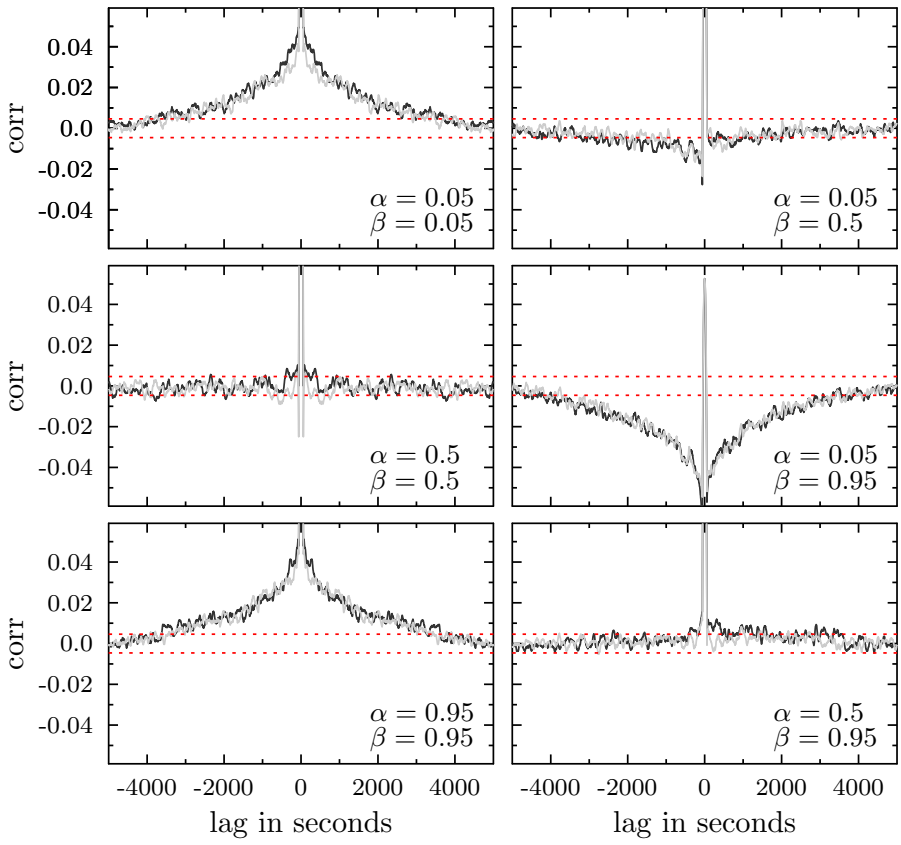

Figure 3.1: Quantile correlation function for Abercrombie & Fitch Co. (ANF) for 2007 (black) and 2008 (grey).

negative returns, while the $(0.95, 0.95)$ quantiles indirectly correlate the largest positive returns. We bring to mind the discussion in the previous section 3.2. In theory, the $(0.95, 0.95)$ quantiles give the correlation of the 95% of the smallest returns in the time series according to equation (3.1). This is equivalent to saying that it provides the correlation of the largest 5% of returns. We can switch both lesser-than signs in equation (3.1) to greater signs and the quantile correlation function will not change as long as the change is performed for both signs. We observe a non-zero correlation which decays to zero on a time scale of one hour.

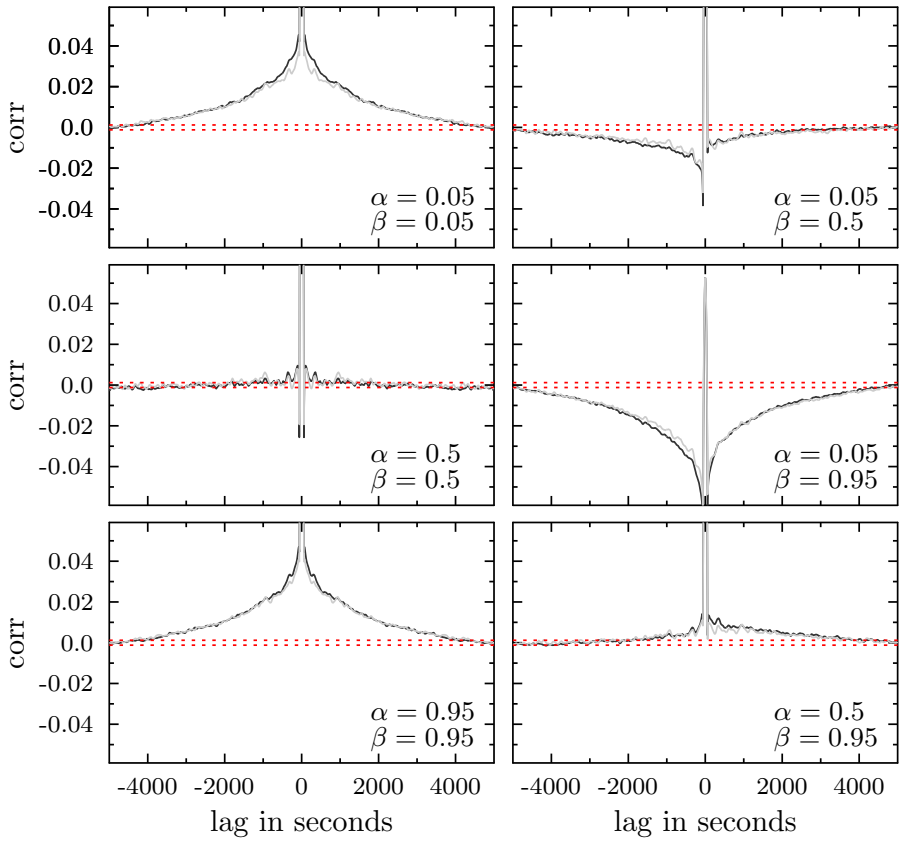

Figure 3.2: Average quantile correlation function for 479 and 488 stocks from the S&P 500 index for 2007 (black) and 2008 (grey).

We notice that in comparison to the usually used autocorrelation of absolute or squared returns the absolute values of the quantile-based correlation are smaller. The reason lies in the filtered time series which only contain zeroes and ones. Hence, the absolute value of the correlation is smaller, because the amount of information is reduced compared to the original time series.

The $(0.5, 0.5)$ quantiles uncover the correlation of the sign of the returns. Strictly speaking this is only the case if the distribution of returns has zero mean and is symmetric. This case corresponds to the autocorrelation of the return time series which is zero. We observe that the quantile correlation function fluctuates within the confidence bands, *i.e.*, there is no significant correlation. However, we notice that the quantile correlation does not fluctuate precisely around zero. The reason lies in the slight asymmetry of the empirical return distribution. For stochastic processes which yield a symmetric return distribution we find that the quantile correlation fluctuates exactly around zero in section 3.3.2.

If the probabilities for the quantiles are chosen equally, *i.e.*, $\alpha = \beta$, the quantile-based correlation functions must be symmetric for positive and negative lags, because it is the autocorrelation of the filtered time series.

Figure	Dataset	Year	ΔA
3.1	ANF	2007	8%
3.1	ANF	2008	5%
3.2	S&P 500	2008	11%
3.2	S&P 500	2008	5%
3.4	INDEX	2007	19%
3.4	INDEX	2008	6%
3.7	GJR-GARCH	2007	7%
3.7	GJR-GARCH	2008	1%
3.8	GJR-GARCH	2007	4%
3.8	GJR-GARCH	2008	1%

Table 3.1: Normalized difference ΔA of the area under the curve for the $(0.05, 0.95)$ quantiles.

In contrast, we observe salient asymmetries if we choose different quantiles, *i.e.*, $\alpha \neq \beta$. Given a quick look the asymmetry in the $(0.05, 0.95)$ quantiles may pass unnoticed due to the small size of the individual figures. However, a closer inspection reveals that the area under the curve is smaller for positive lags. To provide a quantitative measure we calculate the normalized difference

$$\Delta A = \frac{A_- - A_+}{A_- + A_+} \tag{3.6}$$

between the areas under the curve for negative and positive lags, where $A_\pm$ is

$$A_\pm = \sum_{l=\pm 1}^{\pm T/2} |\mathrm{qcf}_l(0.05, 0.95)| \quad . \tag{3.7}$$

The measure runs from minus one to plus one. For minus one the whole area

lies on the positive lag side and for plus one on the negative lag side. If the area is distributed equally to the negative and positive lags the measure yields zero. The normalized differences are listed in table 3.1. We find that the area under the curve for the negative wing of the quantile correlation function is 8% (2007) and 5% (2008) larger compared to the positive side.

As we pointed out previously, we have to be cautious in the interpretation of the probabilities α and β. In figure 3.1 we see the correlation of the smallest 5% of returns with the smallest 95% of returns and observe a negative correlation. More interesting is how the smallest and largest 5% of returns are correlated. Here, we have the first case where the sign of the quantile correlation plays a role. Talking about the largest 5% of returns in the time series implies that we have to change the lesser-than sign in equation (3.1) to a greater-than sign. So we observe a positive correlation if we talk about the smallest and largest returns, because the sign of the quantile correlation function changes. The positive correlation slowly decays to zero and is reminiscent of the volatility clustering observed for equal probabilities $\alpha = \beta$. However, the asymmetry between positive and negative lags shows the occurrence of the leverage effect.

The average quantile-based correlation function for all stocks from the S&P 500 index in the year 2007 (black) and 2008 (grey) is shown in figure 3.2. The general features remain the same compared to a single stock. The plots we have shown up to this point have the advantage of displaying the quantile-based correlation for the whole lag axis at the expense of only showing six quantile pairs. Another way of viewing the quantile correlation function is to calculate a probability-probability plot as shown in figure 3.3. This gives a more detailed view for all combinations of (α, β) pairs. However, it is limited to one lag per plot. We notice that the plot also contains the information for the according negative lag. If we swap the probability levels $(\alpha, \beta) \to (\beta, \alpha)$ in equation (3.4) the lag axis changes its sign $l \to -l$. The peaks for small $(0.05, 0.05)$ and large probabilities $(0.95, 0.95)$ are clearly visible and decay for larger lags. We also observe the asymmetries for probabilities $\alpha \neq \beta$ on the left and right hand side of the plot. Near the positive negative peaks at the edges of the plot we notice plateau-like areas.

In addition, we calculated a homogeneously weighted index from all stocks, see figure 3.4. We observe that the asymmetry for the $(0.05, 0.95)$ quantiles becomes more pronounced in comparison to the average over all stocks, compare table 3.1. This behavior can be attributed to the "correlation leverage effect" as studied in reference [117]. The authors find that the volatility of the index is comprised of the volatility of the single stocks and the average correlation between these stocks, which leads to a stronger leverage effect for indices. However, the absolute values of the quantile correlation are smaller compared to figure 3.2.

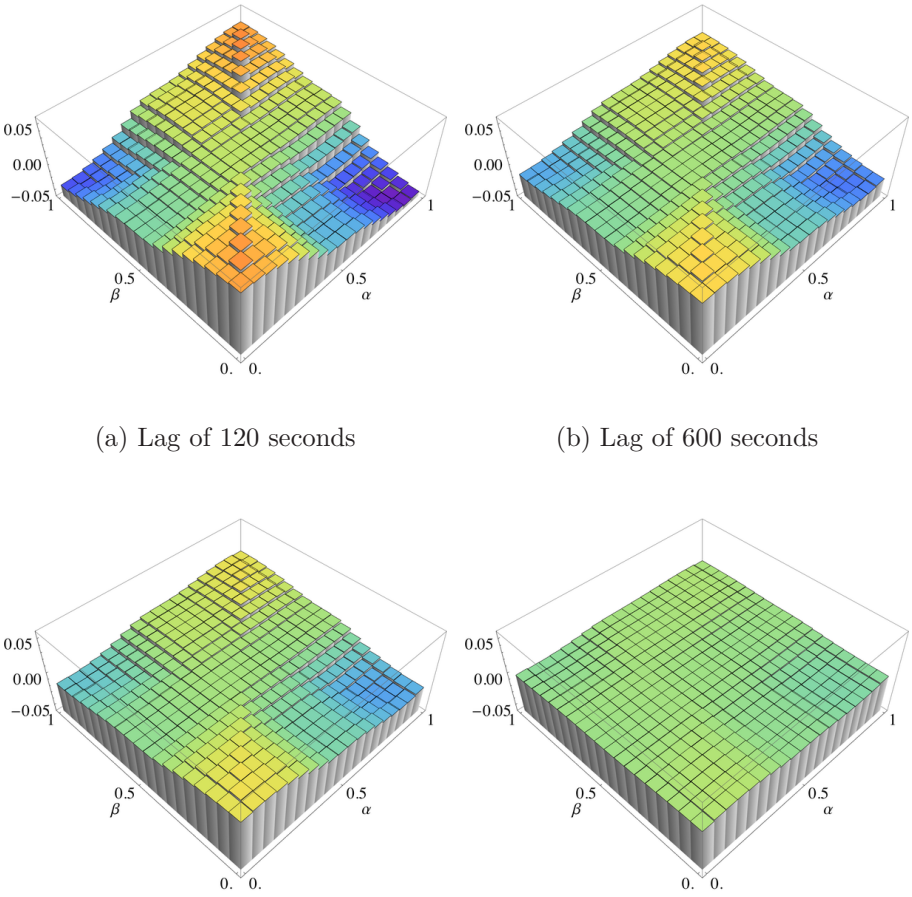

(a) Lag of 120 seconds

(b) Lag of 600 seconds

(c) Lag of 1200 seconds

(d) Lag of 3600 seconds

Figure 3.3: Average quantile correlation function for fixed lags calculated from the S&P 500 stocks in 2007 for four different lags.

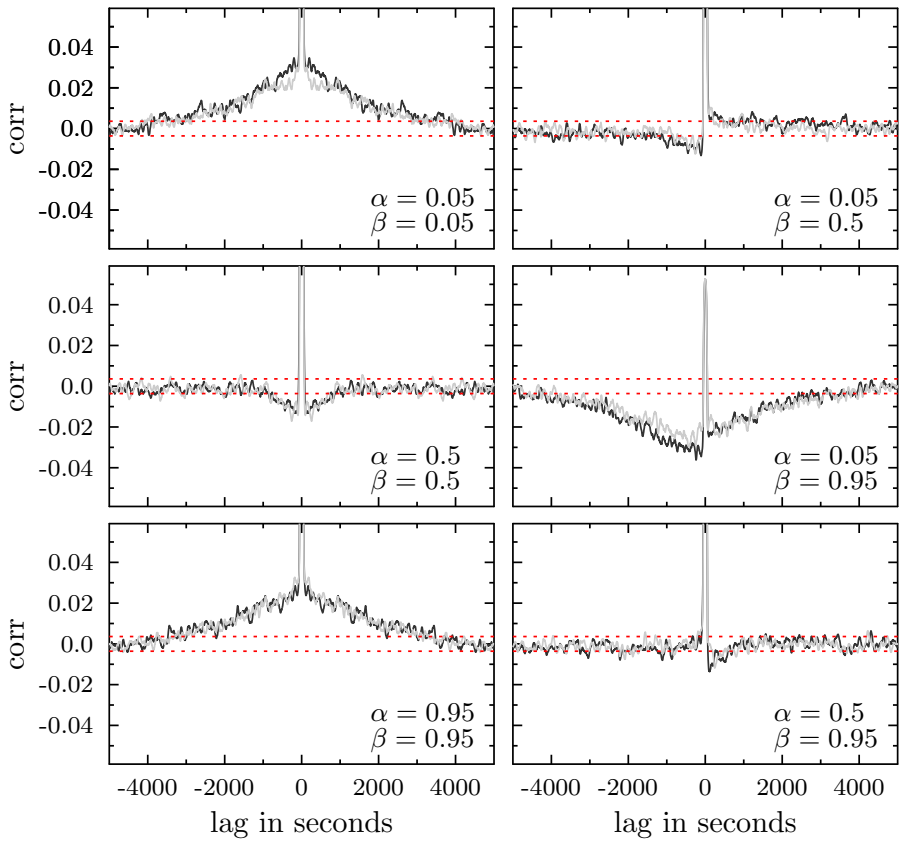

Figure 3.4: Quantile correlation function for an equally weighted index calculated from the S&P 500 stocks for 2007 (black) and 2008 (grey).

3.3.2 GARCH processes

We study the quantile correlation function for three exemplary processes of the GARCH family which are shown in figure 3.5. For the classic GARCH process see equation (2.20) in chapter 2. We continue to use the notation established for the GARCH process in the previous chapter and focus the discussion solely on the modelling of the time dependent variances $\sigma^2(t)$.

We study two extensions to the GARCH model which take the asymmetry into account. The exponential general autoregressive conditional heteroskedastic (EGARCH) model assumes that the logarithmic variances can be described by

$$\begin{aligned}\log\sigma^2(t) = \omega + \alpha_1(|\varepsilon(t-1)| - \langle|\varepsilon(t-1)|\rangle) \\ + \gamma_1\varepsilon(t-1) + \beta_1\log\sigma^2(t-1) \quad ,\end{aligned} \tag{3.8}$$

where ω, α_1 and β_1 are coefficients. We notice that for negative values of the asymmetry parameter γ_1 negative events have a larger impact on future volatilities than positive events. The Glosten-Jagannathan-Runkle GARCH (GJR-GARCH) model proposes to model the variances according to

$$\sigma^2(t) = \omega + \alpha_1 G^2(t-1) + \beta_1\sigma^2(t-1) + \gamma_1 G^2(t-1)I(t-1) \tag{3.9}$$

and with the indicator function

$$I(t-1) = \begin{cases} 0 & , \quad \text{if } G(t-1) \geq 0 \\ 1 & , \quad \text{if } G(t-1) < 0 \end{cases} \quad . \tag{3.10}$$

In all three cases we use GARCH processes of the order (1,1) and choose the same parameters for all processes as far as possible. We use $\omega = 0.00001$, $\alpha_1 = 0.05$ and $\beta_1 = 0.9$ for the GARCH coefficients and $\mu = 0.001$ for the drift. The asymmetry parameter is $\gamma_1 = -0.06$ and $\gamma_1 = 0.06$ for the EGARCH and GJR-GARCH, respectively. We choose these parameters to better work out the characteristic shape of the quantile correlation for different GARCH processes. For example the asymmetry parameter is chosen to be relatively large compared to empirically observed values to better see the asymmetries. We notice that we should only compare figure 3.5 to empirical results on a qualitative level. We will try different approaches to fit the GARCH model in the following sections. To keep the notation in agreement with the literature and the `rugarch` [118] R package we denote the GARCH parameters with α_1 and β_1 and do not confuse them with the probabilities for the (α, β) quantiles.

By design the classic GARCH process (grey) is symmetric. It comes as no surprise that we observe no significant asymmetries. We picked two common modifications to the classic GARCH, the EGARCH (black) and GJR-GARCH

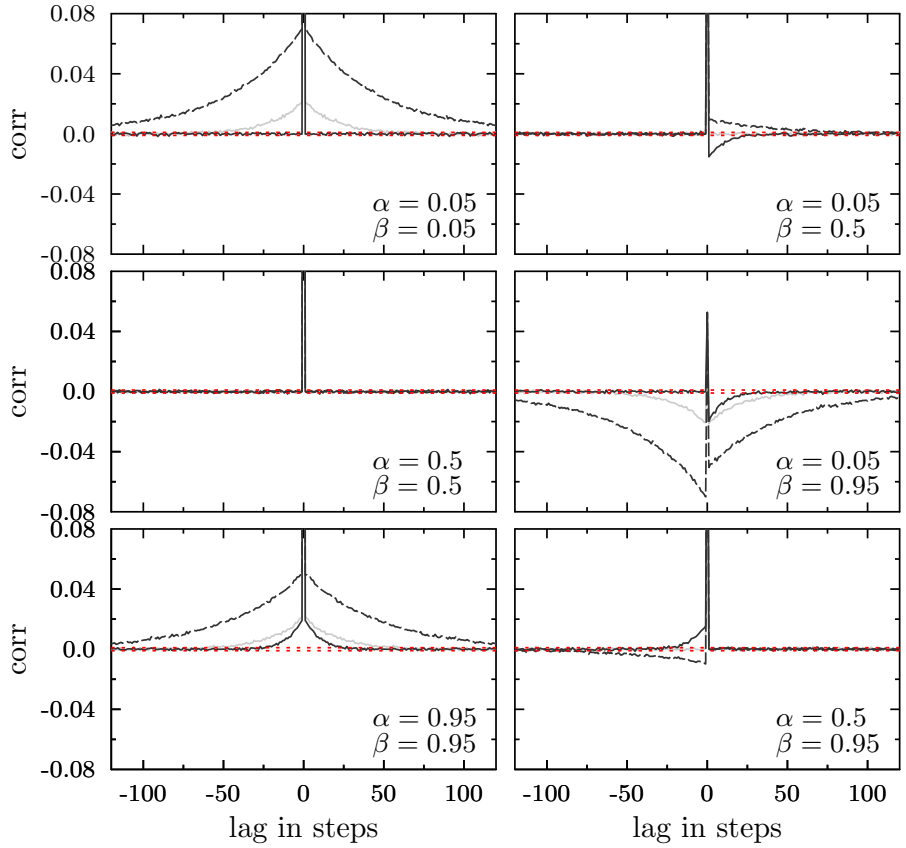

Figure 3.5: Quantile correlation function for three stochastic processes GARCH (grey), GJR-GARCH (dashed) and EGARCH (black).

(dashed), which are designed to model the empirically observed asymmetries. The degree of the asymmetry is controlled by an additional parameter γ_1.

For the EGARCH process we only observe a clustering of large positive returns and zero correlation for small negative returns. For the $(0.05, 0.95)$ quantiles only positive lags have a negative correlation, while negative lags do not show any correlation. The GJR-GARCH shows clustering of large negative and positive returns and asymmetric non-zero correlations for the $(0.05, 0.95)$ quantiles. This asymmetry is also observable in the absolute height of the quantile-based correlation function for the $(0.05, 0.05)$ and $(0.95, 0.95)$ quantiles.

For the three GARCH processes we observe that the quantile-based correlation of the $(0.5, 0.5)$ quantiles is indeed exactly the correlation of the return sign, because the innovations for the GARCH processes are drawn from a normal distribution. Therefore, the distribution of returns is symmetric and the

quantile-based correlation function is zero.

While the asymmetric GARCH processes indeed show asymmetric behavior in the correlation of very small and large returns the quantile correlation function uncovers some remarkable differences to empirical data. For the $(0.05, 0.5)$ and $(0.5, 0.95)$ the GJR-GARCH and EGARCH show only non-zero behavior for the positive or negative lags, respectively. In addition, the EGARCH only shows non-zero correlations for positive lags for the $(0.05, 0.95)$ quantiles.

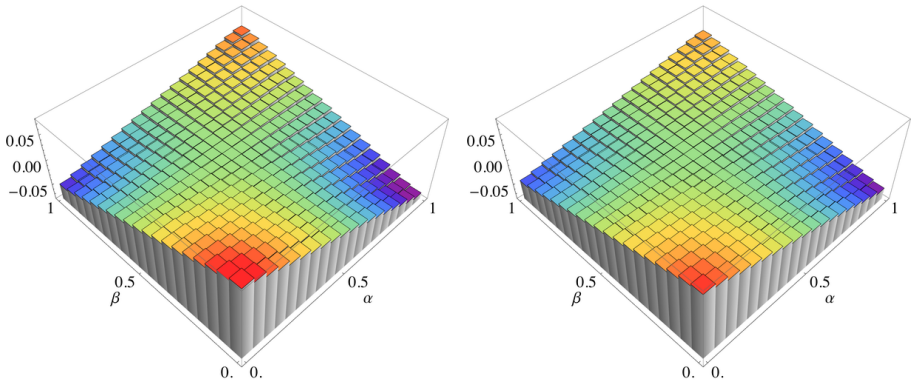

(a) GJR-GARCH, $l = 2$ steps

(b) GJR-GARCH, $l = 10$ steps

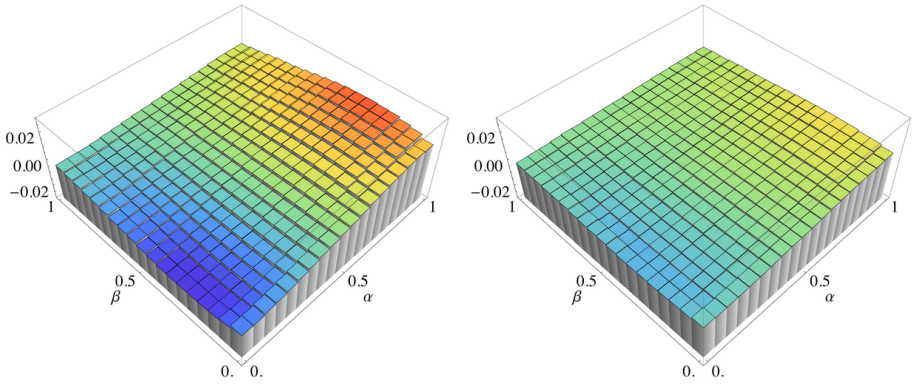

(c) EGARCH, $l = 2$ steps

(d) EGARCH, $l = 10$ steps

Figure 3.6: Quantile correlation function for fixed lags calculated for the GJR-GARCH and EGARCH processes shown in figure 3.5.

Figure 3.6 shows the probability-probability plot for the GJR-GARCH and EGARCH for fixed lags of two and ten steps. The overall shape of the plot for the GJR-GARCH resembles the empirical data. However, it looks much

smoother and ideal compared to the empirical data. Importantly, the more plateau-like structure we observed in figure 3.3 is not there. The asymmetry for the $(0.05, 0.95)$ probabilities for positive and negative lags is clearly visible. We recall that swapping the probabilities $(\alpha, \beta) \to (\beta, \alpha)$ inverts the lag axis.

The results for the EGARCH look strikingly different from the empirical data. We observe a non-zero correlation for positive lags around the $(0.05, 0.95)$ probabilities (right side of the plot) and for positive and negative lags around the $(0.95, 0.95)$ probabilities. There is no correlation for small returns around the $(0.05, 0.05$ probabilities and for the negative lag axis around the $(0.05, 0.95)$ probabilities (left side of the plot).

Fitting each individual day

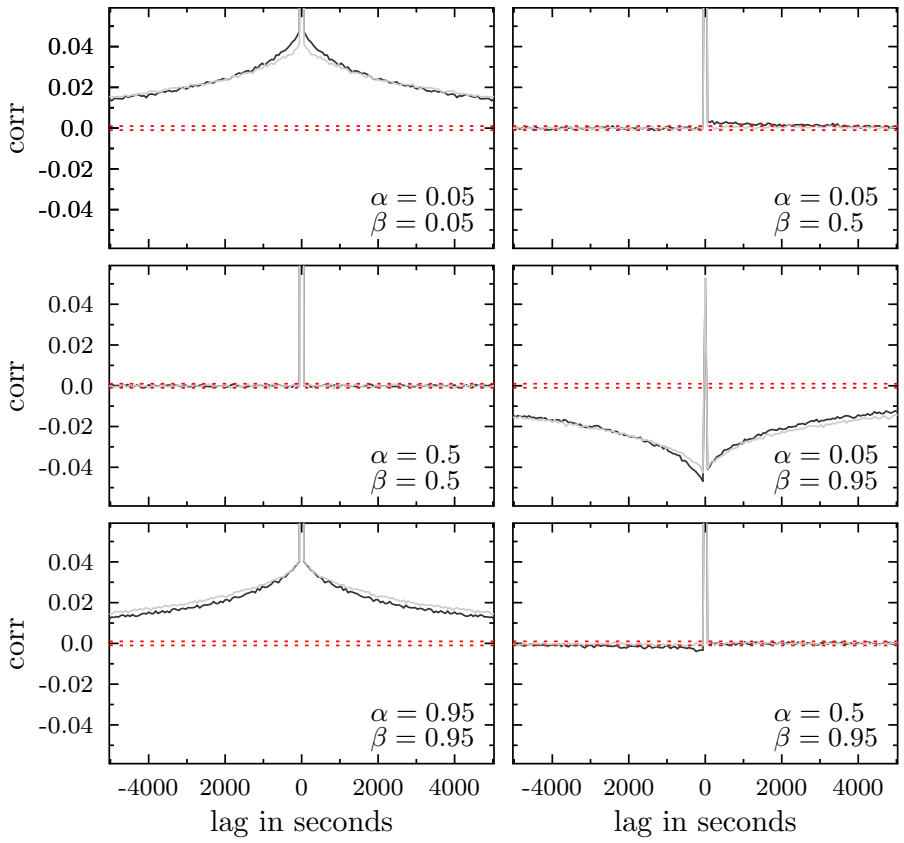

Figure 3.7: Quantile correlation function for GJR-GARCH fitted to each trading day of the equally weighted S&P 500 index for 2007 (black) and 2008 (grey).

We identified the GJR-GARCH to be the best candidate of the three processes to describe the empirical data in section 3.3.2. We use the equally weighted index of the S&P 500 stocks for 2007 and 2008 and fit the GJR-GARCH model to each individual trading day, *i.e.*, we receive 250 individual parameter sets $(\mu, \omega, \alpha_1, \beta_1, \gamma_1)$ for each year. We then use each parameter set to simulate a time series and calculate the quantile correlation function. The average for the years 2007 and 2008 is shown in figure 3.7. However, this approach does not create comparable results to the empirically observed quantile correlation function for the index, see figure 3.4. The quantile correlation function decays more slowly for the $(0.05, 0.05)$, $(0.95, 0.95)$ and $(0.05, 0.95)$ probabilities. The asymmetries are less striking for 2007, where the area under the curve only differs by 7% in contrast to 19% for the index and for 2008 it is neglectable (1%). Nonetheless, for the $(0.05, 0.5)$ and $(0.5, 0.95)$ probabilities the speed of the decay is comparable to the empirical data, but the qualitative shape of the quantile correlation function does not fit the empirical data.

Average parameters

Averaging over time series simulated from 250 individual parameter sets does not yield results which meet the empirical data. Therefore, we calculate a single set of parameters for each year by averaging the parameters obtained by the fit in the previous section. We then simulate 250 time series from this parameter set, calculate the quantile correlation function and average the result. For 2007 we find $\mu = -0.0008$, $\omega = 0.0009$, $\alpha_1 = 0.0527$, $\beta_1 = 0.8986$ and $\gamma_1 = 0.0218$. In 2008 we find $\mu = -0.0026$, $\omega = 0.0667$, $\alpha_1 = 0.0484$, $\beta_1 = 0.9191$ and $\gamma_1 = 0.0025$. For 2007, averaging the parameters yields, at least on an absolute scale, similar results to the empirical data. However, the same restrictions mentioned previously apply. The normalized difference between negative and positive lags is 4%, the asymmetry is clearly visible. For 2008 the averaging yields a ten times smaller asymmetry parameter γ_1 compared to 2007. We notice that the GARCH fit can result in positive and negative values for γ_1, which compensate each other to nearly zero. Thus, there is nearly no asymmetry observable for 2008.

Both approaches to fit the GJR-GARCH model to empirical intraday data yield no satisfying results.

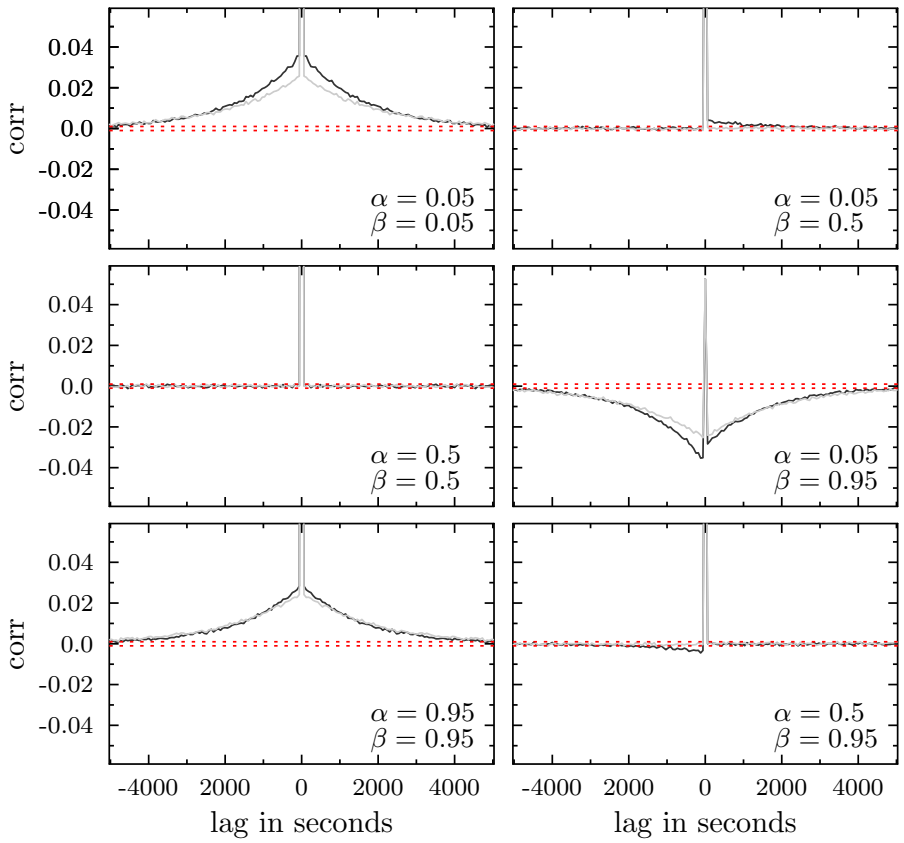

Figure 3.8: Quantile correlation function for the GJR-GARCH process simulated from an averaged set of parameters received from the equally weighted S&P 500 index for 2007 (black) and 2008 (grey).

3.4 Conclusion

The quantile correlation function is an excellent tool to study financial time series. It provides an extensive overview of the temporal dependencies within the time series. The information goes beyond what is provided by the autocorrelation of absolute or squared returns. The asymmetries in the positive and negative lags indicate the leverage effect.

The comparison to three stochastic processes from the GARCH family exposes differences to the empirical data. While the stochastic processes which include an asymmetry parameter are able to reproduce the leverage effect on a qualitative level they fail to fully reproduce the empirical findings. We advertize the use of the quantile-based correlation function as a benchmark for stochastic processes or as a tool to assess the limits of a given stochastic process. In general the quantile-based correlation function can help to raise the bar for the agreement of time series obtained from stochastic processes with empirical data.

Chapter 4

Addressing the non-stationarity of correlations

4.1 Introduction

The volatility of financial time series is highly non-stationary and changes quickly, see section 1.8 and figure 1.7. We have seen how the non-stationarity leads to challenges for the covariance estimation in chapter 2. Another example is the ever changing structure of the correlation matrix. This behavior is discussed in section 1.8. In an empirical study by Münnix *et al.* [75] it has been shown that a distance measure between correlation matrices at different points in time can be used to identify different states of a financial market. The correlation matrix is able to characterize the financial market.

In addition, we observe very large events much more often than we would expect from a normal distribution. The occurrence of financial crises is not a problem which is limited to the last century [119]. There is evidence that the Roman Empire faced several financial crises [120, 121]. In 1623 during the Thirty Years' War a financial crisis hit the city states of the Holy Roman Empire [121]. The city states debased their currencies in an attempt to fill their war chests. This crisis is of particular historic interest, because it involved only the debasement of metallic currency (coins). However, most financial crises are linked to financial markets. One early example is the Bengal Bubble of 1769 [121] which primarily revolves around the overvaluation of the famous East India Company. More recent examples include the dot-com bubble in 2001 and the financial crisis of 2008. This poses the question whether these extreme events are inherent in the system or the result of an external shock.

Financial markets can be considered as complex systems—in the sense of a system with many degrees of freedom.

In physics a standard tool to describe systems with many degrees of freedom is ensemble average. The concept proved highly successful in thermodynamics. A system in equilibrium with many particles can for example be characterized by a set of macroscopic variables, such as its temperature, volume and number of particles. This is achieved by averaging over an ensemble of all microstates for the system. We do not want to overstretch the analogy here, but the idea to use an ensemble approach to describe financial markets seems reasonable.

The key to capturing the structure of the financial market is the correlation matrix.

Due to the measurement noise it is impossible to know the exact covariance or correlation matrix for one realization of a sample. Estimating the covariance matrix from empirical data always requires a sufficiently long average over multiple realizations. Our ansatz assumes that each realization is drawn from a multivariate normal distribution with a randomly drawn covariance or correlation matrix. We derive the sample statistics for this case by averaging the multivariate normal distribution over an ensemble of random correlation matrices. This approach takes the fluctuations of the correlation matrix into account.

The derivation of the correlation-averaged normal distribution is published in [3] and was announced in Europhysics Letters [1] including parts of the empirical study. The full empirical study will be available as a working paper [5].

This chapter is organized as follows: We construct the correlation-averaged normal distribution in section 4.2 and visualize it for the bivariate case in section 4.3. In section 4.4 we carry out an extensive empirical study to validate our ansatz for financial time series. We conclude our results in section 4.5.

4.2 Constructing the correlation-averaged normal distribution

While we constructed the distribution with its application to credit risk in mind, see chapter 5, it became apparent that it has a general relevance for multivariate correlated time series. Therefore, we present the derivation here using a general notation.

Let us assume that each realization of a K dimensional random vector x is drawn from a multivariate normal distribution

$$g(x|\Sigma_t) = \frac{1}{\sqrt{2\pi}^K} \frac{1}{\sqrt{\det \Sigma_t}} \exp\left(-\frac{1}{2} x^\dagger \Sigma_t^{-1} x\right) \quad , \tag{4.1}$$

where Σ_t is the covariance matrix for this realization. The transpose of a vector or matrix is denoted by a dagger $\dagger$. In the case of non-stationary time series the covariance matrix Σ_t will be different for each time step. We defer the discussion of the validity of this assumption in the context of financial time series to section 4.4. In reality, we know that the covariance matrix Σ is not stationary between observations. Therefore, it is our aim to account for this non-stationarity. Our ansatz is to replace the covariance matrix by a random matrix

$$\Sigma_t \quad \longrightarrow \quad \sigma W W^\dagger \sigma \quad , \tag{4.2}$$

with the $K \times K$ diagonal matrices $\sigma = \mathrm{diag}(\sigma_1, \ldots, \sigma_K)$ containing the standard deviations. Random matrices proved successful in nuclear physics since the 1950s to describe many-body systems, for example, the spectra of heavy atomic nuclei and have various other applications, see reference [122] for a review. The elements of the $K \times N$ random matrix W are drawn from a multivariate normal distribution

$$w(W|C,N) = \sqrt{\frac{N}{2\pi}}^{KN} \frac{1}{\sqrt{\det C}^N} \exp\left(-\frac{N}{2} \operatorname{tr} W^\dagger C^{-1} W\right) \quad , \tag{4.3}$$

where C is the average correlation matrix. The ensemble of random correlation matrices $WW^\dagger$ follows a Wishart distribution [123]

$$\tilde{w}(WW^\dagger|C,N) = \frac{\sqrt{N}^{KN} \sqrt{\det WW^\dagger}^{N-K-1}}{\sqrt{2}^{KN} \Gamma_K(N/2) \sqrt{\det C}^N} \exp\left(-\frac{N}{2} \operatorname{tr} C^{-1} WW^\dagger\right) \quad , \tag{4.4}$$

with the multivariate Gamma function

$$\Gamma_K(a) = \pi^{K(K-1)/4} \prod_{k=1}^{K} \Gamma(a + (1-k)/2) \quad . \tag{4.5}$$

This ensemble of Wishart correlation matrices fluctuates around the average correlation matrix C. By means of this construction the ensemble average of $WW^\dagger$,

$$\left\langle WW^\dagger \right\rangle = \int \mathrm{d}[W] \; w(W|C,N) \; WW^\dagger = C \quad , \tag{4.6}$$

yields the average correlation matrix C. The measure $d[W]$ denotes the product of the differentials of the matrix elements.

In this context it is worth pointing out that the variance of the Wishart distributed (4.4) elements of the correlation matrix $WW^\dagger$ is

$$\mathrm{var}\,(WW^\dagger)_{kl} = \frac{C_{kl}^2 + 1}{N} \quad . \tag{4.7}$$

This will aid us in understanding later on when we discuss the meaning of the parameter N. We notice that the parameter N is proportional to the inverse variance of the Wishart distribution. The parameter determines the strength of the fluctuations around the average correlation matrix C. For larger values of N the elements of the matrix $WW^\dagger$ fluctuate less. Obviously, for the limit $N \to \infty$ the variance becomes zero, effectively suppressing all fluctuations. In addition, the parameter N can be viewed as the length of fictitious time series in the data matrices W with dimension $K \times N$.

The basic idea of our approach is to take fluctuating correlations into account by averaging the multivariate normal distribution (4.1) over the distribution (4.3) of the elements of W

$$\langle g \rangle(x|C,N) = \int \mathrm{d}[W]\; w(W|C,N)\; g(x|\sigma W W^\dagger \sigma) \quad . \tag{4.8}$$

In the statistics literature this approach is known as *compounding* [124] or *mixture* [125, 126] in the case of univariate distributions, where a new univariate distribution is constructed by averaging over a parameter of the distribution. For the following calculation it is advantageous to write the multivariate normal distribution (4.1) as a Fourier transform and we replace the covariance matrix Σ_t with the random matrix $\sigma W W^\dagger \sigma$

$$g(x|\sigma W W^\dagger \sigma) = \frac{1}{(2\pi)^K} \int \mathrm{d}[\omega]\; \mathrm{e}^{-\,\mathrm{i}\,\omega^\dagger x} \exp\left(-\frac{1}{2}\omega^\dagger \sigma W W^\dagger \sigma\, \omega\right) \quad , \tag{4.9}$$

where ω is the K dimensional vector of Fourier variables and the measure $\mathrm{d}[\omega]$ is the product of the differentials of the individual elements. The integration runs from $-\infty$ to ∞ for each ω_k. We insert the Fourier transform (4.9) and the distribution (4.3) into equation (4.8) and receive

$$\begin{aligned}\langle g \rangle(x|C,N) = \int \mathrm{d}[W] \left(\frac{N}{2\pi}\right)^{KN} \exp\left(-\frac{N}{2}\,\mathrm{tr}\, W^\dagger C^{-1} W\right) \\ \times \frac{\sqrt{\det C}^{-N}}{(2\pi)^K} \int \mathrm{d}[\omega]\; \mathrm{e}^{-\,\mathrm{i}\,\omega^\dagger x} \exp\left(-\frac{1}{2}\omega^\dagger \sigma W W^\dagger \sigma \omega\right)\end{aligned} \tag{4.10}$$

as the starting point for our calculation. We notice that the bilinear form $\omega^\dagger \sigma W W^\dagger \sigma \omega$ is a scalar and express it in form of a trace $\mathrm{tr}(\sigma\omega\omega^\dagger \sigma W W^\dagger)$. Rearranging the terms yields

$$\begin{aligned}\langle g \rangle(x|C,N) = \left(\frac{N}{2\pi}\right)^{KN} \frac{\sqrt{\det C}^{-N}}{(2\pi)^K} \int \mathrm{d}[\omega]\; \mathrm{e}^{-\,\mathrm{i}\,\omega^\dagger x} \int \mathrm{d}[W] \\ \times \exp\left(-\frac{N}{2}\,\mathrm{tr}\left(W^\dagger C^{-1} W\right) - \frac{1}{2}\,\mathrm{tr}\left(\sigma\omega\omega^\dagger \sigma W W^\dagger\right)\right) \quad .\end{aligned} \tag{4.11}$$

The trace is a linear operator and invariant under cyclic permutations allowing

us to join the two traces and rearrange the argument,

$$\langle g\rangle(x|C,N) = \sqrt{\frac{N}{2\pi}}^{KN} \frac{\sqrt{\det C}^{-N}}{(2\pi)^K} \int \mathrm{d}[\omega]\ \mathrm{e}^{-\mathrm{i}\,\omega^\dagger x} \int \mathrm{d}[W] \times \exp\left(-\frac{1}{2}\,\mathrm{tr}\left(WW^\dagger\left(NC^{-1}+\sigma\omega\omega^\dagger\sigma\right)\right)\right) \quad . \tag{4.12}$$

In equation (4.12) we notice that the second integral over W is just a Gaussian and arrive at

$$\langle g\rangle(x|C,N) = \frac{\sqrt{N}^{KN}\sqrt{\det C}^{-N}}{(2\pi)^K} \int \mathrm{d}[\omega]\ \frac{\mathrm{e}^{-\mathrm{i}\,\omega^\dagger x}}{\sqrt{\det(NC^{-1}+\sigma\omega\omega^\dagger\sigma)}^{N}} \quad . \tag{4.13}$$

Now we rewrite the determinant

$$\det(NC^{-1}+\sigma\omega\omega^\dagger\sigma) = N^K \det(C^{-1}+\frac{1}{N}\sigma\omega\omega^\dagger\sigma) \tag{4.14}$$

and apply a result [127]

$$\det(X+ab^\dagger) = (1+b^\dagger X^{-1}a)\det(X) \tag{4.15}$$

of Sylvester's determinant theorem [128]. The quadratic $K\times K$ matrix X has to be invertible, which is the case for C^{-1} and a and b are K dimensional vectors. In addition, the matrix $ab^\dagger$ must have rank one. This condition is fulfilled because $\sigma\omega\omega^\dagger\sigma$ is a dyadic matrix and we arrive at

$$N^K \det(C^{-1}+\frac{1}{N}\sigma\omega\omega^\dagger\sigma) = N^K(1+\frac{1}{N}\omega^\dagger\sigma C\sigma\omega)\det C^{-1} \quad . \tag{4.16}$$

Replacing the determinant in equation (4.13) with expression (4.16) yields

$$\langle g\rangle(x|C,N) = \frac{1}{(2\pi)^K}\int \mathrm{d}[\omega]\ \mathrm{e}^{-\mathrm{i}\,\omega^\dagger x}\frac{1}{\sqrt{1+\omega^\dagger\sigma C\sigma\omega/N}^{N}} \quad . \tag{4.17}$$

We use the representation

$$\frac{1}{a^\eta} = \frac{1}{\Gamma(\eta)}\int_0^\infty \mathrm{d}z\ z^{\eta-1}\mathrm{e}^{-az} \tag{4.18}$$

of the Gamma function with the real and positive variables a and η. We choose $a = 1+\omega^\dagger\sigma C\sigma\omega/N$ and $\eta = N/2$. Inserting equation (4.18) into

equation (4.17) yields

$$\langle g\rangle(x|C,N) = \frac{1}{(2\pi)^K\Gamma(N/2)}\int_0^\infty \mathrm{d}z\; z^{N/2-1}\mathrm{e}^{-z} \times \int \mathrm{d}[\omega]\; \mathrm{e}^{-\,\mathrm{i}\,\omega^\dagger x}\exp\left(-\frac{z}{N}\omega^\dagger\sigma C\sigma\omega\right) \quad . \tag{4.19}$$

The second last step is to perform the inverse Fourier transform. We replace the correlation matrix C with the new fixed covariance matrix

$$\Sigma = \sigma C\sigma \quad . \tag{4.20}$$

To solve the Fourier integral in equation (4.19), we have to factorize the integral in components of ω. Therefore, we diagonalize the matrix $\Sigma = U^\dagger\hat{\Sigma}U$, where $\hat{\Sigma}$ is a diagonal matrix which contains the eigenvalues of Σ and U is a $K\times K$ orthogonal matrix. Then, we substitute $\eta = U\omega$ and write the K dimensional integral in component-wise fashion

$$\begin{aligned}&\int \mathrm{d}[\omega]\; \mathrm{e}^{-\,\mathrm{i}\,\omega^\dagger x}\exp\left(-\frac{z}{N}\omega^\dagger U^\dagger\hat{\Sigma}U\omega\right)\\ =&\prod_{k=1}^K\int_{-\infty}^{+\infty}\mathrm{d}\eta_k\; \mathrm{e}^{-\,\mathrm{i}\,\eta_k(Ux)_k}\exp\left(-\frac{z}{N}\hat{\Sigma}_k\eta_k^2\right) \quad .\end{aligned} \tag{4.21}$$

We perform the integration in η_k

$$\begin{aligned}&\prod_{k=1}^K\int_{-\infty}^{+\infty}\mathrm{d}\eta_k\; \mathrm{e}^{-\,\mathrm{i}\,\eta_k(Ux)_k}\exp\left(-\frac{z}{N}\hat{\Sigma}_k\eta_k^2\right)\\ =&\prod_{k=1}^K\sqrt{\frac{\pi N}{z}}\frac{1}{\sqrt{\hat{\Sigma}_k}}\exp\left(-\frac{N}{4z}(Ux)_k^2\hat{\Sigma}_k^{-1}\right) \qquad (4.22)\\ =&\sqrt{\frac{\pi N}{z}}^K\frac{1}{\sqrt{\det\Sigma}}\exp\left(-\frac{N}{4z}\sum_{k=1}^K(Ux)_k^2\hat{\Sigma}_k^{-1}\right) \quad . \qquad (4.23)\end{aligned}$$

We recall that the diagonalization $\Sigma = U^\dagger\hat{\Sigma}U$ has no effect on the determinant due to matrix similarity. Therefore, we write $\det\hat{\Sigma} = \det\Sigma$. In addition, we can replace the bilinear form $x^\dagger U^\dagger\hat{\Sigma}^{-1}Ux$ in the exponential with $x^\dagger\Sigma^{-1}x$.

Performing the inverse Fourier transform in equation (4.19) yields

$$\langle g\rangle(x|\Sigma,N) = \frac{1}{(2\pi)^K\Gamma(N/2)\sqrt{\det\Sigma}}\int_0^\infty \mathrm{d}z\; z^{N/2-1}\mathrm{e}^{-z} \times\sqrt{\frac{\pi N}{z}}^K \exp\left(-\frac{N}{4z}x^\dagger\Sigma^{-1}x\right) \quad . \tag{4.24}$$

Finally, we use the integral representation of the modified Bessel function $\mathcal{K}$ of the second kind of order ν, see equation 10.32.10 in reference [129],

$$\mathcal{K}_\nu(t) = \frac{1}{2}\left(\frac{1}{2}t\right)^\nu \int_0^\infty \mathrm{d}z \exp\left(-z-\frac{t^2}{4z}\right) z^{-\nu-1} \tag{4.25}$$

to cast equation (4.24) into the form

$$\langle g\rangle(x|\Sigma,N) = \sqrt{\frac{N}{4\pi}}^K \frac{\sqrt{2}^{K-N+2}}{\Gamma(N/2)} \frac{\sqrt{Nx^\dagger\Sigma^{-1}x}^{\frac{N-K}{2}}}{\sqrt{\det\Sigma}} \mathcal{K}_{\frac{K-N}{2}}\left(\sqrt{Nx^\dagger\Sigma^{-1}x}\right), \tag{4.26}$$

with the modified Bessel function $\mathcal{K}$ of the second kind of order $(K-N)/2$. The distribution (4.26) only depends on one free parameter N, which according to equation (4.7) controls the strength of the fluctuations around the empirically obtainable average covariance matrix Σ. The sample vector x enters the distribution only via the bilinear form $x^\dagger\Sigma^{-1}x$. Interestingly, a univariate distribution of the form (4.26) was received in reference [130] with a compounding ansatz to describe the scattering of microwaves in random potentials. However, in this case, only the square of the scalar intensity enters the distribution. Our multivariate result takes fluctuating correlations around an average covariance matrix Σ into account. For $N = K+1$ our result is exponential, while in general the tails of the distribution show single-exponential behavior. The tail gets heavier for smaller values of N.

4.3 Visualizing the bivariate case

To visualize the distribution we calculate the two-dimensional (bivariate) case with $x = (x_1, x_2)$ and with the covariance matrix

$$\Sigma = \begin{bmatrix} 1 & \varrho \\ \varrho & 1 \end{bmatrix} \tag{4.27}$$

with standard deviation unity and correlation coefficient ϱ. Inserting the two dimensional vector x and covariance matrix Σ into equation (4.26) yields

$$\langle g\rangle(x|\varrho,N) = \frac{N}{4\pi}\frac{\sqrt{2}^{4-N}}{\Gamma(N/2)}\frac{\sqrt{N(x_1^2-2x_1x_2\varrho+x_2^2)/(1-\varrho^2)}^{\frac{N-2}{2}}}{\sqrt{1-\varrho^2}} \times \mathcal{K}_{\frac{2-N}{2}}\left(\sqrt{N(x_1^2-2x_1x_2\varrho+x_2^2)/(1-\varrho^2)}\right) \quad . \tag{4.28}$$

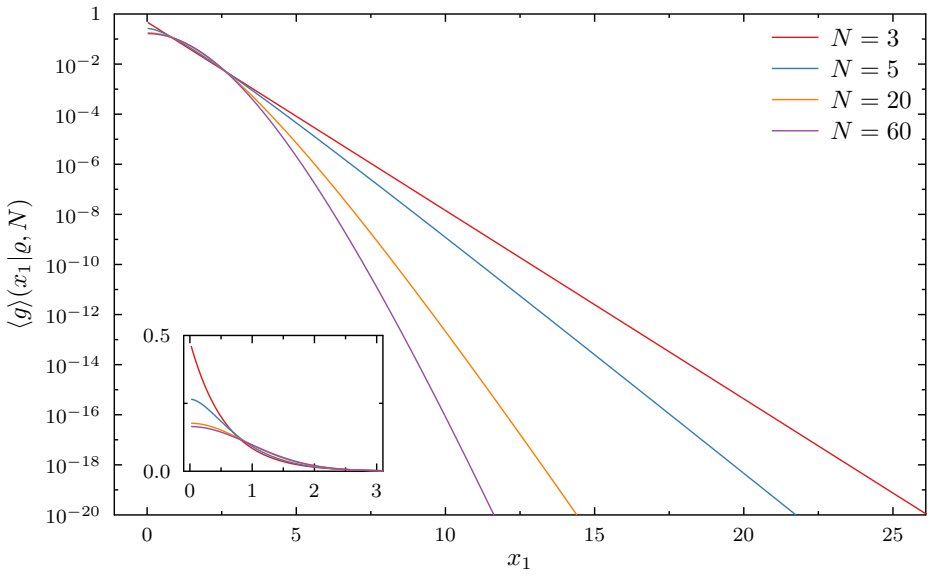

Figure 4.1: Linear-log plot of the tail behavior for the bivariate correlation-averaged normal distribution along the positive x_1 axis ($x_2 = 0$) for $\varrho = 0$. The linear inset shows the front part of the distribution.

Figure 4.1 provides an overview of the tail behavior for different values of N. We plot the distribution for $x_2 = 0$ along the positive x_1 axis. The negative tail looks the same due to symmetry. For $N = 3$ the distribution is exponential and smaller values of N result in a heavier tail.

The probability density function is shown in figure 4.2 for three different correlation coefficients $\varrho = -0.4, 0, 0.4$ and two values of $N = 5$ and $N = 20$.

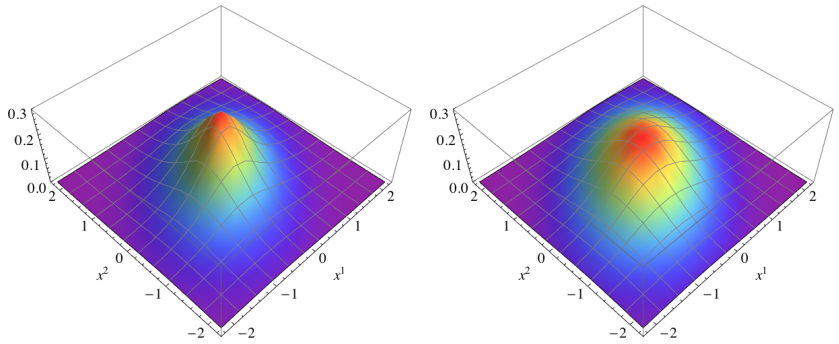

(a) $\varrho = 0.4$, $N = 5$

(b) $\varrho = 0.4$, $N = 20$

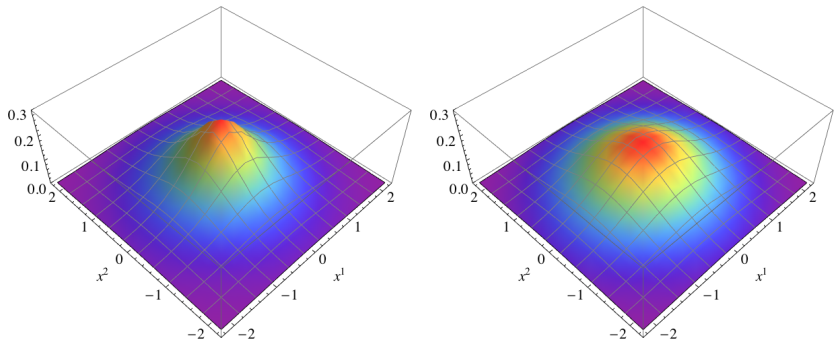

(c) $\varrho = 0$, $N = 5$

(d) $\varrho = 0$, $N = 20$

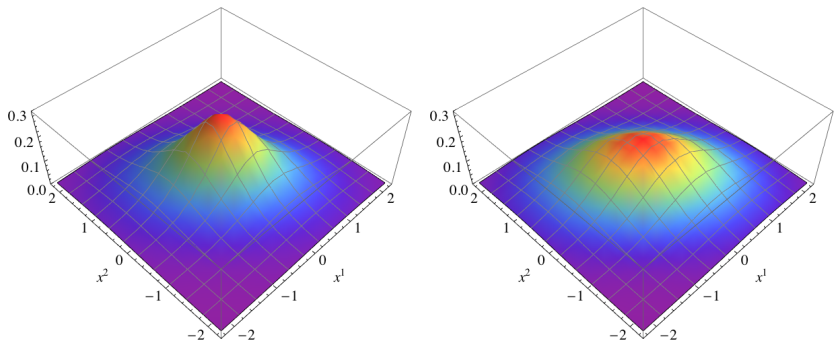

(e) $\varrho = -0.4$, $N = 5$

(f) $\varrho = -0.4$, $N = 20$

Figure 4.2: Bivariate correlation-averaged normal distribution for different correlation coefficients ϱ and two choices of $N = 5$ and $N = 20$.

4.4 Empirical validation of our ansatz for financial time series

During the construction of the correlation-averaged normal distribution in section 4.2 we assumed that each realization of the sample is drawn from a multivariate normal distribution (4.1) with a different covariance matrix Σ_t for each realization. However, we pointed out that it is impossible to measure the covariance matrix Σ_t from a single realization. Therefore, we have to compromise and estimate from multiple realizations. The aim here is to use a time horizon which is short enough to be considered stationary and long enough to not only contain measurement noise. We denote this covariance matrix as Σ_{st} in contrast to the covariance matrix Σ_t for a single realization.

There are two things we show here. First, we have to confirm that the correlation-averaged normal distribution is able to describe the empirical multivariate return distribution. The discussion will primarily revolve around the assumption of a quasi-stationary covariance matrix Σ_{st} on short time horizons. Second, we need to discuss how to obtain the right values for the parameter N from the empirical data.

For later purposes we introduce a correlation matrix with a simplified structure, *i.e.*, homogeneous correlations between stocks. We construct this matrix so that all off-diagonal elements have a value of $C_{k\neq l} = c$

$$C = \begin{bmatrix} 1 & c & c & \cdots & c \\ c & 1 & c & \cdots & c \\ c & c & \ddots & & \vdots \\ \vdots & \vdots & & \ddots & \vdots \\ c & c & \cdots & \cdots & 1 \end{bmatrix} \quad . \tag{4.29}$$

This construction has two advantages. We can simplify the parameter space of the correlation matrix to only one parameter and it will allow us to make analytical progress in chapter 5.

We take all price time series from Yahoo Finance [35]. For this study we use the adjusted daily prices and compile two different stock selections. The first set contains stocks from the Standard & Poor's 500 index (S&P 500), while the second set consists of stocks traded at the NASDAQ. For each time horizon we take only stocks into account which were continuously traded during the period. The S&P 500 consists mostly of the best performing companies within the United States of America. In contrast, taking all stocks which are traded at the NASDAQ into account makes a much broader selection across companies with regard to their success.

As discussed in section 1.7, we calculate the returns of the prices, see equation 1.11. The return depends on the chosen return interval Δt, we use daily

($\Delta t = 1$ trading day) and monthly ($\Delta t = 20$ trading days) returns in this analysis.

4.4.1 Multivariate normal distribution for returns

During the derivation of the correlation-averaged multivariate normal distribution we assumed that each realization of the random vector is drawn from a multivariate normal distribution (4.1). However, we discussed earlier that in the case of empirical data we cannot estimate the covariance matrix Σ_t for one realization. We have to estimate a covariance matrix Σ_{st} on a longer time horizon but short enough to view it as quasi-stationary. In the case of financial time series this means that the multivariate returns should be described by

$$g(r|\Sigma_{\text{st}}) = \frac{1}{\sqrt{\det(2\pi\Sigma_{\text{st}})}} \exp\left(-\frac{1}{2} r^{\dagger} \Sigma_{\text{st}}^{-1} r\right) \quad , \tag{4.30}$$

on short time horizons, where r is the K dimensional return vector.

To verify this assumption, we split the return time series into short non-overlapping time intervals of 25 trading days. It is very important to understand that this time interval has nothing to do with the return time interval Δt. We first calculate the return time series for a given return interval $\Delta t = 1$ trading day and after that partition the resulting time series into small slices of 25 trading days. Now, we claim that on this short time interval the covariance matrix Σ_{st} can be viewed as constant. As a side note, we know that the covariance matrix will be non-invertible, because the length of the time series (25 data points) is shorter than the dimension of the matrix (> 300 stocks). This poses no problems from a mathematical standpoint, because the distribution in equation (4.30) is properly defined by δ-functions in the case of non-invertible covariance matrices.

To progress further, we calculate the 2×2 covariance $\Sigma_{\text{st}}^{(k,l)}$ for all possible combinations of the stocks (k, l) in the selection. In contrast to the full covariance matrix, the bivariate covariance matrix is always invertible. The distribution of the pairs of returns (r_k, r_l) should then be bivariate normal distributed. In a last step, we rotate the vector of return pairs (r_k, r_l) into the eigenbasis of $\Sigma_{\text{st}}^{(k,l)}$ and normalize the elements of the resulting vector by dividing with the square root of the corresponding eigenvalues. The elements of the rotated vector of return pairs should then follow a normal distribution. We create a histogram from all these elements. The distribution of the aggregated pairs of returns is shown in figure 4.3. The distribution to the left shows the aggregated results for 307 stocks of the S&P 500 index, which were continuously traded during the period of 1992-2012. The distribution on the right is created from 2667 stocks which were traded between 2002 and 2012 on the NASDAQ stock exchange. The full list of stocks is shown in appendix B. For comparison a normal distribution is shown (red circles). We observe a good

agreement over four orders of magnitude between the distribution of aggregated pairs of returns and the normal distribution. In reverse, this underlines that we can assume that the multivariate return distribution can be described on short time horizons by a multivariate normal distribution and a fixed covariance matrix Σ_{st}. We use the pairs of returns to reduce the dimension and to be able to easily illustrate the agreement with a normal distribution.

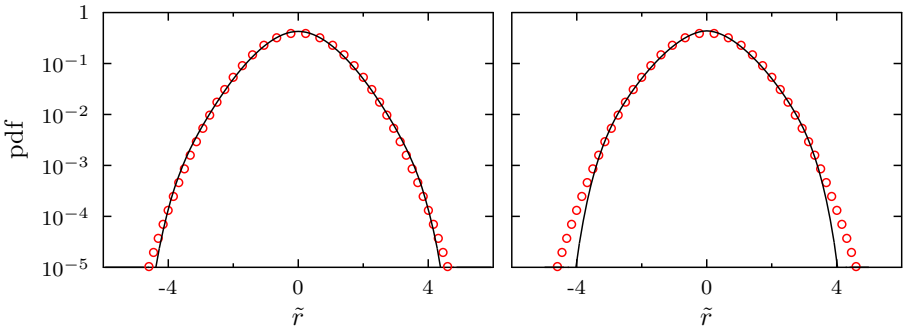

Figure 4.3: Aggregated return distributions for fixed covariance matrices. The circles show a normal distribution. On the left is the S&P 500 dataset between 1992 to 2012 and on the right is the NASDAQ dataset from 2002 to 2012.

4.4.2 Rotated and scaled returns

The previous section showed a first reasoning why our assumption of multivariate normal distributed returns (4.30) is valid on short time horizons. Nonetheless, we want to present another argument to further justify our assumptions. In particular, we assumed in equation (4.4) that the ensemble of random correlation matrices follows a Wishart distribution. Here, we show that the empirical data is well described by the correlation-averaged normal distribution and thereby show the validity of these assumptions *ex post*. Starting from our correlation-averaged return distribution (4.26), we calculate the distribution of rotated and scaled returns. Again, it is our aim to reduce the dimension to better visualize the comparison. We rotate the vector r into the eigenbasis of the covariance matrix Σ and normalize the elements of the resulting vector with its corresponding eigenvalue. The integral now factorizes. Then, we integrate out all degrees of freedom until only one is left. We arrive at the distribution of the rotated and scaled returns

$$\langle g \rangle(\tilde{r}|N) = \frac{\sqrt{2}^{1-N}\sqrt{N}}{\sqrt{\pi}\Gamma(N/2)} \sqrt{N\tilde{r}^2}^{(N-1)/2} \mathcal{K}_{(N-1)/2}\left(\sqrt{N\tilde{r}^2}\right) \quad , \tag{4.31}$$

where $\tilde{r}$ denotes the rotated and scaled return. We notice that the order of the Bessel function now is $(N-1)/2$.

We can apply the same procedure to multivariate returns obtained from empirical data. This approach allows us to calculate the distribution of the rotated and scaled returns for the average covariance matrix Σ or the average covariance matrix $\hat{\Sigma} = \sigma C \sigma$ with the homogeneous correlation matrix from equation (4.29). The results can then be compared to the theoretical distribution in equation (4.31).

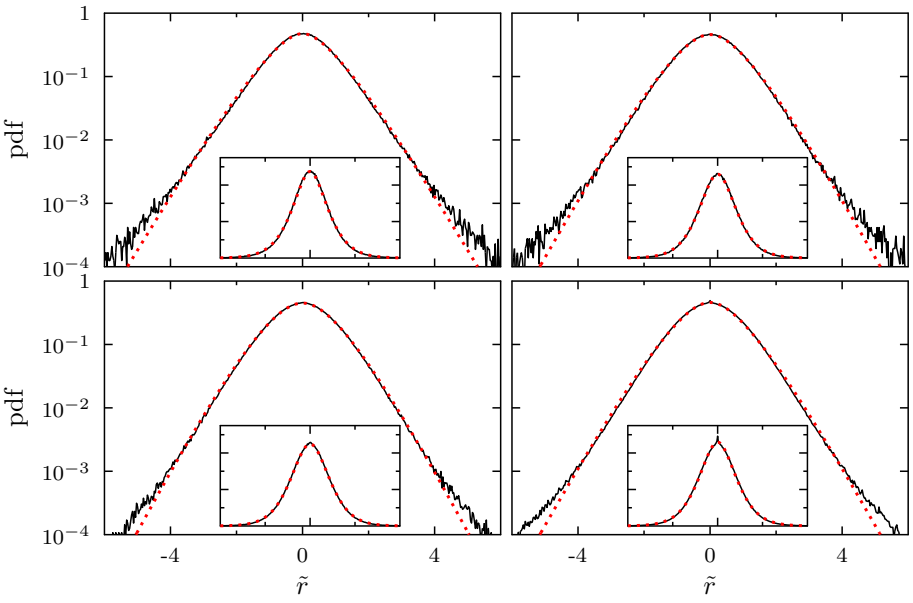

Figure 4.4: Aggregated distributions for the rotated and scaled daily returns. The empirical distribution is shown in black and the theoretical result is red and dotted. The parameter N is around six. Top left/right: S&P 500 (1992-2012) / (2002-2012), bottom left/right: NASDAQ (1992-2012) / (2002-2012).

First, we discuss the results for the non-homogeneous average covariance matrix Σ, which are shown in figures 4.4 and 4.5 for daily and monthly returns, respectively. We performed the empirical study on four different data sets. The first dataset consists of 307 stocks from the S&P 500 index which were continuously traded in the period from 1992-2012 (top left). The second set includes 439 stocks from the S&P 500 during the years from 2002 to 2012 (top right). Then we use 708 and 2667 stocks from NASDAQ on the time horizons stated above (bottom left/right), respectively. A complete list of the stocks used is presented in appendix B. To determine the best selection for the parameter N, we use the Cramer-von Mises test. We calculate

the confidence level for each integer value of N and choose the value with the highest confidence probability, see table 4.1. For daily returns we find

	S&P 500		NASDAQ	
figure	1992-2012	2002-2012	1992-2012	2002-2012
4.4	5	6	7	6
4.5	14	22	20	20
4.6	4	4	4	4

Table 4.1: Values for the parameter N used in Figs. 4.4 to 4.6.

that values around six describe the data well, while for monthly returns larger values around $N = 20$ are necessary. We find that equation (4.31) describes the empirically obtained distributions of the rotated and scaled returns very well. They fit up to four decimal powers. Second, we study the distribution of the rotated and scaled returns for the homogeneous correlation matrix, see equation (4.29). The homogeneous correlation matrix has the same value on all off-diagonal elements. We determine the average correlation level c and the volatilities on each time horizon and calculate the covariance matrix according to equation (4.20). Then, we rotate the multivariate return vector into the eigenbasis of this covariance matrix $\hat{\Sigma}$. This allows us to investigate if the missing correlation structure does matter in describing the multivariate return distribution. For this matrix we find smaller values for the parameter N, which describes the fluctuations around the average correlation matrix. The S&P 500 and NASDAQ data is described well by $N = 4$. The resulting probability distributions are shown in figure 4.6. The top line shows the S&P 500 data for the years 1992 to 2012 and from 2002 to 2012, the bottom line shows the NASDAQ data. We observe that smaller values around $N = 4$ are needed to describe the distribution of monthly rotated and scaled returns if we use the covariance matrix with homogeneous correlation structure. Compare this to larger values around $N = 20$ that we find for the full covariance matrix in figures 4.4 and 4.5. While deriving the correlation-averaged multivariate normal distribution in section 4.2, we noted that the parameter N is proportional to the inverse variance, see equation (4.7), of the Wishart distributed elements of the random matrix. Here, the meaning of the parameter becomes intuitively clear. The covariance matrix $\hat{\Sigma}$ lacks the correlation structure of the empirical correlation matrix. Therefore, it is no surprise that stronger fluctuations are required to account for the missing structure. Due to the inverse nature of the parameter N smaller values are needed for larger fluctuations. In figure 4.7 the dependence of the parameter N on the return interval Δt is shown. The presented N values have the highest confidence level using in the Cramer-von Mises test. Larger return intervals require values around $N = 5$ to describe the empirical data best, in the case of our covariance matrix with

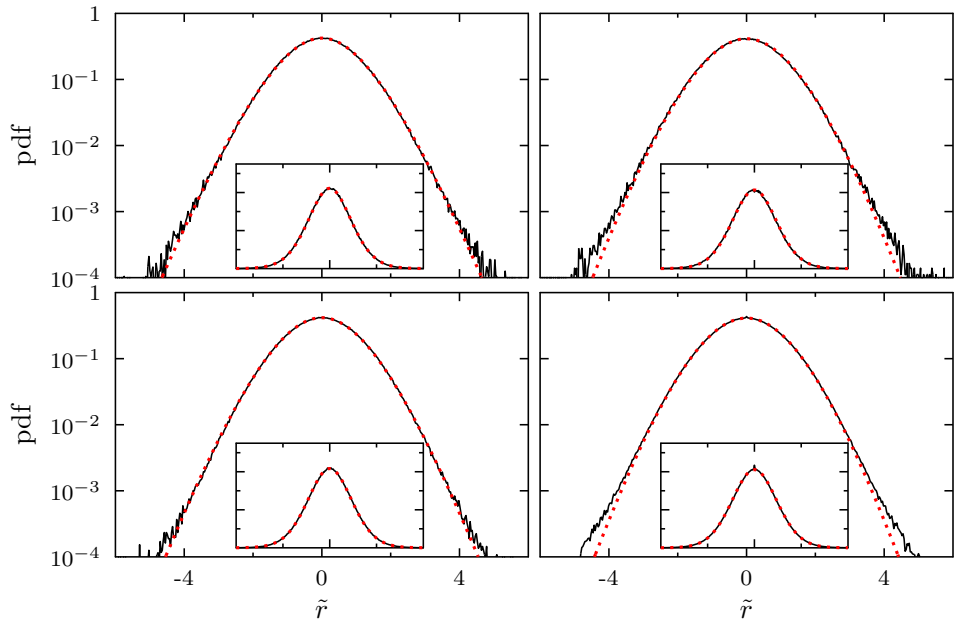

Figure 4.5: Aggregated distributions for the rotated and scaled monthly returns. The empirical distribution is shown in black and the theoretical result is red and dotted. Values around twenty are needed for the parameter N to describe the data. Top left/right: S&P 500 (1992-2012) / (2002-2012), bottom left/right: NASDAQ (1992-2012) / (2002-2012).

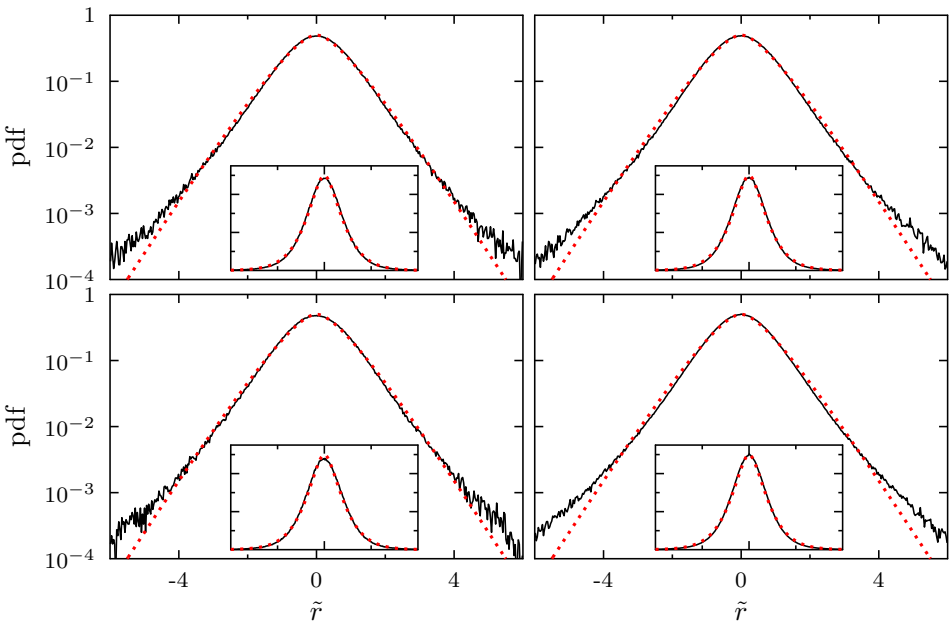

Figure 4.6: Aggregated distributions for the rotated and scaled monthly returns using the covariance matrix $\hat{\Sigma}$ with homogeneous correlation structure. The empirical distribution is shown in black and the theoretical result is red and dotted. The S&P 500 and the NASDAQ data uses $N = 4$. Top left/right: S&P 500 (1992-2012) / (2002-2012), bottom left/right: NASDAQ (1992-2012) / (2002-2012). The average correlation levels are $c = 0.26, 0.35, 0.21$ and $c = 0.25$, respectively.

homogeneous correlations. The aggregated distributions for the rotated and scaled yearly returns is shown in appendix D and fits the data well for $N = 6$.

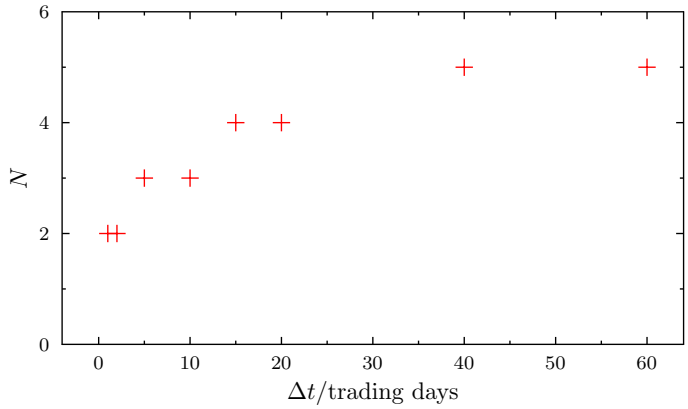

Figure 4.7: Parameter N versus the return interval Δt in the case of a covariance matrix with homogeneous correlation structure.

4.4.3 Variance

Besides the data driven approaches of the previous sections, there is another argument to estimate the magnitude of the parameter N. Our model assumes that the K dimensional multivariate return vector

$$r = W\varepsilon$$

is described by a random $K \times N$ matrix W with independent rows and a stochastic part ε. The N dimensional vector ε has entries which are *i.i.d.* normally distributed random numbers with zero mean $\langle\varepsilon\rangle = 0$ and variance $\langle\varepsilon^2\rangle = 1$. We calculate the variance of the expression

$$x = \operatorname{tr} rr^T = r^T r = \sum_{kij} W_{ki}\varepsilon_i W_{kj}\varepsilon_j \quad ,$$

and arrive at

$$\langle x^2\rangle = 4\left(\frac{1}{2} + c^2\right)\frac{K^2}{N} + 2c^2K^2 + 4(1-c^2)\frac{K}{N} + 2(1-c^2)K \quad .$$

We compare this variance to the empirical results and find for our data sets that N values smaller than 5 are necessary to receive a comparable variance.

4.5 Conclusion

Multivariate data often includes a significant amount of non-stationary features. We addressed this non-stationarity by averaging a multivariate normal distribution over an ensemble of correlation matrices with Wishart distributed elements. The ensemble fluctuates around an average empirical covariance matrix, which can be estimated on the whole time horizon in question. The fluctuations of the ensemble around this covariance matrix are controlled by a single parameter. With our ansatz we effectively reduce the whole complexity of a correlated non-stationary financial market to one free parameter. The parameter can be estimated from empirical data and we find that our ansatz describes the empirical data on a time horizon of 20 years very well.

By taking the non-stationarity into account we constructed a correlation-averaged multivariate normal distribution, which can be expressed as a modified Bessel function of the second kind. The tails of the distribution decay exponentially and clearly deviate from a multivariate normal distribution, *i.e.*, they are far heavier. Therefore, we conclude that the heavy tails are a consequence of the non-stationarity of the financial markets. From this perspective, the appearance of very large events, *e.g.*, financial crises, is far more common than normality would let us think and is inherent in financial markets.

Chapter 5

Credit risk: Taking fluctuating asset correlations into account

5.1 Introduction

The collapse of the investment bank Lehman Brothers on September 15, 2008 revealed the consequences of the sub-prime mortgage crisis to the public [22]. Between 2004-2007 banks in the United States of America gave variable interest loans to individuals who normally would not be able to afford a house. This led to a rise in housing prices which further fueled the view that the mortgage on a house is safe because of rising house prices in the future. The burst of the housing bubble in 2006 proved the opposite. The damage was not done by a single large debtor defaulting, but the correlated default of many small obligors [131]. The breakdown of Lehman Brothers had severe consequences for the trust between banks, which for fear of other banks defaulting, stopped lending money to each other. Confronted with these refinancing risks the banks harshly reduced the number of credits given to small and midsize businesses. Many companies rely on credits for their daily operation, because they have to pay up front for the resources required in the production cycles. Lacking these credits weaker companies without financial reserves had to cease operation. The resulting recession led to a rise of the default probability [132]. These devastating consequences show the importance of gaining a better understanding of the risks inherent in the financial system. In recent years economists have pointed out several issues with the current state of credit risk management and proposed different approaches to improve the situation, see [133–141] for an overview.

It all boils down to the estimation of the loss distribution for a large portfolio of credit contracts. The typical shape of a loss distribution for credit portfolios is shown in figure 5.1. It differs from the hypothetical loss distribution for a portfolio of stocks, which we saw in figure 1.8. The loss distribution has a characteristic shape due to the fundamental properties of credit contracts. One of the simplest credit contracts is called zero-coupon bond. The principle is illustrated in figure 5.2. The investor or creditor buys the bond from the obligor at a discounted price. At the maturity time the obligor must pay back the face value of the bond to the creditor. The face value is higher than

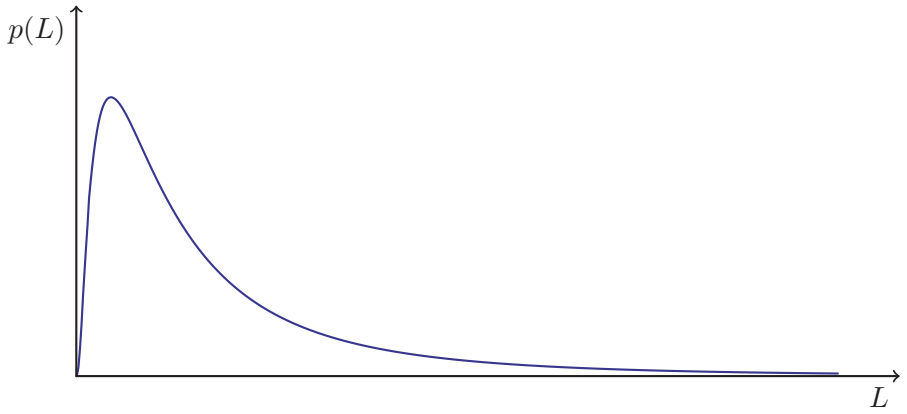

Figure 5.1: Schematic drawing of a typical loss distribution $p(L)$ versus the relative loss L.

the discounted price of the bond. The difference is the profit the creditor makes by lending his money to the obligor. This is only true if the obligor is able to fully pay back the face value and does not default. In reality the creditor has to incorporate a risk compensation, which typically depends on the creditworthiness of the obligor. In the case of a zero-coupon bond the creditor is not entitled to interest payments before the maturity time. The bond is named after this fact, *i.e.*, the creditor does not receive "coupon" payments. From the zero-coupon bond we can learn a typical characteristic of credit contracts. The maximum profit an investor can achieve is limited to the difference between face value and the discounted price of the bond. On the other hand, the maximum loss is losing the whole amount of money given to the obligor.

Typically, a creditor lends money to many entities and therefore has a portfolio consisting of a large number of contracts. Most obligors will be able to pay back their debt and only a small fraction of the portfolio will be lost, as seen in the peak of figure 5.1. Such small losses are normal and are taken into account by the investor in form of a risk premium. The real danger lies in the heavy tail of the loss distribution. The rare freak events, which cause the large losses, as seen during the subprime crisis, can take down whole creditors. Assessing how strong this tail is, is very important to determine risk compensation and capital requirements of banks. Financial institutions often claim that diversification is able to lower the risk of a portfolio. While this is true for portfolios consisting of stocks, it does not work for portfolios of credit contracts. The main reason lies in the asymmetry of the loss distribution for credit portfolios in contrast to the symmetric loss distribution of stock portfolios. The maximum profit of the bank is only the interest and risk compensation if no credit defaults. On the other hand the greatest possible loss

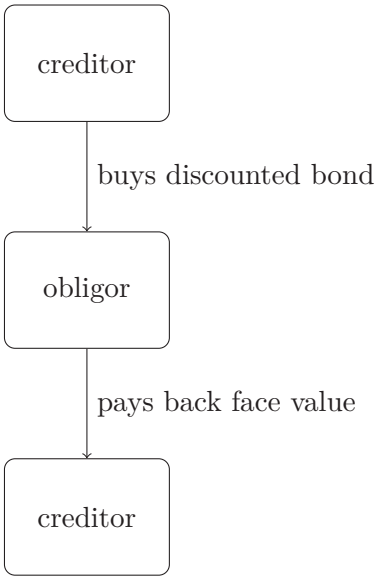

Figure 5.2: The creditor buys the discounted bond from the obligor. At a future point in time the obligor pays back the face value of the bond.

is the complete loss of the money lent. Taking the correlations into account is very important to assess the strength of the tail for the loss distribution of credit portfolios, for example collateralized debt obligations (CDOs). Even in the presence of weak correlations diversification cannot reduce the portfolio risk, which has been shown for first passage models [142, 143] and numerically for the Merton model [144, 145].

Here, we plan to extend the Merton model to take fluctuating correlations between asset values into account. We constructed a distribution in chapter 4, which is able to describe multivariate asset returns and addresses the non-stationarity of the covariance or correlation matrix. To make analytical progress we have to introduce a covariance matrix with homogeneous correlation structure. Combining this distribution with the Merton model applies the concept of ensemble average to credit risk modelling and was first studied for an average correlation level of zero in reference [146]. This allows us to greatly simplify the parameter space to two main parameters. The strength of the fluctuations is governed by the parameter N. The second parameter c is the average correlation level between assets. We are even able to calculate a limiting loss distribution for the case of infinite portfolio size. This helps us to gain a quantitative understanding why the effect of diversification is very limited for credit portfolios.

This chapter is structured as follows: In section 5.2 we briefly discuss two

common approaches to credit risk modeling, the reduced form models and structural models. Then we study how the Merton model works in section 5.3.1. In chapter 4 we constructed a correlation-averaged multivariate normal distribution. We will use this distribution to describe the asset value of the obligor at maturity time in section 5.3.2. In addition, we carry out Monte-Carlo simulations to determine Value at Risk (VaR) and the Expected Tail Loss (ETL) for our average loss distribution in section 5.4.2. The simulations show that it is a reasonable assumption to omit the structure of the correlation matrix if the heterogeneous empirical volatilities are used. Furthermore, the simulation results emphasize the importance of taking fluctuating correlations into account.

The analytical results presented in this chapter are published in Europysics Letters [2]. The VaR and ETL Monte-Carlo simulations will be available as a working paper [5].

5.2 Credit risk modeling

There are two common kinds of credit risk models [147]: reduced form and structural models. Reduced form models describe the default probability and recovery rate with a functional dependence on some macroeconomic risk factors and a risk factor for the specific asset. Often, such models assume a simple function for the default probability which lacks a deeper economic interpretation.

On the other hand, structural models take an underlying stochastic process to model the asset value. If the asset value drops below the face value of the credit contract a default occurs. Depending on the model a default only occurs if the asset value is below the face value at the maturity time of the contract or as soon as the asset value drops below the face value. The latter are called first passage structural models, see *e.g.* references [142, 143]. We use the Merton model as a basis, where only the asset value at maturity time is considered.

5.3 Structural credit risk model with fluctuating asset correlations

5.3.1 Merton model

We extend the structural credit risk model of Merton [148], which he developed in 1974 along the lines of the Black and Scholes option pricing theory. The close connection to Black and Scholes will become apparent during the explanation of the Merton model.

Merton assumes a greatly simplified debt structure of a company. All debt claims against a company are consolidated into a single bond with face value

F_k. We denote different companies with the subscript k. Furthermore, it is assumed that the liquidation in case of bankruptcy is free of charge and the debt and equity of the company can be traded without restrictions. We suppose that the total value of a company $V_k(t)$ at time t can be described by a geometric Brownian motion

$$\mathrm{d}V_k(t) = \mu_k V_k(t)\mathrm{d}t + \sigma_k V_k(t)\mathrm{d}W(t) \quad , \tag{5.1}$$

where $\mathrm{d}W(t)$ is a Wiener process and $V_k(0) > 0$. μ_k is the drift and σ_k is the volatility of the asset value for company k. If at the bond's maturity time T the asset value of the company is below the face value, $V_k(T) < F_k$, the obligor is not able to pay back his debt, a default occurs. In this case the bondholders have the right to take over all assets of the company and liquidate them. If the face value is smaller than the asset value, the company can pay back its obligations and no default or loss occurs. Both cases are illustrated in figure 5.3 for a hypothetical path of the geometric Brownian motion. But how

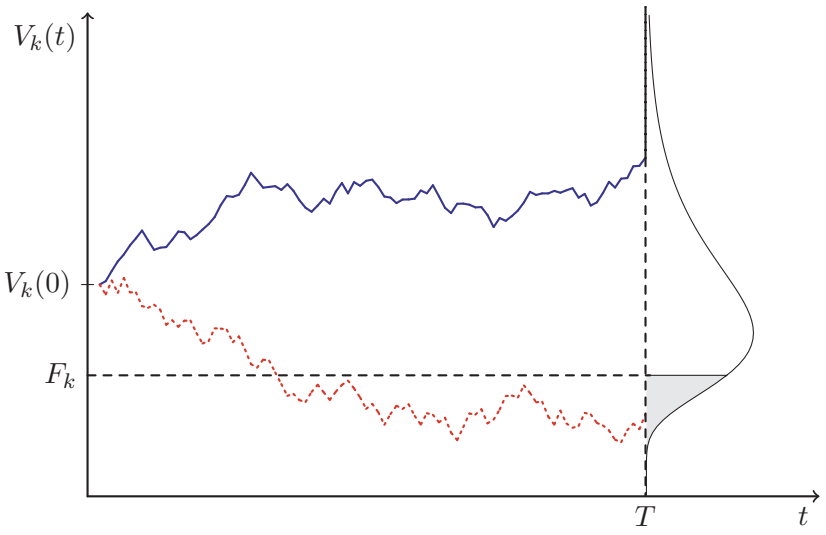

Figure 5.3: In the Merton model a default occurs if the asset value $V_k(t)$ is below the face value F_k at time T (dotted line). Otherwise the obliger can pay back the debt (solid line). The grey area under the curve corresponds to the default probability.

to determine the asset value of a company in reality? It was Merton's seminal idea to use the stock price $S_k(t)$ of the company, because it should reflect how much a company is worth. From the perspective of a shareholder the value of his share is reduced at maturity time T by the amount of debt paid back, *i.e.*, the face value of the contract. If the company defaults the shares become

worthless. This can be written as

$$S_k(T) = \max(V_k(T) - F_k, 0) \quad . \tag{5.2}$$

The total value of the company gets smaller by paying back the face value F_k of the bond. Should a default occur the shareholders are not liable for the losses, *i.e.*, they do not have to compensate the bondholders, hence the zero in equation (5.2). This resembles a European call option, compare section 1.3, where the equity of the company is an option on the assets of the company. Therefore, the default probability at maturity T viewed at time t is already known from the Black and Scholes theory of option pricing

$$P_k(V_k(T) \leq F_k) = N\left(-\frac{\log(V_k(t)/F_k) + (\mu - \sigma^2/2)(T-t)}{\sigma\sqrt{T-t}}\right) \quad , \tag{5.3}$$

where $N(\cdot)$ denotes the standard normal cumulative distribution, see equation (1.4).

After this historic note how the Merton model developed along the lines of the Black and Scholes model, we set up the Merton model for our needs. Suppose we have a portfolio of credit contracts for K companies. We write the normalized loss of the k-th contract for our credit portfolio as

$$L_k = \frac{F_k - V_k(T)}{F_k}\Theta(F_k - V_k(T)) \quad , \tag{5.4}$$

where $\Theta(x)$ denotes the Heaviside step function

$$\Theta(x) = \begin{cases} 0, & x < 0 \\ 1, & x \geq 0 \end{cases} \quad . \tag{5.5}$$

The Heaviside step function $\Theta(F_k - V_k(T))$ is unity only if the face value F_k is larger than the remaining asset value of the obligor $V_k(T)$, otherwise zero. This construction guarantees that the loss L_k is always equal or greater than zero and equal or lesser than one.

The sum of the individual losses L_k, which are weighted by their fraction f_k of the portfolio, gives the total loss of the portfolio

$$L = \sum_{k=1}^{K} f_k L_k \quad , \quad f_k = \frac{F_k}{\sum_{i=1}^{K} F_i} \quad . \tag{5.6}$$

To calculate the loss distribution we have to integrate over the distribution of asset values $g(V|\Sigma)$ at maturity time T with $V = (V_1(T), \ldots, V_K(T))$ and filter for a given loss L using the conditions of equation (5.6), see reference [146].

We start with the filter integral

$$p(L) = \int\limits_{[0,\infty)^K} \mathrm{d}[V] g(V|\Sigma) \delta \left(L - \sum_{k=1}^{K} f_k L_k \right) \quad , \tag{5.7}$$

where the measure $\mathrm{d}[V]$ is the product of the differentials for each asset k and express the δ-function as an integral over ν

$$p(L) = \int\limits_{0}^{\infty} \mathrm{d}[V] g(V|\Sigma) \frac{1}{2\pi} \int\limits_{-\infty}^{+\infty} \mathrm{d}\nu \exp \left(-\mathrm{i}\,\nu L + \mathrm{i}\,\nu \sum_{k=1}^{K} f_k L_k \right) \quad . \tag{5.8}$$

Inserting the individual loss from equation (5.4) and reordering the terms yields

$$\begin{aligned} p(L) = \frac{1}{2\pi} \int\limits_{-\infty}^{+\infty} \mathrm{d}\nu \; \mathrm{e}^{-\mathrm{i}\,\nu L} \\ \times \prod_{k=1}^{K} \left[\int\limits_{0}^{\infty} \mathrm{d}V_k(T) \, \mathrm{e}^{\mathrm{i}\,\nu f_k (1 - V_k(T)/F_k) \Theta(F_k - V_k(T))} \right] g(V|\Sigma) \end{aligned} \quad . \tag{5.9}$$

We split the range of integration to get rid of the Heaviside function and end up with the general loss distribution for the Merton model

$$\begin{aligned} p(L) = \frac{1}{2\pi} \int\limits_{-\infty}^{+\infty} \mathrm{d}\nu \; \mathrm{e}^{-\mathrm{i}\,\nu L} \\ \times \prod_{k=1}^{K} \left[\int\limits_{0}^{F_k} \mathrm{d}V_k(T) \, \mathrm{e}^{\mathrm{i}\,\nu f_k (1 - V_k(T)/F_k)} + \int\limits_{F_k}^{\infty} \mathrm{d}V_k(T) \right] g(V|\Sigma) \end{aligned} \quad . \tag{5.10}$$

The crucial part is to find a suitable function to describe the distribution of asset values $g(V|\Sigma)$ at maturity time T. The distribution should provide a realistic description of the correlated asset values including the heavy tails. In addition, it has to model the empirically known non-stationarity of the correlation structure and covariances. Moreover, it needs to be analytically tractable. The random matrix ansatz in chapter 4 allowed us to construct a correlation-averaged multivariate normal distribution which fulfills these requirements. The steps to adopt this distribution as the distribution of asset values at maturity time will be the topic of the next section 5.3.2.

5.3.2 An ensemble approach: average asset value distribution

We use the correlation-averaged multivariate normal distribution, which we obtained by ensemble average, in chapter 4. A very important empirical observation is that the returns of different stocks are correlated, see section 1.8. Even more important, the correlations are non-stationary, *i.e.*, the structure of the correlation matrix changes in time. Our correlation-averaged multivariate normal distribution takes this non-stationarity into account. We know from the empirical study in section 4.4 that the empirical multivariate distribution of returns is described well by the correlation-averaged multivariate normal distribution. We recall the definition of the return

$$r_k(t) = \frac{S_k(t+\Delta t) - S_k(t)}{S_k(t)} \tag{5.11}$$

for the k-th stock, where Δt is the return interval. The correlation-averaged multivariate normal distribution allows us to capture the multivariate return distribution only with the parameter N and the average correlation matrix C. Unfortunately, we cannot make analytical progress for the loss distribution for arbitrary correlation matrices, because the K dimensional integral in equation (4.19) would not necessarily factorize. We already introduced a simplified homogeneous correlation matrix (4.29) in section 4.4, which we will utilize now. Here, we have to perform a coordinate transformation for the correlation-averaged normal distribution from the returns r to the asset values V assuming the geometric Brownian motion used in the Merton model.

As we are interested in the distribution of asset values at maturity time T, the return interval Δt will be determined by the maturity time T,

$$\Delta t = T \quad . \tag{5.12}$$

This connection plays an important role as it sets the return interval for the estimation of the parameter N and allows us to calibrate the loss distribution to empirical data.

In chapter 4, we found the general result for the correlation-averaged multivariate normal distribution for an arbitrary average covariance matrix Σ

$$\langle g \rangle (r|\Sigma, N) = \frac{\sqrt{N}^K}{\sqrt{2}^{N-2}\Gamma(N/2)\sqrt{\det(2\pi\Sigma)}} \frac{\mathcal{K}_{(K-N)/2}\left(\sqrt{N r^\dagger \Sigma^{-1} r}\right)}{\sqrt{N r^\dagger \Sigma^{-1} r}^{(K-N)/2}} \quad , \tag{5.13}$$

where $\mathcal{K}$ is the modified Bessel function of the second kind and of order $(K-N)/2$. We substitute the covariance matrix Σ for the correlation matrix C, according to $\Sigma = \sigma C \sigma$. Here, it is advantageous to use the Fourier representation, see equation (4.19), of the correlation-averaged multivariate normal

distribution to make analytical progress

$$\langle g\rangle(r|C,N) = \frac{1}{2^{N/2}\Gamma(N/2)} \int_0^\infty \mathrm{d}z\ z^{N/2-1}\mathrm{e}^{-z/2} \int \frac{\mathrm{d}[\omega]}{(2\pi)^K} \exp\left(-\mathrm{i}\omega^\dagger r - \frac{z}{2N}\omega^\dagger \sigma C \sigma \omega\right) \ , \tag{5.14}$$

where $\sigma = \mathrm{diag}(\sigma_1, \ldots, \sigma_K)$ contains the standard deviations for each of the K assets. The measure $d[\omega]$ is the product of the differentials for each element of ω. We omit the time dependence of the K dimensional return vector $r(t)$ to simplify the notation. The vector ω contains the K Fourier variables and the parameter N is proportional to the inverse variance, see equation (4.7). The relevance of N for financial data has already been discussed in section 4.4.

To factorize the Fourier integral we have to introduce a correlation matrix with a simplified structure, *i.e.*, homogeneous correlations between assets. We already mentioned this matrix during the empirical study in section 4.4, see equation (4.29). This matrix can be expressed as

$$C = (1-c)\mathbb{1} + cee^\dagger \quad , \tag{5.15}$$

where e is a K dimensional vector with ones as its elements and $\mathbb{1}$ is the $K \times K$ identity matrix. This matrix describes homogeneous correlations between all stocks. We insert the homogeneous correlation matrix (5.15) into the general result of the correlation-averaged return distribution (5.14), which yields

$$\langle g\rangle(r|c,N) = \frac{1}{2^{N/2}\Gamma(N/2)} \int_0^\infty \mathrm{d}z\ z^{N/2-1}e^{-z/2} \int \frac{\mathrm{d}[\omega]}{(2\pi)^K} \exp\left(-\mathrm{i}\omega^\dagger r - \frac{z}{2N}\omega^\dagger \sigma \left((1-c)\mathbb{1} + cee^\dagger\right)\sigma\omega\right) \ . \tag{5.16}$$

Splitting the exponential function into two terms, we arrive at

$$\begin{aligned}\langle g\rangle(r|c,N) =& \frac{1}{2^{N/2}\Gamma(N/2)} \int_0^\infty \mathrm{d}z\ z^{N/2-1}e^{-z/2} \\ & \times \int \frac{\mathrm{d}[\omega]}{(2\pi)^K} \exp\left(-\mathrm{i}\omega^\dagger r - \frac{z}{2N}\omega^\dagger \sigma^2 \omega(1-c)\right) \\ & \times \exp\left(-\frac{zc}{2N}(\omega^\dagger \sigma e)^2\right) \ . \end{aligned} \tag{5.17}$$

Now, we express the second exponential as an integral

$$\begin{aligned}&\exp\left(-\frac{zc}{2N}(\omega^\dagger\sigma e)^2\right)\\&=\sqrt{\frac{N}{2\pi zc}}\int_{-\infty}^{+\infty}\mathrm{d}u\ \exp\left(-\mathrm{i}\,u\omega^\dagger\sigma e\right)\exp\left(-\frac{N}{2zc}u^2\right)\quad,\end{aligned}\tag{5.18}$$

to make the Fourier integral in equation (5.17) solvable. The disadvantage is the introduction of a new integral over u.

Performing the inverse Fourier transform in ω yields

$$\begin{aligned}\langle g\rangle(r|c,N)=\frac{1}{2^{N/2}\Gamma(N/2)}\frac{1}{\det\sigma}\int_0^\infty\mathrm{d}z\ z^{N/2-1}\mathrm{e}^{-z/2}\sqrt{\frac{N}{2\pi zc}}\sqrt{\frac{N}{2\pi z(1-c)}}^K\\\times\int_{-\infty}^{+\infty}\mathrm{d}u\,\mathrm{e}^{-Nu^2/(2cz)}\exp\left(-\frac{(r+u\sigma e)^\dagger\sigma^{-2}(r+u\sigma e)}{2z(1-c)/N}\right).\end{aligned}\tag{5.19}$$

We notice that the bilinear form

$$(r+u\sigma e)^\dagger\sigma^{-2}(r+u\sigma e)=\sum_k(r_k+u\sigma_k)^2\sigma_k^{-2}\tag{5.20}$$

can be written as a sum and we recall that the K dimensional vector e contains ones as elements. This yields

$$\begin{aligned}\langle g\rangle(r|c,N)=\frac{1}{2^{N/2}\Gamma(N/2)}\frac{1}{\det\sigma}\int_0^\infty\mathrm{d}z\ z^{N/2-1}\mathrm{e}^{-z/2}\\\times\sqrt{\frac{N}{2\pi zc}}\sqrt{\frac{N}{2\pi z(1-c)}}^K\int_{-\infty}^{+\infty}\mathrm{d}u\ \exp\left(-\frac{N}{2zc}u^2\right)\\\times\exp\left(-\sum_{k=1}^K\frac{N}{2z(1-c)\sigma_k^2}(r_k+u\sigma_k)^2\right)\quad.\end{aligned}\tag{5.21}$$

To get rid of the singularities for the case of fluctuating correlations around zero, $c=0$, we substitute $u=q\sqrt{c}$. The limits of the integration are not affected and we change back the notation $q\to u$ as the integration in u is only a helper integral and has no economic interpretation.

We arrive at the correlation-averaged multivariate normal distribution of returns

$$\begin{aligned}\langle g\rangle(r|c,N) = \frac{1}{2^{N/2}\Gamma(N/2)}\frac{1}{\det\sigma}\int_0^\infty \mathrm{d}z\ z^{N/2-1}\mathrm{e}^{-z/2} \\ \times\sqrt{\frac{N}{2\pi z}}\sqrt{\frac{N}{2\pi z(1-c)}}^{K}\int_{-\infty}^{+\infty}\mathrm{d}u\ \exp\left(-\frac{N}{2z}u^2\right) \\ \times\exp\left(-\sum_{k=1}^{K}\frac{N}{2z(1-c)\sigma_k^2}(r_k+u\sqrt{c}\sigma_k)^2\right)\end{aligned} \tag{5.22}$$

with fluctuating correlations around the average correlation level c. When we later insert the asset value distribution (5.22) into equation (5.10), we want to achieve a factorization of the V_k-integrals. Therefore, we do not carry out the integration in u now.

The last step in the construction of the average asset value distribution is to make the switch from returns r to asset values V. In the spirit of the Merton model, we assume that the asset prices follow a geometric Brownian motion. Therefore, we perform the change of variables

$$r_k \longrightarrow \ln\frac{V_k(T)}{V_{k0}} - \left(\mu_k - \frac{\rho_k^2}{2}\right)T \quad , \tag{5.23}$$

where we denote $V_k(0)$ as V_{k0}. The term $\rho_k^2/2$ is a result of Itō's Lemma [149]. We notice that the formerly dimensionless standard deviations σ_k have to be substituted for the volatilities ρ_k with dimension inverse square root of time according to

$$\sigma_k = \rho_k\sqrt{T} \quad , \tag{5.24}$$

where T is the maturity time. The drift terms μ_k have the dimension of inverse time. This construction ensures that the dimensionless returns r are substituted by a dimensionless quantity.

Finally, we arrive at the result for the average asset value distribution at maturity time T

$$\begin{aligned}\langle g\rangle(V|c,N) = \frac{1}{2^{N/2}\Gamma(N/2)\det\rho}\left(\prod_{k=1}^{K}\frac{1}{V_k(T)}\right)\int_0^\infty \mathrm{d}z\ z^{N/2-1}\mathrm{e}^{-z/2} \\ \times\sqrt{\frac{N}{2\pi z}}\sqrt{\frac{N}{2\pi z(1-c)T}}^{K}\int_{-\infty}^{+\infty}\mathrm{d}u\ \exp\left(-\frac{N}{2z}u^2\right) \\ \times\exp\left(-\sum_{k=1}^{K}\frac{N\left(\ln\frac{V_k(T)}{V_{k0}}-(\mu_k-\frac{\rho_k^2}{2})T+u\sqrt{cT}\rho_k\right)^2}{2z(1-c)T\rho_k^2}\right).\end{aligned} \tag{5.25}$$

The product $\prod_{k=1}^{K}V_k^{-1}(T)$ is the result of the Jacobian determinant due to the change of variables from returns to asset values.

With the average asset value distribution at hand, we can calculate the average loss distribution $\langle p\rangle(L|c,N)$.

5.3.3 Average loss distribution

Now, we have all the necessary prerequisites to calculate the average loss distribution $\langle p \rangle(L|c,N)$, which takes fluctuating correlations between the asset values into account. We start by inserting the average asset value distribution (5.25) in component-wise fashion into the loss distribution (5.10) and sort the terms

$$\begin{aligned}\langle p \rangle(L|c,N) = & \frac{1}{2\pi 2^{N/2}\Gamma(N/2)} \int_0^\infty \mathrm{d}z \; z^{N/2-1}\mathrm{e}^{-z/2} \\ & \times \sqrt{\frac{N}{2\pi z}} \int_{-\infty}^{+\infty} \mathrm{d}u \; \exp\left(-\frac{N}{2z}u^2\right) \int_{-\infty}^{+\infty} \mathrm{d}\nu \; \mathrm{e}^{-\mathrm{i}\nu L} \\ & \times \prod_{k=1}^{K} \left[\int_0^{F_k} \mathrm{d}V_k(T) \exp\left(\mathrm{i}\nu f_k(1 - \frac{V_k(T)}{F_k})\right) + \int_{F_k}^{\infty} \mathrm{d}V_k(T) \right] \\ & \times \left(\prod_{k=1}^{K} \frac{1}{V_k(T)\rho_k} \right) \sqrt{\frac{N}{2\pi z(1-c)T}}^{K} \\ & \times \exp\left(- \sum_{k=1}^{K} \frac{N\left(\ln\frac{V_k(T)}{V_{k0}} - (\mu_k - \frac{\rho_2^k}{2})T + \sqrt{cT}u\rho_k\right)^2}{2z(1-c)T\rho_k^2} \right) . \end{aligned} \tag{5.26}$$

We notice that the determinant $\det\rho$ in equation (5.25) can be written as a product of its diagonal elements, because ρ is a diagonal matrix. We see that the sum in the exponential can be expressed as a product of K exponentials. From this point on, we omit the time dependence T on V_k to simplify the notation. Consolidating everything into one product from $k = 1$ to K yields

$$\begin{aligned}\langle p \rangle(L|c,N) = & \frac{1}{2\pi 2^{N/2}\Gamma(N/2)} \int_0^\infty \mathrm{d}z \; z^{N/2-1}\mathrm{e}^{-z/2} \\ & \times \sqrt{\frac{N}{2\pi z}} \int_{-\infty}^{+\infty} \mathrm{d}u \; \exp\left(-\frac{N}{2z}u^2\right) \int_{-\infty}^{+\infty} \mathrm{d}\nu \; \mathrm{e}^{-\mathrm{i}\nu L} \; \kappa(\nu,z,u) \end{aligned} \tag{5.27}$$

with

$$\kappa(\nu,z,u)=\prod_{k=1}^{K}\left[\int_0^{F_k}\mathrm{d}V_k\exp\left(\mathrm{i}\,\nu f_k(1-\frac{V_k}{F_k})\right)+\int_{F_k}^{\infty}\mathrm{d}V_k\right]\phi(k,z,u) \quad (5.28)$$

and

$$\begin{aligned}\phi(k,z,u)=&\frac{\sqrt{N}}{\sqrt{2\pi z(1-c)T}V_k\rho_k}\\ &\times\exp\left(-\frac{N\left(\ln\frac{V_k}{V_{k0}}-\left(\mu_k-\frac{\rho_k^2}{2}\right)T+\sqrt{cT}u\rho_k\right)^2}{2z(1-c)T\rho_k^2}\right).\end{aligned} \quad (5.29)$$

We observe that the factor before the exponential function normalizes the expression to unity. To make analytical progress we write the product in equation (5.28) as a composition of the logarithm with the exponential function and arrive at

$$\kappa(\nu,z,u)=\exp\left(\sum_{k=1}^{K}\ln\left(\left[\int_0^{F_k}\mathrm{d}V_k\mathrm{e}^{\mathrm{i}\,\nu f_k(1-V_k/F_k)}+\int_{F_k}^{\infty}\mathrm{d}V_k\right]\phi(k,z,u)\right)\right). \quad (5.30)$$

We now carry out two substitutions $V_k = V_{k0}\exp\left(\sqrt{z}\hat{V}_k+\left(\mu_k-\rho_k^2/2\right)T\right)$ and $u=\sqrt{z}\xi$ to make a later numerical evaluation of the integrals easier. The latter substitution does not alter the limits of the integration and we change back the notation $\xi\to u$ as the integration in u is only a helper integral and has no economic meaning. The substitutions yield

$$\begin{aligned}\langle p\rangle(L|c,N)=&\frac{1}{2\pi 2^{N/2}\Gamma(N/2)}\int_0^{\infty}\mathrm{d}z\;z^{N/2-1}\mathrm{e}^{-z/2}\sqrt{\frac{N}{2\pi}}\int_{-\infty}^{+\infty}\mathrm{d}u\;\mathrm{e}^{-Nu^2/2}\\ &\times\int_{-\infty}^{+\infty}\mathrm{d}\nu\;\mathrm{e}^{-\mathrm{i}\,\nu L}\;\kappa(\nu,z,u)\end{aligned} \quad (5.31)$$

with

$$\kappa(\nu,z,u)=\exp\left(\sum_{k=1}^{K}\ln\left(\mathcal{T}(k,\nu,z)\frac{\sqrt{N}\exp\left(-\frac{N(\hat{V}_k+\sqrt{cT}u\rho_k)^2}{2T(1-c)\rho_k^2}\right)}{\rho_k\sqrt{2T\pi(1-c)}}\right)\right) \quad (5.32)$$

and with the integration operator

$$\mathcal{T}(k,\nu,z) = \left[\int_{-\infty}^{\hat{F}_k} \mathrm{d}\hat{V}_k \exp\left(\mathrm{i}\,\nu f_k \left(1 - \frac{V_{k0}}{F_k} \mathrm{e}^{\sqrt{z}\hat{V}_k + \mu_k T - \frac{\rho_k^2}{2}T} \right) \right) + \int_{\hat{F}_k}^{\infty} \mathrm{d}\hat{V}_k \right] . \tag{5.33}$$

The new upper limit of the integral is

$$\hat{F}_k = \frac{1}{\sqrt{z}} \left(\ln \frac{F_k}{V_{k0}} - \left(\mu_k - \frac{\rho_k^2}{2} \right) T \right) \quad . \tag{5.34}$$

We assume that the contracts in the portfolio have weights of equal magnitude in the order of $f_k \approx 1/K$. This assumption is reasonable, because the investor tries to diversify as much as possible to reduce his risk, *i.e.*, K is large. This allows us later to carry out a second order approximation in f_k and we will be able to solve the $\mathrm{d}\nu$-integral. Therefore, we expand the exponential function in equation (5.33)

$$\begin{aligned} & \exp\left(\mathrm{i}\,\nu f_k \left(1 - \frac{V_{k0}}{F_k} \exp\left(\sqrt{z}\hat{V}_k + \left(\mu_k - \frac{\rho_k^2}{2} \right) T \right) \right) \right) \\ = & \sum_{j=0}^{\infty} \frac{(\mathrm{i}\,\nu f_k)^j}{j!} \left(1 - \frac{V_{k0}}{F_k} \exp\left(\sqrt{z}\hat{V}_k + \left(\mu_k - \frac{\rho_k^2}{2} \right) T \right) \right)^j \\ = & 1 + \sum_{j=1}^{\infty} \frac{(\mathrm{i}\,\nu f_k)^j}{j!} \left(1 - \frac{V_{k0}}{F_k} \exp\left(\sqrt{z}\hat{V}_k + \left(\mu_k - \frac{\rho_k^2}{2} \right) T \right) \right)^j \end{aligned} \tag{5.35}$$

and insert the result into the average loss distribution $\langle g \rangle(L|c,N)$. The expansion only affects the operator $\mathcal{T}(k,\nu,z)$, see equation (5.33). We arrive at

$$\kappa(\nu,z,u) = \exp\left(\sum_{k=1}^{K} \ln \left(\mathcal{T}(k,\nu,z) \frac{\sqrt{N} \exp\left(-\frac{N\left(\hat{V}_k + \sqrt{cT}u\rho_k \right)^2}{2T(1-c)\rho_k^2} \right)}{\rho_k \sqrt{2\pi T(1-c)}} \right) \right) \tag{5.36}$$

with

$$\mathcal{T}(k,\nu,z) = \left[\int_{-\infty}^{\hat{F}_k} \mathrm{d}\hat{V}_k \sum_{j=1}^{\infty} \frac{(\mathrm{i}\,\nu f_k)^j}{j!} \left(1 - \frac{V_{k0}}{F_k} \mathrm{e}^{\sqrt{z}\hat{V}_k + \mu_k T - \frac{\rho_k^2}{2}T} \right)^j + \int_{-\infty}^{+\infty} \mathrm{d}\hat{V}_k \right] . \tag{5.37}$$

The expansion of the exponential function (5.35) has given us an additional term of 1 before the sum, which inserted into equation (5.33) results in an additional integral from $-\infty$ to $\hat{F}_k$. We join the second integration from $\hat{F}_k$ to $+\infty$ with this integral and receive an integral over the whole real axis. We constructed the term after the operator to be normalized if integrated over the whole domain. Therefore, the second integral yields one, and we arrive at

$$\kappa(\nu,z,u) = \exp\left(\sum_{k=1}^{K}\ln\left(1+\sum_{j=1}^{\infty}\frac{(\mathrm{i}\,\nu f_k)^j}{j!}\frac{\sqrt{N}}{\rho_k\sqrt{2\pi T(1-c)}}\right.\right.$$
$$\times\int_{-\infty}^{\hat{F}_k}\mathrm{d}\hat{V}_k\,\left(1-\frac{V_{k0}}{F_k}\exp\left(\sqrt{z}\hat{V}_k+\left(\mu_k-\frac{\rho_k^2}{2}\right)T\right)\right)^j$$
$$\left.\left.\times\exp\left(-\frac{N\left(\hat{V}_k+\sqrt{cT}u\rho_k\right)^2}{2T(1-c)\rho_k^2}\right)\right)\right) \quad . \tag{5.38}$$

This simplifies the κ function to

$$\kappa(\nu,z,u) = \exp\left(\sum_{k=1}^{K}\ln\left(1+\sum_{j=1}^{\infty}\frac{(\mathrm{i}\,\nu f_k)^j}{j!}m_{jk}(z,u)\right)\right) \tag{5.39}$$

with the j-th moment

$$m_{jk}(z,u) = \frac{\sqrt{N}}{\rho_k\sqrt{2\pi T(1-c)}}$$
$$\times\int_{-\infty}^{\hat{F}_k}\mathrm{d}\hat{V}_k\,\left(1-\frac{V_{k0}}{F_k}\exp\left(\sqrt{z}\hat{V}_k+\left(\mu_k-\frac{\rho_k^2}{2}\right)T\right)\right)^j$$
$$\times\exp\left(-\frac{N\left(\hat{V}_k+\sqrt{cT}u\rho_k\right)^2}{2T(1-c)\rho_k^2}\right) \quad . \tag{5.40}$$

The explicit expressions for the first three moments $j = 0, 1, 2$ are shown for the case of homogeneous portfolios with $f_k = 1/K$ in appendix C.

Inserting equation (5.39) into the average loss distribution (5.31) up to the second order, *i.e.*, $j = 1, 2$ and expanding the logarithm collecting only terms up to the second order in f_k yields

$$\begin{aligned}\langle p\rangle(L|c,N) \approx & \frac{1}{2\pi 2^{N/2}\Gamma(N/2)} \int_0^\infty \mathrm{d}z\ z^{N/2-1}\mathrm{e}^{-z/2}\sqrt{\frac{N}{2\pi}} \int_{-\infty}^{+\infty} \mathrm{d}u\ \mathrm{e}^{-Nu^2/2} \\ & \times \int_{-\infty}^{+\infty} \mathrm{d}\nu\ \mathrm{e}^{-\mathrm{i}\,\nu L} \exp\left(\sum_{k=1}^{K}\left(\mathrm{i}\,\nu f_k m_{1k}(z,u)\right.\right. \\ & \left.\left. -\frac{\nu^2 f_k^2}{2}\left(m_{2k}(z,u) - m_{1k}^2(z,u)\right)\right)\right) \quad . \end{aligned} \tag{5.41}$$

We rearrange the terms in the argument of the exponential function and arrive at

$$\begin{aligned}\langle p\rangle(L|c,N) = & \frac{1}{2\pi 2^{N/2}\Gamma(N/2)} \int_0^\infty \mathrm{d}z\ z^{N/2-1}\mathrm{e}^{-z/2}\sqrt{\frac{N}{2\pi}} \int_{-\infty}^{+\infty} \mathrm{d}u\ \mathrm{e}^{-Nu^2/2} \\ & \times \int_{-\infty}^{+\infty} \mathrm{d}\nu\ \exp\left(\mathrm{i}\,\nu\left(\sum_{k=1}^{K} f_k m_{1k}(z,u) - L\right)\right. \\ & \left. -\frac{\nu^2}{2}\left(\sum_{k=1}^{K} f_k^2\left(m_{2k}(z,u) - m_{1k}^2(z,u)\right)\right)\right) . \end{aligned} \tag{5.42}$$

At this point we are able to solve the ν-integral

$$\begin{aligned} & \int_{-\infty}^{+\infty} \mathrm{d}\nu \exp\left(\mathrm{i}\,\nu\left(\underbrace{\sum_{k=1}^{K} f_k m_{1k}(z,u)}_{M_1(z,u)} - L\right)\right. \\ & \qquad \left. -\frac{\nu^2}{2}\left(\underbrace{\sum_{k=1}^{K} f_k^2\left(m_{2k}(z,u) - m_{1k}^2(z,u)\right)}_{M_2(z,u)}\right)\right) \\ & = \frac{\sqrt{2\pi}}{\sqrt{M_2(z,u)}} \exp\left(-\frac{(L - M_1(z,u))^2}{2M_2(z,u)}\right) \quad . \end{aligned} \tag{5.43}$$

Here, we define the functions

$$M_1(z,u) = \sum_{k=1}^{K} f_k m_{1k}(z,u) \tag{5.44}$$

and

$$M_2(z,u) = \sum_{k=1}^{K} f_k^2 \left(m_{2k}(z,u) - m_{1k}^2(z,u) \right) \quad , \tag{5.45}$$

to simplify the notation. We arrive at the final result for the average loss distribution

$$\begin{aligned} \langle p \rangle (L|c,N) = & \frac{1}{\sqrt{2\pi} 2^{N/2} \Gamma(N/2)} \int_0^\infty \mathrm{d}z \; z^{N/2-1} \mathrm{e}^{-z/2} \sqrt{\frac{N}{2\pi}} \int_{-\infty}^{+\infty} \mathrm{d}u \; \mathrm{e}^{-Nu^2/2} \\ & \times \frac{1}{\sqrt{M_2(z,u)}} \exp\left(-\frac{(L - M_1(z,u))^2}{2M_2(z,u)} \right) , \end{aligned} \tag{5.46}$$

which takes non-stationary correlations into account. The z- and u-integral must be evaluated numerically due to their complexity. We defer the discussion of the average loss distribution to section 5.4. First, we discuss the loss distribution for homogeneous portfolios in section 5.3.4. The expression (5.46) allows us to derive a limiting distribution of infinite portfolio size for homogeneous portfolios in section 5.3.5.

5.3.4 Homogeneous portfolio

For a homogeneous portfolio all contracts have the same face value $F_k = F$, variance $\sigma_k^2 = \sigma^2$, drift $\mu_k = \mu$ and start asset value $V_{k0} = V_0$. Generally speaking, the k-dependence is dropped from the average loss distribution. This greatly simplifies the moment functions (5.44) and (5.45), which makes the numerical evaluation of the average loss distribution substantially faster. The j-th moment reads

$$\begin{aligned} m_j(z,u) = & \frac{\sqrt{N}}{\rho\sqrt{2\pi T(1-c)}} \int_{-\infty}^{\hat{F}} \mathrm{d}\hat{V} \left(1 - \frac{V_0}{F} \exp\left(\sqrt{z}\hat{V} + \left(\mu - \frac{\rho^2}{2} \right) T \right) \right)^j \\ & \times \exp\left(-\frac{N\left(\hat{V} + \sqrt{cT}u\rho \right)^2}{2T(1-c)\rho^2} \right) \end{aligned} \tag{5.47}$$

with the upper limit

$$\hat{F} = \frac{1}{\sqrt{z}} \left(\ln \frac{F}{V_0} - \left(\mu - \frac{\rho^2}{2} \right) T \right) \tag{5.48}$$

and $\hat{V} = (\ln(V(T)/V_0) - (\mu - \rho^2/2)T)/\sqrt{z}$. The portfolio weights are simply

$$f_k = \frac{1}{K} \tag{5.49}$$

due to the normalization of the weights (5.6), *i.e.*, all credit contracts have the same weight. The functions $M_1(z,u)$ and $M_2(z,u)$ simplify to

$$\begin{aligned} M_1(z,u) &= m_1(z,u) \\ M_2(z,u) &= \frac{1}{K}\left(m_2(z,u) - m_1^2(z,u)\right) \quad . \end{aligned} \tag{5.50}$$

The first three moments $j = 0, 1, 2$, which are required for M_1 and M_2, are shown in appendix C.

5.3.5 Limit for very large homogeneous portfolios

We derive a limiting function for very large ($K \to \infty$) portfolios. This will allow us to study the effect of diversification on portfolio risk. By using the homogeneous moments (5.50) in the average loss distribution (5.46) we receive the homogeneous average loss distribution

$$\begin{aligned} \langle p \rangle(L|c,N) = \frac{1}{\sqrt{2\pi}2^{N/2}\Gamma(N/2)} \int_0^\infty \mathrm{d}z \; z^{N/2-1}\mathrm{e}^{-z/2} \sqrt{\frac{N}{2\pi}} \int_{-\infty}^{+\infty} \mathrm{d}u \; \mathrm{e}^{-Nu^2/2} \\ \times \frac{1}{\sqrt{M_2(z,u)}} \exp\left(-\frac{(L - M_1(z,u))^2}{2M_2(z,u)}\right) \quad . \end{aligned} \tag{5.51}$$

We notice that the second line of the equation can be expressed as a delta function

$$\frac{1}{\sqrt{2\pi M_2(z,u)}} \exp\left(-\frac{(L - M_1(z,u))^2}{2M_2(z,u)}\right) = \delta(L - M_1(z,u)) \tag{5.52}$$

if $M_2(z,u) \to 0$ goes to zero. This is exactly the case for $K \to \infty$, compare equation (5.50). We arrive at

$$\begin{aligned} \langle p \rangle(L|c,N) = \frac{1}{2^{N/2}\Gamma(N/2)} \int_0^\infty \mathrm{d}z \, z^{N/2-1}\mathrm{e}^{-z/2} \sqrt{\frac{N}{2\pi}} \\ \times \int_{-\infty}^{+\infty} \mathrm{d}u \, \exp\left(-\frac{N}{2}u^2\right) \delta(L - m_1(z,u)) \quad . \end{aligned} \tag{5.53}$$

We use the integral form of the generalized scaling property

$$\int_{-\infty}^{+\infty} \mathrm{d}u\, h(u)\delta(f(u)) = \frac{h(u_0)}{|\partial f(u_0)/\partial u_0|} \tag{5.54}$$

for the δ-function, where u_0 is the real root of the function $f(u)$. The δ-function in equation (5.53) contributes only to the u-integral if its argument is zero. The argument of the delta function is

$$f(z,u) = L - m_1(z,u) \tag{5.55}$$

and we calculate the inverse function $u_0(L,z)$ of

$$0 = L - m_1(z,u_0) \quad . \tag{5.56}$$

To simplify the notation we drop the arguments of u_0. The partial derivative of the δ-functions' argument at u_0 is

$$\left|\frac{\partial f(z,u)}{\partial u}\right|_{z,u_0} = \left|\frac{\partial m_1(z,u)}{\partial u}\right|_{z,u_0} \quad . \tag{5.57}$$

Now, we solve the u-integral with the generalized scaling property of the delta function. This leads to the average loss distribution for the limit case $K \to \infty$

$$\begin{aligned}\langle p\rangle(L|c,N) = {} & \frac{1}{2^{N/2}\Gamma(N/2)}\sqrt{\frac{N}{2\pi}}\int_0^\infty \mathrm{d}z\, z^{N/2-1}\mathrm{e}^{-z/2} \\ & \times \exp\left(-\frac{N}{2}u_0^2\right)\frac{1}{|\partial m_1(z,u)/\partial u|_{z,u_0}} \quad .\end{aligned} \tag{5.58}$$

The L dependence is now hidden in the inverse function u_0 according to equation (5.55). We will defer the discussion of the implications for credit portfolios to section 5.4.

5.4 Limits of stationary asset correlations

In section 5.4.1 we show the average loss distribution and its parameter dependence for empirically obtained parameters. Monte-Carlo simulations are carried out in section 5.4.2 to study the VaR and ETL properties of our average loss distribution.

5.4.1 Average loss distribution

In section 4.4, we have given an empirical justification for our correlation-averaged multivariate normal distribution (5.14). The distribution is able

to describe the empirically observed multivariate returns. We use this distribution to model the distribution of the asset values (5.25) in the Merton model at the maturity time T. There are four parameters in the case of ho-

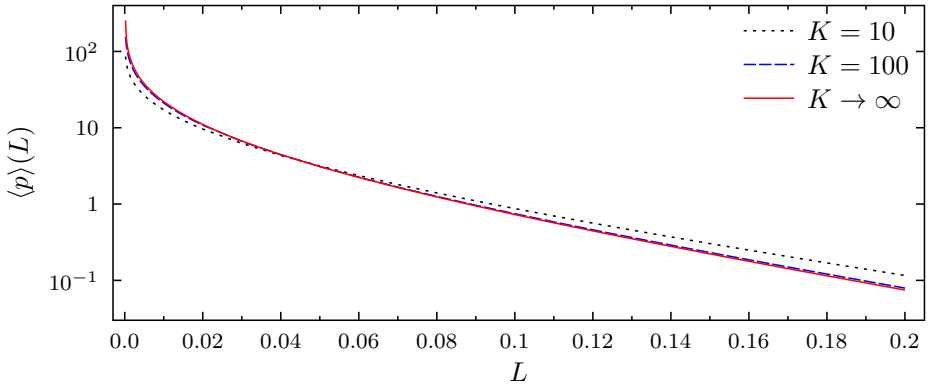

(a) $T = 20$ trading days

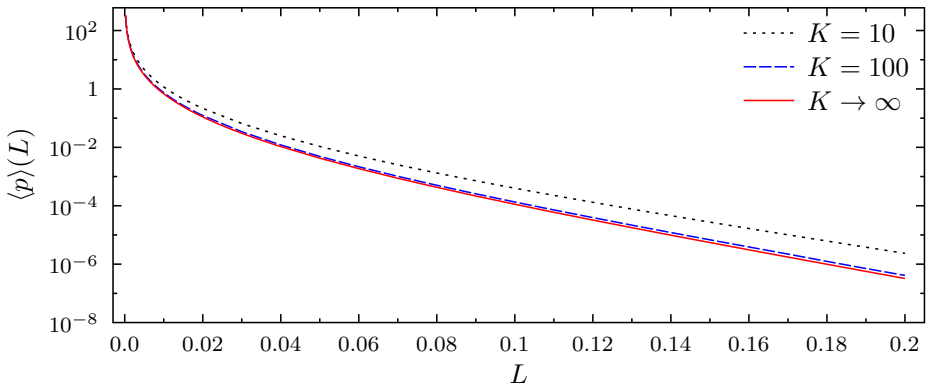

(b) $T = 1$ year

Figure 5.4: The average loss distribution for portfolio sizes of $K = 10$ and $K = 100$. In addition the limit $K \to \infty$ is shown. The parameters are $N = 4.2$, $\mu = 0.013$ month^{-1}, $\sigma = 0.1$ month$^{-1/2}$, $T = 20$ trading days and an average correlation level of $c = 0.26$ (top). For a maturity time of $T = 1$ year, $N = 6.0$, $\mu = 0.17$ year^{-1}, $\sigma = 0.35$ year$^{-1/2}$ and an average correlation level of $c = 0.28$ (bottom).

mogeneous portfolios. The average drift μ, the average volatility σ and the average correlation level c are easily obtainable from empirical data. The last parameter N, which controls the fluctuations around the average correlation matrix, should be estimated according to section 4.4. Smaller values of N lead to stronger fluctuations. The average loss distribution with fluctuating

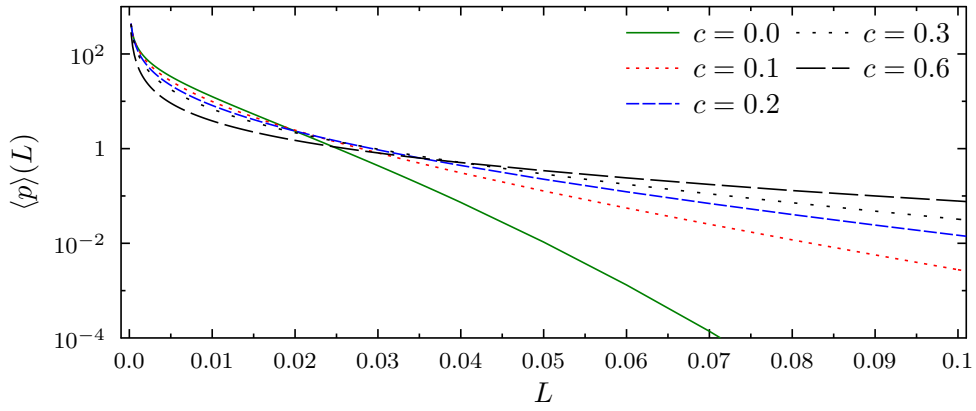

Figure 5.5: Average loss distribution for different average correlation levels c. The parameters are $\mu = 0.013$ month^{-1}, $\sigma = 0.1$ month$^{-1/2}$, $T = 1$ month, $K = 100$ and $N = 4.2$.

correlations $\langle p \rangle(L|c, N)$ between asset values for the Merton model is shown in figure 5.4. We choose different values for the size of the portfolio $K = 10, 100$ and present the limiting case for infinite sized portfolios $K \to \infty$. The remaining parameters are fixed at typical values obtained from empirical data, see the caption of figure 5.4 for the values. Non-integer values for N are obtained with a least squares fit and confirmed by the Cramer-von Mises test. For the face value, we choose $F = 75$ and the initial asset value at time $t = 0$ is $V_0 = 100$. The distribution shows slowly decreasing heavy tails. We im-

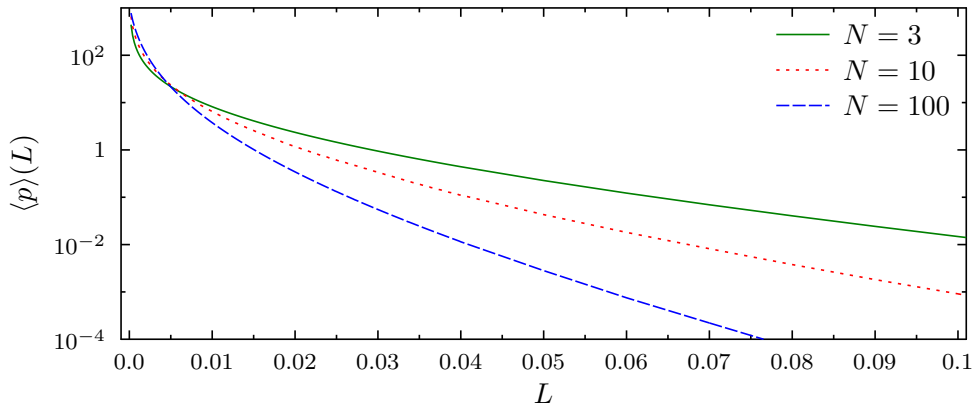

Figure 5.6: Average loss distribution for different values of N. The parameters are $\mu = 0.015$ month^{-1}, $\sigma = 0.25$ month$^{-1/2}$, $T = 1$ month, $K = 500$ and $c = 0.2$

mediately notice, that increasing the portfolio size from 10 to 100 contracts leads to a small decrease in risk. However, the advantages of diversification quickly vanish, as increasing the portfolio size any further quickly converges to the loss distribution for portfolios of infinite size. Here, we come to a nice quantitative understanding why diversification is not working in the presence of even weakly correlated assets. Figure 5.5 shows that the situation becomes worse for stronger average correlations between the assets. The tail of the average loss distribution gets wider with increasing average correlation level c and so the chance of larger losses grows. The influence of the parameter N is presented in figure 5.6. The smaller N the greater the probability of large losses gets. This is in accordance with our interpretation of the parameter N. Stronger fluctuations of the correlation lead to an increase in risk. In this context it is alarming that in general smaller values of N are needed to describe the data.

5.4.2 Value at Risk and Expected Tail Loss

Until now, we have only studied the homogeneous case with average drift μ, volatilities σ and our homogeneous correlation matrix. The rationale behind this simplification is to make analytical progress in the calculation. Here, we study how good the assumption of homogeneous portfolios is and have a deeper look at empirical covariances. We use Value at Risk (VaR) and Expected Tail Loss (ETL) to quantify the portfolio risk. To achieve this we use Monte-Carlo simulations.

For each Monte-Carlo simulation step we calculate the K dimensional vector

$$V(T) = V_0 \exp\left(\frac{\sqrt{T}}{\sqrt{N}}\sigma\left(U^{-1}\,\Lambda\,\mathcal{N}\right)n + \mu T - \frac{1}{2}\sigma^2 eT\right) \quad , \tag{5.59}$$

containing the asset values at maturity time T. The elements of the $K \times N$ matrix $\mathcal{N}$ are drawn from a standard normal distribution, as the elements of the N dimensional vector n. The diagonal matrix $\sigma = \mathrm{diag}(\sigma_1, \ldots, \sigma_K)$ contains the volatilities for each stock. The K dimensional drift vector μ stores the average for each asset. The vector e is K dimensional and contains only ones. The columns of the matrix U are the eigenvectors of the correlation matrix C, while the matrix Λ has the eigenvalues of the correlation matrix as diagonal elements. The K dimensional vector V_0 holds the initial price of the asset at the beginning of the credit contract. For each simulation step we calculate the portfolio loss

$$L^{(\mathrm{MC})} = \frac{1}{K}\sum_{k=0}^{K}\frac{F_k - V_k(T)}{F_k}\Theta(F_k - V_k(T)) \quad , \tag{5.60}$$

where the Heaviside function filters out all cases where the price at maturity

time $V_k(T)$ is larger than the face value F_k, *i.e.*, taking only losses into account. We run 50 million simulation steps and sort the results into a histogram, which yields the loss distribution for fluctuating correlations.

First, we investigate the capabilities of the covariance matrix with homogeneous correlation structure to estimate the VaR and the ETL. A classic approach in financial applications is to estimate a covariance matrix over a longer period of time to reduce measurement noise, say five years for example. This covariance matrix is then used as input for portfolio optimization or other risk frameworks. Following these lines, we want to know how our covariance matrix with homogeneous correlations compares to the full covariance matrix.

Time horizon for estimation	K	N_{hom}	N_{emp}	$\bar{\sigma}$ in month$^{-1/2}$	$\bar{\mu}$ in month^{-1}	c
2006-2010	465	5	12	0.11	0.009	0.40
2002-2004	436	5	14	0.10	0.015	0.30
2008-2010	478	5	7	0.12	0.01	0.46

Table 5.1: Parameters used for the different time horizons.

On the time horizons shown in table 5.1, we estimate the sample covariance matrix for stocks from the S&P 500 index for monthly returns. The portfolio is comprised only of stocks which were continuously traded during the time period in question. In addition, we estimate the average drift $\bar{\mu}$, volatility $\bar{\sigma}$ and correlation level c. The parameter N is determined as described in section 4.4 for each time horizon. For the numerical simulations only integer values of N can be used, in contrast to the analytic result. During the financial crisis a smaller value of $N_{\text{emp}} = 7$ is necessary to model the higher than usual fluctuations of the variances. We run Monte-Carlo simulations for the full empirical sample covariance matrix and for our homogeneous covariance matrix and calculate the VaR and ETL from the resulting loss distribution.

We calculate the relative deviation of the VaR and ETL for different probability levels of $\alpha = 0.99, 0.995, 0.999$ between the empirical covariance matrix and the covariance matrix with homogeneous correlation structure. For the latter we have two possible choices. We can take the average homogeneous volatilities and drift to calculate the covariance matrix from our homogeneous correlation matrix. Then the covariance matrix is also homogeneous. Alternatively, we can take heterogeneous drift and volatilities. The resulting covariance matrix then has a homogeneous correlation structure, but consists of heterogeneous volatilities. The homogeneous covariance matrix resembles the homogeneous case discussed in section 5.3.4 and the results are shown in table 5.2. The results for the second case with heterogeneous drift and volatility vector is shown in table 5.3. Positive values denote that the covariance

time	F/V_0	δVaR 99.0 in %	δVaR 99.5 in %	δVaR 99.9 in %	δETL 99.0 in %	δETL 99.5 in %	δETL 99.9 in %
2006-2010	0.75	-45.5	-35.0	-13.5	-26.0	-18.0	-1.0
	0.80	-21.0	-12.5	3.0	-6.5	-0.5	11.5
	0.85	-4.5	1.0	11.0	4.0	8.0	15.5
	0.90	3.0	6.5	12.0	8.0	10.5	15.0
2002-2004	0.75	-69.5	-60.0	-38.0	-51.0	-42.5	-22.0
	0.80	-41.0	-30.5	-9.0	-23.0	-14.0	3.5
	0.85	-12.5	-4.0	11.0	0.5	7.0	18.5
	0.90	4.5	9.0	17.5	11.5	15.0	22.0
2008-2010	0.75	-42.5	-33.5	-17.0	-27.0	-21.0	-8.5
	0.80	-21.5	-15.5	-4.0	-11.5	-7.0	1.0
	0.85	-8.0	-4.0	2.5	-2.0	0.5	5.0
	0.90	-1.0	1.0	5.0	2.0	3.5	6.5

Table 5.2: Relative deviation δ of the VaR and ETL between the covariance matrix with homogeneous correlation structure and an empirical covariance matrix in percent. We use homogeneous volatility and drift vectors. Positive values denote that the covariance matrix with homogeneous correlation structure overestimates VaR and ETL, while negative values show an underestimation. We present the VaR and ETL at 99%, 99.5% and 99.9%.

matrix with homogeneous correlation structure overestimates VaR and ETL, while negative values show an underestimation. We round all values to increments of 0.5. In the case of homogeneous volatilities and drift we find that the covariance matrix with homogeneous correlation structure underestimates the risk in most instances. If we use heterogeneous volatilities and drifts, we find that the covariance matrix with homogeneous correlation structure is an appropriate fit and has a tendency to slightly overestimate the VaR and ETL. A clear trend is visible, which shows that for larger leverages F/V_0 the deviations from the empirical covariance matrix decrease. This shows that the structure of the correlation matrix plays a secondary role and underlines the importance of estimating the volatilities as well as possible. We learned a similar lesson in chapter 2, where better volatility estimation techniques improved the spatial dependence model significantly.

In the first part of our numerical study we exclusively used our random matrix approach which takes fluctuating correlations into account. The following simulations compare this approach to a conventional model with stationary correlations. Stationary correlations correspond to the case $N \to \infty$, which effectively reduces the variance of the elements of the random matrix to zero.

time	F/V_0	δVaR 99.0 in %	δVaR 99.5 in %	δVaR 99.9 in %	δETL 99.0 in %	δETL 99.5 in %	δETL 99.9 in %
2006-2010	0.75	18.0	18.5	20.0	19.5	20.0	22.5
	0.80	12.0	13.0	16.0	14.0	15.0	18.0
	0.85	7.5	9.0	12.5	10.0	12.0	15.0
	0.90	5.0	6.5	10.5	8.0	9.5	12.5
2002-2004	0.75	12.0	14.0	19.5	16.5	18.5	24.0
	0.80	12.0	14.5	20.5	17.0	19.0	24.5
	0.85	11.5	14.5	20.0	16.0	18.5	23.0
	0.90	10.0	12.5	17.0	14.0	15.5	19.5
2008-2010	0.75	-1.0	-1.5	-0.50	-1.0	-1.0	0.5
	0.80	-2.0	-2.0	-0.0	-1.0	-0.5	1.5
	0.85	-2.0	-1.5	1.0	-0.5	0.0	2.0
	0.90	-1.5	-0.5	1.5	0.0	1.0	3.0

Table 5.3: Relative deviation δ of the VaR and ETL between the covariance matrix with homogeneous correlation structure and an empirical covariance matrix in percent. We use the empirically found volatilities and drift for each stock. Positive values denote that the covariance matrix with homogeneous correlation structure overestimates VaR and ETL, while negative values show an underestimation. We present the VaR and ETL at 99%, 99.5% and 99.9%.

We calculate the relative deviation of the VaR for $N \to \infty$ and for different values of N. We use the empirical covariance matrix from the time horizon of 2006-2010, *i.e.*, the volatilities and drift are heterogeneous vectors. We found $N = 12$ for the covariance matrix and for this N the VaR is underestimated between 30% and 40%, see figure 5.7. We call to mind that an empirical covariance matrix requires larger values for the parameter N as discussed in section 4.4.

Figure 5.8 shows the dependence of the average correlation level c for the covariance matrix with homogeneous correlation structure. Again, we show how much stationary correlations underestimate the VaR dependent compared to fluctuating correlations. The VaR is underestimated by roughly 45% for common empirically observed average correlation levels between 0.2 and 0.4.

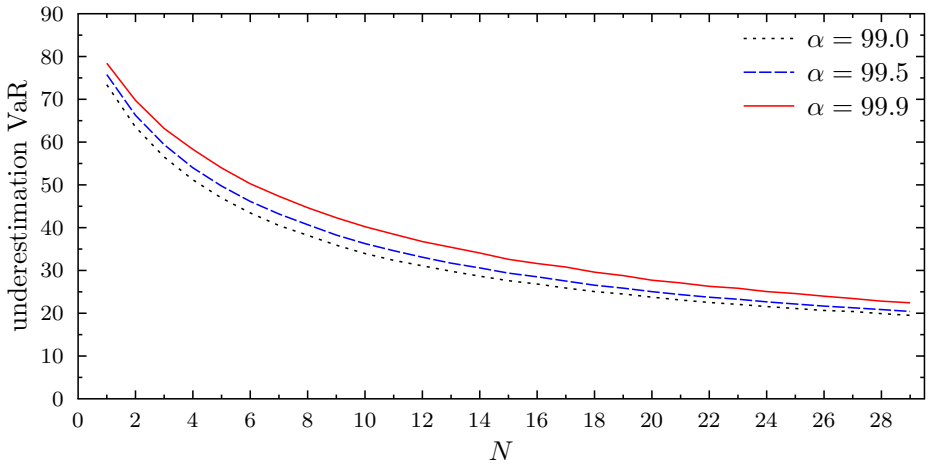

Figure 5.7: Underestimation of the VaR for the empirical covariance matrix (2006-2010) if fluctuating correlations are not taken into account. Comparison for different values of N. The empirically obtained value for the covariance matrix is $N_{\text{emp}} = 12$.

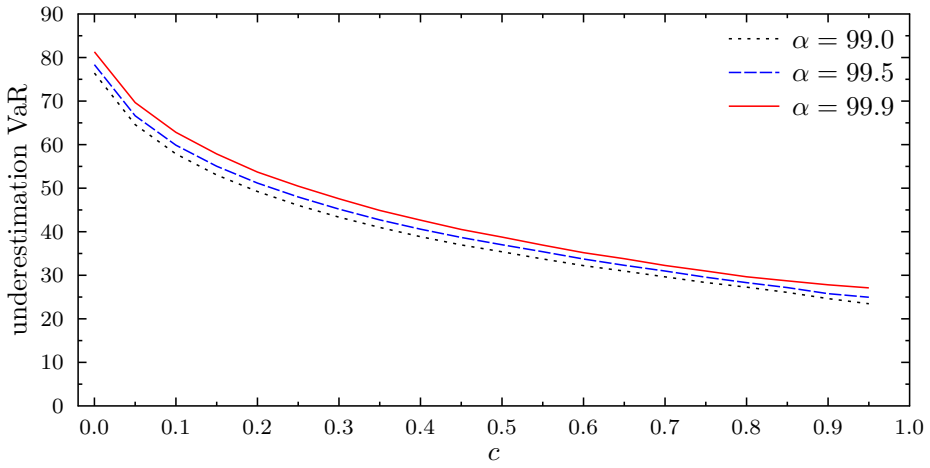

Figure 5.8: Underestimation of the VaR in the case of the covariance matrix with homogeneous correlation structure if fluctuating correlations are not taken into account. We use homogeneous volatilities and drifts. Parameters are $N = 5$, $K = 500$, $\bar{\sigma} = 0.25$ year$^{-1/2}$, $\bar{\mu} = 0.15$ year^{-1} and different values of c.

5.5 Conclusion

In chapter 4 we constructed a correlation-averaged normal distribution to address the non-stationarity inherent in correlated financial time series. We carried out an empirical study in section 4.4 to validate our random matrix ansatz for financial time series. In this chapter we inserted the correlation-averaged normal distribution after a change of variables from returns to asset values as a realistic distribution to describe the asset values into the Merton model.

We constructed the average loss distribution for a portfolio of credit contracts in the case of a homogeneous correlation matrix. The homogeneous correlation matrix allows us to consider fluctuations around arbitrary average correlation levels, which generalizes previous studies [146]. We find that for realistic average correlation levels the tails of the loss distribution become even heavier than for an average correlation level of zero. Taking the non-stationarity of correlations and covariances into account uncovers an intrinsic risk to credit portfolios. In addition, our model gives a vivid quantitative description why for credit portfolios the benefits of diversification are very limited if correlations between the assets are present. We derived an analytic expression for the limiting case for a portfolio of infinite size and find that the risk is not significantly lowered compared to a portfolio with one hundred credit contracts. In reality, banks have thousands of credit contracts and therefore do not operate in regions where diversification is able to lower the risk.

We further carried out Monte-Carlo simulations for VaR and ETL. The analysis shows that the assumption of a homogeneous correlation structure yields good results if the heterogeneous volatilities are taken into account. This underlines the importance of good estimation techniques for variances. In addition, the simulations show that not taking the non-stationarity into account the VaR is underestimated by roughly 40%. While using the full covariance matrix requires the use of numerics the analytical results have another benefit. They allow us to capture the financial market with only two "macroscopic" parameters, the average correlation level c and the strength of the fluctuations N around the homogeneous correlation matrix. We achieved this by leveraging a concept from statistical physics: ensemble average.

A quantitative understanding of the effects of non-stationarity is very important for risk management. This understanding can help to improve the risk estimation for financial products which are built around a selection of multiple credit contracts such as collateralized debt obligations (CDOs).

Chapter 6

Summary and outlook

The basic idea of econophysics is to apply methods and concepts of (statistical) physics to economics problems. The academic training of physicists includes a strong emphasis on analyzing empirical data on the one hand and building models to describe the data on the other hand. This uniquely enables physicists to contribute to some economics problems where large amounts of empirical data are available, *e.g.*, financial markets.

We started in chapter 2 by investigating the effects of non-stationarity inherent in the covariance matrix in a practical setting, *i.e.*, portfolio optimization and saw how important it is to take the non-stationarity into account. Different combinations of methods to improve the estimation of the covariance matrix were studied by us. The results showed that sophisticated methods are necessary to remove the negative effects of the non-stationarity.

Two of the refinement methods are based on a stochastic process (GARCH). While the results are satisfying, it raised the question how well stochastic processes describe the empirical data. We carried out an extensive empirical study on intraday data employing the quantile-based correlation method of Dette *et. al* in chapter 3. We find that it provides an extensive overview of the temporal dependencies in financial return time series. Being able to choose the quantile pair freely for the filtered time series allows us to observe volatility clustering, the leverage effect and asymmetries between positive and negative lags. Providing such a detailed picture of the time series makes an excellent tool to analyze the agreement of stochastic processes with empirical data. While it is beyond the scope of this work to test all known processes we find some shortcomings for popular GARCH type processes. Importantly, the EGARCH does not reproduce the empirical findings. On the other hand, the GJR-GARCH is at least able to replicate the basic empirical features. We strongly advertize the use of the quantile-based correlation function to study financial time series.

With the practical consequences of non-stationarity and the shortcomings of stochastic processes in mind we develop a better statistical description of financial markets as a whole. We addressed the problems of non-stationarity in the covariance matrix by assuming that each realization of a multivariate sample vector is drawn from a multivariate normal distribution with its own random covariance matrix. Averaging the multivariate normal distribution

over an ensemble of matrices, where the elements are drawn from a Wishart distribution, yields a realistic distribution to describe the multivariate return distribution.

This approach is reminiscent of an ensemble average in statistical physics, where a system with many degrees of freedom is captured by a set of macroscopic variables. We are able to capture the financial market with our multivariate approach by an average covariance matrix and one parameter governing the strength of the fluctuations around this average matrix. We conclude that in this framework the instability of financial markets is inherent in the system and a direct result of the non-stationarity.

We find that the empirical rotated and scaled returns are well described by the correlation-averaged normal distribution over three orders of magnitude. Additional research conducted by Chetalova *et. al.* shows that the portfolio returns of randomly selected portfolios also show a good agreement with our approach. Nonetheless, deviations exist in the far tails of the distribution. Current research in our group by Meudt *et. al.* is based on the groundwork laid by the ensemble approach and gives confidence that the agreement with empirical data can be even further improved by drawing the elements of the correlation matrix from alternative distributions instead of the Wishart distribution. This underlines the strength of the concept to apply ensemble averaging to financial markets.

The correlation-averaged normal distribution provides a new view on financial markets and allows us to contribute a realistic asset value distribution for the Merton model. During our credit risk studies we are able to further simplify the description of financial markets by introducing a correlation matrix with a homogeneous correlation structure. This allows us to boil down the parameter space for the correlations from $K(K-1)/2$ to only two parameters, the average correlation level between assets and the strength of the fluctuations. We are able to specify an expression for the average loss distribution and it is even possible to state a limiting distribution in the case of infinite portfolio size. This allows us to contribute a generic understanding why the benefits of diversification are very limited for portfolios of credit contracts.

We use Monte-Carlo simulations to calculate the Value at Risk and Expected Tail Loss and find that the introduction of the homogeneous correlation matrix is justified. However, it is important to use heterogeneous volatilities to come as close as possible to the full covariance matrix. This again underlines the results from chapter 2 and how important it is to estimate the volatilities as well as possible.

Methods from statistical physics and a data driven approach common in physics are well-suited to capture complex systems. This contributes to a better understanding of financial markets.

Appendix A

TAQ details

The TAQ data format is described in reference [150]. The last three columns for the price data as shown in section 1.5 give additional information on each date. The first of the three columns is always set to zero for data after June 28, 2006 and is related to a now defunct regulatory rule (Rule 127). The second column contains a correction indicator. The possible values and their meaning are taken from reference [150] and shown in table A.1. We take only trades into account which have a correction indicator of zero or one. The third column

Value	Meaning
	Good trades:
0	Regular trade that was not corrected, changed, or signified as cancel or error.
1	Original trade which was later corrected. This record contains the original time and the corrected data for the trade.
2	Symbol correction (out of time sequence).
	Original trade records:
7	Trade cancelled due to error.
8	Trade cancelled.
9	Trade cancelled due to symbol correction.
	Correction instructions:
10	Cancel record (associated with 8).
11	Error record (associated with 7).
12	Correction record (associated with 1; contains corrected time and original data).

Table A.1: Possible values of the correction indicator in the TAQ database.

states the sale condition, which can consist of up to four letters. However, the TAQ database on DVD only includes the first two letters. Providing a list of all possible conditions is beyond the scope of this section, see reference [150]. We only take regular trades into account which either have a blank or @ as condition.

The following stocks were included in the empirical study in chapter 3:

S&P 500 2007 (479 stocks):

A (NYSE), AA (NASDAQ), AAPL (NASDAQ), ABC (NYSE), ABT (NASDAQ), ACE (NYSE), ADBE (NASDAQ), ADI (NASDAQ), ADM (NYSE), ADP (NASDAQ), ADSK (NASDAQ), AEE (NYSE), AEP (NYSE), AES (NASDAQ), AET (NYSE), AFL (NYSE), AGN (NYSE), AIG (NASD ADF), AIV (NYSE), AIZ (NYSE), AKAM (NASDAQ), AKS (NASDAQ), ALL (NYSE), ALTR (NASDAQ), AMAT (NASDAQ), AMD (NASD ADF), AMGN (NASDAQ), AMP (NYSE), AMT (NYSE), AMZN (NASDAQ), AN (NYSE), ANF (NYSE), ANR (NYSE), APA (NASD ADF), APC (NASDAQ), APD (NYSE), APH (NYSE), APOL (NASDAQ), ARG (NYSE), ATI (NYSE), AVB (NYSE), AVP (NYSE), AVY (NYSE), AXP (NASDAQ), AZO (NYSE), BA (NYSE), BAC (NASDAQ), BAX (NYSE), BBBY (NASDAQ), BBT (NASDAQ), BBY (NASDAQ), BCR (NYSE), BDX (NYSE), BEN (NYSE), BHI (NASDAQ), BIG (NYSE), BIIB (NASDAQ), BK (NYSE), BLK (NYSE), BLL (NYSE), BMC (NYSE), BMS (NYSE), BMY (NASDAQ), BRCM (NASDAQ), BSX (NASDAQ), BTU (NASDAQ), BXP (NYSE), C (NASDAQ), CA (NASDAQ), CAG (NASDAQ), CAH (NYSE), CAM (NYSE), CAT (NASDAQ), CB (NYSE), CBG (NYSE), CBS (NASDAQ), CCE (NYSE), CCL (NYSE), CEG (NYSE), CELG (NASDAQ), CERN (NASDAQ), CF (NYSE), CHK (NASD ADF), CHRW (NASDAQ), CI (NYSE), CINF (NASDAQ), CL (NYSE), CLF (NASDAQ), CLX (NYSE), CMA (NYSE), CMCSA (NASDAQ), CME (NASDAQ), CMG (NYSE), CMI (NASDAQ), CMS (NYSE), CNP (NYSE), CNX (NASDAQ), COF (NASDAQ), COG (NYSE), COH (NASDAQ), COL (NYSE), COP (NASDAQ), COST (NASDAQ), COV (NASDAQ), CPB (NYSE), CPWR (NASDAQ), CRM (NYSE), CSC (NYSE), CSCO (NASDAQ), CSX (NYSE), CTAS (NASDAQ), CTL (NYSE), CTSH (NASDAQ), CTXS (NASDAQ), CVC (NYSE), CVH (NYSE), CVS (NASDAQ), CVX (NASDAQ), D (NYSE), DD (NASDAQ), DE (NASD ADF), DELL (NASDAQ), DF (NYSE), DFS (NASDAQ), DGX (NYSE), DHI (NASDAQ), DHR (NYSE), DIS (NASDAQ), DISCA (NASDAQ), DNB (NYSE), DNR (NYSE), DO (NYSE), DOV (NYSE), DOW (NASDAQ), DRI (NYSE), DTE (NYSE), DTV (NASDAQ), DUK (NASD ADF), DV (NYSE), DVA (NYSE), DVN (NASDAQ), EBAY (NASDAQ), ECL (NYSE), ED (NYSE), EFX (NYSE), EIX (NYSE), EL (NYSE), EMC (NASDAQ), EMN (NYSE), EMR (NASDAQ), EOG (NASDAQ), EP (NASD ADF), EQR (NYSE), EQT (NYSE), ERTS (NASDAQ), ESRX (NASDAQ), ETFC (NASD ADF), ETN (NYSE), ETR (NYSE), EW (NYSE), EXC (NYSE), EXPD (NASDAQ), EXPE (NASDAQ), F (NASD ADF), FAST (NASDAQ), FCX (NASD ADF), FDO (NYSE), FDX (NYSE), FE (NYSE), FFIV (NASDAQ), FHN (NASDAQ), FII (NYSE), FIS (NYSE), FISV (NASDAQ), FITB (NASDAQ), FLIR (NASDAQ), FLR (NYSE), FLS (NYSE), FMC (NYSE), FO (NYSE), FRX (NYSE), FSLR (NASDAQ), FTI (NYSE), GAS (NYSE), GCI (NYSE), GD (NYSE), GE (NASD ADF), GILD (NASDAQ), GIS (NYSE), GLW (NASDAQ), GME (NYSE), GNW (NASD ADF), GOOG (NASDAQ), GPC (NYSE), GPS (NASDAQ), GR (NYSE), GS (NASD ADF), GT (NYSE), GWW (NYSE), HAL (NASDAQ), HAR (NYSE), HAS (NYSE), HBAN (NASDAQ), HCBK (NASDAQ), HCN (NYSE), HCP (NYSE), HD (NASDAQ), HES (NYSE), HIG (NASD ADF), HNZ (NYSE), HOG (NYSE), HON (NASDAQ), HOT (NYSE), HP (NYSE), HPQ (NASDAQ), HRB (NYSE), HRL (NYSE), HRS (NYSE), HSP (NYSE), HST (NASDAQ), HSY (NYSE), HUM (NYSE), IBM (NYSE), ICE (NYSE), IFF (NYSE), IGT (NYSE), INTC (NASDAQ), INTU (NASDAQ), IP (NASDAQ), IPG (NASDAQ), IR (NYSE), IRM (NYSE), ISRG (NASDAQ), ITT (NYSE), ITW (NYSE), IVZ (NYSE), JBL (NASD ADF), JCI (NYSE), JCP (NASDAQ), JDSU (NASDAQ), JEC (NYSE), JNJ (NASDAQ), JNPR (NASDAQ), JNS (NYSE), JOYG (NASDAQ), JPM (NASDAQ), JWN (NASDAQ), K (NYSE), KEY (NASDAQ), KFT (NASDAQ), KIM (NYSE), KLAC (NASDAQ), KMB (NYSE), KMX (NYSE), KO (NASDAQ), KR (NASDAQ), KSS (NASDAQ), LEG (NYSE), LEN (NASDAQ), LH (NYSE), LLL (NYSE), LLTC (NASDAQ), LLY (NASDAQ), LM (NYSE), LMT (NYSE), LNC (NYSE), LOW (NASDAQ), LSI (NASDAQ), LTD (NASDAQ), LUK (NYSE), LUV (NASDAQ), LXK (NYSE), M (NASDAQ), MA (NASDAQ), MAR (NYSE), MAS (NYSE), MAT (NYSE), MCD (NASDAQ), MCHP (NASDAQ), MCK (NYSE), MCO (NYSE), MDT (NASDAQ), MET (NYSE), MHP (NYSE), MHS (NYSE), MI (NASDAQ), MKC (NYSE), MMC (NYSE), MMM (NYSE), MO (NASD ADF), MOLX (NASDAQ), MON (NASD ADF), MOS (NASD ADF), MRK (NASDAQ), MRO (NASDAQ), MS (NASDAQ), MSFT (NASDAQ), MTB (NYSE), MU (NASDAQ), MUR (NYSE), MWV (NYSE), MYL (NASDAQ), NBL (NYSE), NBR (NASDAQ), NDAQ (NASDAQ), NE (NASDAQ), NEM (NASDAQ), NFLX (NASDAQ), NFX (NYSE), NI (NYSE), NKE (NYSE), NOC (NYSE), NOV (NASD ADF), NRG (NYSE), NSC (NYSE), NTAP (NASDAQ), NTRS (NASDAQ), NU (NYSE), NUE (NASD ADF), NVDA (NASDAQ), NVLS (NASDAQ), NWL (NYSE), NWSA (NASDAQ), NYX (NASD ADF), OI (NYSE), OKE (NYSE), OMC (NYSE), ORCL (NASDAQ), ORLY (NASDAQ), OXY (NASDAQ), PAYX (NASDAQ), PBCT (NASDAQ), PBI (NYSE), PCAR (NASDAQ), PCG (NYSE), PCL (NYSE), PCLN (NASDAQ), PCP (NYSE), PCS (NYSE), PDCO (NASDAQ), PEG (NYSE), PEP (NASDAQ), PFE (NASD ADF), PFG (NYSE), PG (NASDAQ), PGN (NYSE), PGR (NYSE), PH (NYSE), PHM (NASDAQ), PKI (NYSE), PLD (NYSE), PLL (NYSE), PNC (NYSE), PNW (NYSE), POM (NYSE), PPG (NYSE), PPL (NYSE), PRU (NYSE), PSA (NYSE), PWR (NYSE), PX (NYSE), PXD (NYSE), QCOM (NASDAQ), R (NYSE), RAI (NYSE), RDC (NASDAQ), RF (NASDAQ), RHI (NYSE), RHT (NYSE), RL (NYSE), ROK (NYSE), ROP (NYSE), ROST (NASDAQ), RRC (NYSE), RRD (NYSE), RSG (NYSE), RSH (NASDAQ), RTN (NYSE), S (NASD ADF), SAI (NYSE), SBUX (NASDAQ), SCG (NYSE), SCHW (NASDAQ), SE (NASDAQ), SEE (NYSE), SHLD (NASDAQ), SHW (NYSE), SIAL (NASDAQ), SJM (NYSE), SLB (NASDAQ), SLE (NYSE), SLM (NASDAQ), SNA (NYSE), SNDK (NASDAQ), SO (NASDAQ), SPG (NYSE), SPLS (NASDAQ), SRCL (NASDAQ), SRE (NYSE), STI (NYSE), STJ (NASDAQ), STT (NYSE), STZ (NYSE), SVU (NYSE), SWK (NYSE), SWN (NYSE), SWY (NASDAQ), SYK (NYSE), SYMC (NASDAQ), SYY (NYSE), T (NASDAQ), TAP (NYSE), TDC (NYSE), TE (NYSE), TEG (NYSE), TEL (NYSE), TER (NASDAQ), TGT (NASDAQ), THC (NASD ADF), TIE (NASD ADF), TIF (NYSE), TJX (NASDAQ), TLAB (NASDAQ), TMK (NYSE), TMO (NYSE), TROW (NASDAQ), TRV (NYSE), TSN (NYSE), TSO (NASD ADF), TSS (NYSE), TWC (NYSE), TWX (NASD ADF), TXN (NASDAQ), TXT (NYSE), TYC (NYSE), UNH (NASDAQ), UNM (NYSE), UNP (NYSE), UPS (NYSE), URBN (NASDAQ), USB (NASDAQ), UTX (NYSE), VAR (NYSE), VFC (NYSE), VIAB (NYSE), VLO (NASD ADF), VMC (NYSE), VNO (NYSE), VRSN (NASDAQ), VTR (NYSE), VZ (NASDAQ), WAG (NASDAQ), WAT (NYSE), WDC (NASDAQ), WEC (NYSE), WFC (NASDAQ), WFR (NASD ADF), WHR (NYSE), WIN (NYSE), WLP (NYSE), WM (NASD ADF), WMB (NASDAQ), WMT (NASDAQ), WPI (NYSE), WU (NASDAQ), WY (NYSE), WYN (NYSE), WYNN (NASDAQ), X (NASD ADF), XEL (NYSE), XL (NYSE), XLNX (NASDAQ), XOM (NASDAQ), XRAY (NASDAQ), XRX (NASD ADF), YHOO (NASDAQ), YUM (NYSE), ZION (NASDAQ), ZMH (NYSE)

S&P 500 2008 (488 stocks):

A (NYSE), AA (NASDAQ), AAPL (NASDAQ), ABC (NYSE), ABT (NASDAQ), ACE (NYSE), ADBE (NASDAQ), ADI (NASDAQ), ADM (NYSE), ADP (NASDAQ), ADSK (NASDAQ), AEE (NYSE), AEP (NYSE), AES (NASDAQ), AET (NYSE), AFL (NYSE), AGN (NYSE), AIG (NASD ADF), AIV (NYSE), AIZ (NYSE), AKAM (NASDAQ), AKS (NASDAQ), ALL (NYSE), ALTR (NASDAQ), AMAT (NASDAQ), AMD (NASD ADF), AMGN (NASDAQ), AMP (NYSE), AMT (NYSE), AMZN (NASDAQ), AN (NYSE), ANF (NYSE), ANR (NYSE), APA (NASD ADF), APC (NASDAQ), APD (NYSE), APH (NYSE), APOL (NASDAQ), ARG (NYSE), ATI (NYSE), AVB (NYSE), AVP (NYSE), AVY (NYSE), AXP (NASDAQ), AZO (NYSE), BA (NYSE), BAC (NASDAQ), BAX (NYSE), BBBY (NASDAQ), BBT (NASDAQ), BBY (NASDAQ), BCR (NYSE), BDX (NYSE), BEN (NYSE), BHI (NASDAQ), BIG (NYSE), BIIB (NASDAQ), BK (NYSE), BLK (NYSE), BLL (NYSE), BMC (NYSE), BMS (NYSE), BMY (NASDAQ), BRCM (NASDAQ), BSX (NASDAQ), BTU (NASDAQ), BXP (NYSE), C (NASDAQ), CA (NASDAQ), CAG (NASDAQ), CAH (NYSE), CAM (NYSE), CAT (NASDAQ), CB (NYSE), CBG (NYSE), CBS (NASDAQ), CCE (NYSE), CCL (NYSE), CEG (NYSE), CELG (NASDAQ), CERN (NASDAQ), CF (NYSE), CHK (NASD ADF), CHRW (NASDAQ), CI (NYSE), CINF (NASDAQ), CL (NYSE), CLF (NASDAQ), CLX (NYSE), CMA (NYSE), CMCSA (NASDAQ), CME (NASDAQ), CMG (NYSE), CMI (NASDAQ), CMS (NYSE), CNP (NYSE), CNX (NASDAQ), COF (NASDAQ), COG (NYSE), COH (NASDAQ), COL (NYSE), COP (NASDAQ), COST (NASDAQ), COV (NASDAQ), CPB (NYSE), CPWR (NASDAQ), CRM (NYSE),

CSC (NYSE), CSCO (NASDAQ), CSX (NYSE), CTAS (NASDAQ), CTL (NYSE), CTSH (NASDAQ), CTXS (NASDAQ), CVC (NYSE), CVH (NYSE), CVS (NASDAQ), CVX (NASDAQ), D (NYSE), DD (NASDAQ), DE (NASD ADF), DELL (NASDAQ), DF (NYSE), DFS (NASDAQ), DGX (NYSE), DHI (NASDAQ), DHR (NYSE), DIS (NASDAQ), DISCA (NASDAQ), DNB (NYSE), DNR (NYSE), DO (NYSE), DOV (NYSE), DOW (NASDAQ), DPS (NYSE), DRI (NYSE), DTE (NYSE), DTV (NASDAQ), DUK (NASD ADF), DV (NYSE), DVA (NYSE), DVN (NASDAQ), EBAY (NASDAQ), ECL (NYSE), ED (NYSE), EFX (NYSE), EIX (NYSE), EL (NYSE), EMC (NASDAQ), EMN (NYSE), EMR (NASDAQ), EOG (NASDAQ), EP (NASD ADF), EQR (NYSE), EQT (NYSE), ERTS (NASDAQ), ESRX (NASDAQ), ETFC (NASD ADF), ETN (NYSE), ETR (NYSE), EW (NYSE), EXC (NYSE), EXPD (NASDAQ), EXPE (NASDAQ), F (NASD ADF), FAST (NASDAQ), FCX (NASD ADF), FDO (NYSE), FDX (NYSE), FE (NYSE), FFIV (NASDAQ), FHN (NASDAQ), FII (NYSE), FIS (NYSE), FISV (NASDAQ), FITB (NASDAQ), FLIR (NASDAQ), FLR (NYSE), FLS (NYSE), FMC (NYSE), FO (NYSE), FRX (NYSE), FSLR (NASDAQ), FTI (NYSE), FTR (NASDAQ), GAS (NYSE), GCI (NYSE), GD (NYSE), GE (NASD ADF), GILD (NASDAQ), GIS (NYSE), GLW (NASDAQ), GME (NYSE), GNW (NASD ADF), GOOG (NASDAQ), GPC (NYSE), GPS (NASDAQ), GR (NYSE), GS (NASD ADF), GT (NYSE), GWW (NYSE), HAL (NASDAQ), HAR (NYSE), HAS (NYSE), HBAN (NASDAQ), HCBK (NASDAQ), HCN (NYSE), HCP (NYSE), HD (NASDAQ), HES (NYSE), HIG (NASD ADF), HNZ (NYSE), HOG (NYSE), HON (NASDAQ), HOT (NYSE), HP (NYSE), HPQ (NASDAQ), HRB (NYSE), HRL (NYSE), HRS (NYSE), HSP (NYSE), HST (NASDAQ), HSY (NYSE), HUM (NYSE), IBM (NYSE), ICE (NYSE), IFF (NYSE), IGT (NYSE), INTC (NASDAQ), INTU (NASDAQ), IP (NASDAQ), IPG (NASDAQ), IR (NYSE), IRM (NYSE), ISRG (NASDAQ), ITT (NYSE), ITW (NYSE), IVZ (NYSE), JBL (NASD ADF), JCI (NYSE), JCP (NASDAQ), JDSU (NASDAQ), JEC (NYSE), JNJ (NASDAQ), JNPR (NASDAQ), JNS (NYSE), JOYG (NASDAQ), JPM (NASDAQ), JWN (NASDAQ), K (NYSE), KEY (NASDAQ), KFT (NASDAQ), KIM (NYSE), KLAC (NASDAQ), KMB (NYSE), KMX (NYSE), KO (NASDAQ), KR (NASDAQ), KSS (NASDAQ), L (NYSE), LEG (NYSE), LEN (NASDAQ), LH (NYSE), LIFE (NASDAQ), LLL (NYSE), LLTC (NASDAQ), LLY (NASDAQ), LM (NYSE), LMT (NYSE), LNC (NYSE), LO (NYSE), LOW (NASDAQ), LSI (NASDAQ), LTD (NASDAQ), LUK (NYSE), LUV (NASDAQ), LXK (NYSE), M (NASDAQ), MA (NASDAQ), MAR (NYSE), MAS (NYSE), MAT (NYSE), MCD (NASDAQ), MCHP (NASDAQ), MCK (NYSE), MCO (NYSE), MDT (NASDAQ), MET (NYSE), MHP (NYSE), MHS (NYSE), MI (NASDAQ), MKC (NYSE), MMC (NYSE), MMM (NYSE), MO (NASD ADF), MOLX (NASDAQ), MON (NASD ADF), MOS (NASD ADF), MRK (NASDAQ), MRO (NASDAQ), MS (NASDAQ), MSFT (NASDAQ), MTB (NYSE), MU (NASDAQ), MUR (NYSE), MWV (NYSE), MWW (NYSE), MYL (NASDAQ), NBL (NYSE), NBR (NASDAQ), NDAQ (NASDAQ), NE (NASDAQ), NEM (NASDAQ), NFLX (NASDAQ), NFX (NYSE), NI (NYSE), NKE (NYSE), NOC (NYSE), NOV (NASD ADF), NRG (NYSE), NSC (NYSE), NTAP (NASDAQ), NTRS (NASDAQ), NU (NYSE), NUE (NASD ADF), NVDA (NASDAQ), NVLS (NASDAQ), NWL (NYSE), NWSA (NASDAQ), NYX (NASD ADF), OI (NYSE), OKE (NYSE), OMC (NYSE), ORCL (NASDAQ), ORLY (NASDAQ), OXY (NASDAQ), PAYX (NASDAQ), PBCT (NASDAQ), PBI (NYSE), PCAR (NASDAQ), PCG (NYSE), PCL (NYSE), PCLN (NASDAQ), PCP (NYSE), PCS (NYSE), PDCO (NASDAQ), PEG (NYSE), PEP (NASDAQ), PFE (NASD ADF), PFG (NYSE), PG (NASDAQ), PGN (NYSE), PGR (NYSE), PH (NYSE), PHM (NASDAQ), PKI (NYSE), PLD (NYSE), PLL (NYSE), PM (NASD ADF), PNC (NYSE), PNW (NYSE), POM (NYSE), PPG (NYSE), PPL (NYSE), PRU (NYSE), PSA (NYSE), PWR (NYSE), PX (NYSE), PXD (NYSE), QCOM (NASDAQ), R (NYSE), RAI (NYSE), RDC (NASDAQ), RF (NASDAQ), RHI (NYSE), RHT (NYSE), RL (NYSE), ROK (NYSE), ROP (NYSE), ROST (NASDAQ), RRC (NYSE), RRD (NYSE), RSG (NYSE), RSH (NASDAQ), RTN (NYSE), S (NASD ADF), SAI (NYSE), SBUX (NASDAQ), SCG (NYSE), SCHW (NASDAQ), SE (NASDAQ), SEE (NYSE), SHLD (NASDAQ), SHW (NYSE), SIAL (NASDAQ), SJM (NYSE), SLB (NASDAQ), SLE (NYSE), SLM (NASDAQ), SNA (NYSE), SNDK (NASDAQ), SNI (NYSE), SO (NASDAQ), SPG (NYSE), SPLS (NASDAQ), SRCL (NASDAQ), SRE (NYSE), STI (NYSE), STJ (NASDAQ), STT (NYSE), STZ (NYSE), SVU (NYSE), SWK (NYSE), SWN (NYSE), SWY (NASDAQ), SYK (NYSE), SYMC (NASDAQ), SYY (NYSE), T (NASDAQ), TAP (NYSE), TDC (NYSE), TE (NYSE), TEG (NYSE), TEL (NYSE), TER (NASDAQ), TGT (NASDAQ), THC (NASD ADF), TIE (NASD ADF), TIF (NYSE), TJX (NASDAQ), TLAB (NASDAQ), TMK (NYSE), TMO (NYSE), TROW (NASDAQ), TRV (NYSE), TSN (NYSE), TSO (NASD ADF), TSS (NYSE), TWC (NYSE), TWX (NASD ADF), TXN (NASDAQ), TXT (NYSE), TYC (NYSE), UNH (NASDAQ), UNM (NYSE), UNP (NYSE), UPS (NYSE), URBN (NASDAQ), USB (NASDAQ), UTX (NYSE), V (NASD ADF), VAR (NYSE), VFC (NYSE), VIAB (NYSE), VLO (NASD ADF), VMC (NYSE), VNO (NYSE), VRSN (NASDAQ), VTR (NYSE), VZ (NASDAQ), WAG (NASDAQ), WAT (NYSE), WDC (NASDAQ), WEC (NYSE), WFC (NASDAQ), WFR (NASD ADF), WHR (NYSE), WIN (NYSE), WLP (NYSE), WM (NASD ADF), WMB (NASDAQ), WMT (NASDAQ), WPI (NYSE), WU (NASDAQ), WY (NYSE), WYN (NYSE), WYNN (NASDAQ), X (NASD ADF), XEL (NYSE), XL (NYSE), XLNX (NASDAQ), XOM (NASDAQ), XRAY (NASDAQ), XRX (NASD ADF), YHOO (NASDAQ), YUM (NYSE), ZION (NASDAQ), ZMH (NYSE)

Appendix B

Daily stock data

The following stocks were included in the empirical study in section 4.4:

S&P 500 1992-2012 (307 stocks):

AA, AAPL, ABT, ADBE, ADI, ADM, ADP, ADSK, AEP, AES, AET, AFL, AGN, AIG, ALTR, AMAT, AMD, AMGN, AON, APA, APC, APD, APH, ARG, AVP, AVY, AXP, AZO, BA, BAC, BAX, BBT, BBY, BCR, BDX, BEN, BF.B, BHI, BIG, BIIB, BK, BLL, BMC, BMS, BMY, C, CA, CAG, CAH, CAT, CB, CCE, CCL, CELG, CERN, CI, CINF, CL, CLF, CLX, CMA, CMCSA, CMI, CMS, CNP, COG, COP, COST, CPB, CSC, CSCO, CSX, CTAS, CTL, CVH, CVS, CVX, D, DD, DE, DELL, DHR, DIS, DNB, DOV, DOW, DTE, DUK, ECL, ED, EFX, EIX, EMC, EMR, EOG, EQT, ETN, ETR, EXC, F, FAST, FDO, FDX, FHN, FISV, FITB, FLS, FMC, FRX, GAS, GCI, GD, GE, GIS, GLW, GPC, GPS, GT, GWW, HAL, HAS, HBAN, HCP, HD, HES, HNZ, HOG, HON, HOT, HP, HPQ, HRB, HRL, HRS, HST, HSY, HUM, IBM, IFF, IGT, INTC, IP, IPG, IR, ITW, JCI, JCP, JEC, JNJ, JPM, JWN, K, KEY, KIM, KLAC, KMB, KO, KR, L, LEG, LEN, LH, LLTC, LLY, LM, LMT, LNC, LOW, LSI, LTD, LUK, LUV, MAS, MAT, MCD, MDT, MHP, MKC, MMC, MMM, MO, MOLX, MRK, MRO, MSFT, MSI, MTB, MU, MUR, MWV, MYL, NBL, NBR, NE, NEE, NEM, NI, NKE, NOC, NSC, NTRS, NU, NUE, NWL, OI, OKE, OMC, ORCL, OXY, PAYX, PBCT, PBI, PCAR, PCG, PCL, PCP, PEP, PFE, PG, PGR, PH, PHM, PLL, PNC, PNW, POM, PPG, PPL, PSA, QCOM, R, RDC, RF, ROK, ROST, RRD, RSH, RTN, S, SCG, SCHW, SEE, SHW, SIAL, SLB, SLM, SNA, SO, SPLS, STI, STJ, STT, SVU, SWK, SWN, SWY, SYK, SYMC, SYY, T, TAP, TE, TEG, TER, TGT, THC, TIF, TJX, TLAB, TMK, TMO, TROW, TRV, TSN, TSO, TXN, TXT, TYC, UNH, UNP, USB, UTX, VAR, VFC, VLO, VMC, VNO, VZ, WAG, WDC, WEC, WFC, WFM, WHR, WM, WMB, WMT, WPO, WY, X, XEL, XL, XLNX, XOM, XRAY, XRX, ZION

S&P 500 2002-2012 (439 stocks):

A, AA, AAPL, ABC, ABT, ACE, ADBE, ADI, ADM, ADP, ADSK, AEE, AEP, AES, AET, AFL, AGN, AIG, AIV, AKAM, AKS, ALL, ALTR, AMAT, AMD, AMGN, AMT, AMZN, AN, ANF, AON, APA, APC, APD, APH, APOL, ARG, ATI, AVB, AVP, AVY, AXP, AZO, BA, BAC, BAX, BBBY, BBT, BBY, BCR, BDX, BEN, BF.B, BHI, BIG, BIIB, BK, BLK, BLL, BMC, BMS, BMY, BRCM, BRK.B, BSX, BTU, BXP, C, CA, CAG, CAH, CAM, CAT, CB, CCE, CCL, CELG, CERN, CHK, CHRW, CI, CINF, CL, CLF, CLX, CMA, CMCSA, CMI, CMS, CNP, CNX, COF, COG, COH, COL, COP, COST, CPB, CPWR, CSC, CSCO, CSX, CTAS, CTL, CTSH, CTXS, CVC, CVH, CVS, CVX, D, DD, DE, DELL, DF, DGX, DHI, DHR, DIS, DNB, DNR, DO, DOV, DOW, DRI, DTE, DUK, DV, DVA, DVN, EBAY, ECL, ED, EFX, EIX, EL, EMC, EMN, EMR, EOG, EQR, EQT, ESRX, ETFC, ETN, ETR, EW, EXC, EXPD, F, FAST, FCX, FDO, FDX, FE, FFIV, FHN, FII, FIS, FISV, FITB, FLIR, FLR, FLS, FMC, FRX, FTI, FTR, GAS, GCI, GD, GE, GILD, GIS, GLW, GPC, GPS, GS, GT, GWW, HAL, HAR, HAS, HBAN, HCBK, HCN, HCP, HD, HES, HIG, HNZ, HOG, HON, HOT, HP, HPQ, HRB, HRL, HRS, HST, HSY, HUM, IBM, IFF, IGT, INTC, INTU, IP, IPG, IR, IRM, ISRG, ITT, ITW, IVZ, JBL, JCI, JCP, JDSU, JEC, JNJ, JNPR, JNS, JPM, JWN, K, KEY, KIM, KLAC, KMB, KMX, KO, KR, KSS, L, LEG, LEN, LH, LIFE, LLL, LLTC, LLY, LM, LMT, LNC, LOW, LSI, LTD, LUK, LUV, LXK, M, MAR, MAS, MAT, MCD, MCHP, MCK, MCO, MDT, MET, MHP, MKC, MMC, MMM, MO, MOLX, MON, MRK, MRO, MS, MSFT, MSI, MTB, MU, MUR, MWV, MWW, MYL, NBL, NBR, NE, NEE, NEM, NFX, NI, NKE, NOC, NOV, NSC, NTAP, NTRS, NU, NUE, NVDA, NWL, NWSA, OI, OKE, OMC, ORCL, ORLY, OXY, PAYX, PBCT, PBI, PCAR, PCG, PCL, PCLN, PCP, PDCO, PEP, PFE, PFG, PG, PGR, PH, PHM, PKI, PLD, PLL, PNC, PNW, POM, PPG, PPL, PRU, PSA, PWR, PX, PXD, QCOM, R, RAI, RDC, RF, RHI, RHT, RL, ROK, ROP, ROST, RRC, RRD, RSG, RSH, RTN, S, SBUX, SCG, SCHW, SEE, SHW, SIAL, SJM, SLB, SLM, SNA, SNDK, SO, SPG, SPLS, SRCL, SRE, STI, STJ, STT, STZ, SVU, SWK, SWN, SWY, SYK, SYMC, SYY, T, TAP, TE, TEG, TER, TGT, THC, TIE, TIF, TJX, TLAB, TMK, TMO, TROW, TRV, TSN, TSO, TSS, TWX, TXN, TXT, TYC, UNH, UNM, UNP, UPS, URBN, USB, UTX, VAR, VFC, VLO, VMC, VNO, VRSN, VTR, VZ, WAG, WAT, WDC, WEC, WFC, WFM, WFR, WHR, WLP, WM, WMB, WMT, WPI, WPO, WY, X, XEL, XL, XLNX, XOM, XRAY, XRX, YHOO, YUM, ZION, ZMH

NASDAQ 1992-2012 (708 stocks):

AA, AAN, AAPL, AB, ABM, ABMD, ABT, ABX, ACET, ACU, ADBE, ADI, ADM, ADP, ADSK, AE, AEGN, AEP, AES, AET, AFG, AFL, AGN, AGYS, AIG, AIM, AIN, AIR, AIRT, AIT, AJG, ALCO, ALE, ALK, ALOT, ALRN, ALTR, AM, AMAG, AMAT, AMD, AMGN, AMSWA, AMWD, ANN, AON, AP, APA, APAGF, APC, APD, ARL, ARTW, ARW, ASBC, ASBI, ASH, ASNA, ASRV, ATAX, ATML, ATO, ATRO, ATX, AVA, AVP, AVT, AVY, AWR, AXE, AXLL, AXP, AZO, AZZ, B, BA, BAC, BANF, BAX, BBT, BBVA, BBY, BC, BCE, BCPC, BCR, BCS, BDL, BDN, BDX, BEAM, BEAV, BEN, BGG, BHI, BHP, BID, BK, BKH, BKSC, BLL, BMI, BMS, BMTC, BMY, BOBE, BOH, BOTA, BP, BPL, BPOP, BPT, BRE, BRID, BRN, BRS, BRY, BT, BTI, BWINA, BWINB, BWS, BXS, C, CA, CAG, CAH, CAS, CASC, CASY, CAT, CATO, CATY, CB, CBB, CBM, CBRL, CBRX, CBSH, CBT, CBU, CCC, CCE, CCK, CCL, CDE, CDNS, CEC, CELG, CERN, CFI, CFNB, CFR, CGNX, CHD, CHE, CHG, CI, CINF, CKP, CL, CLDX, CLGX, CLX, CMC, CMCSA, CMCSK, CMI, CMO, CMS, CNA, CNBKA, CNL, CNP, CNW, COHU, COO, COP, COST, CP, CPB, CPF, CPK, CQB, CR, CRBC, CRRC, CRS, CRUS, CSC, CSCO, CSH, CSX, CT, CTAS, CTB, CTL, CTS, CVH, CVM, CVS, CVX, CW, CWH, CWT, CY, CYN, CYTR, D, DBD, DCI, DD, DDS, DE, DELL, DGAS, DGICB, DGII, DIS, DLX, DNB, DOV, DOW, DTE, DUK, DX, EA, EAT, ECL, ECOL, ED, EDE, EEP, EFX, EGAS, EGN, EIX, ELSE, ELX, EMC, EMCI, EMR, ENB, ENZN, EOG, EPHC, EQT, ERIC, ESV, ETN, ETR, EV, EXAR, EXC, F, FARM, FAST, FDO, FDX, FELE, FFBC, FHN, FISV, FITB, FL, FLO, FLOW, FLS, FMC, FNP, FOE, FRM, FRT, FRX, FSS, FUL, FUN, FUR, FWLT, GAS, GCI,

GCO, GD, GE, GFI, GGG, GIS, GLCH, GLDC, GLW, GMT, GNTX, GPC, GPS, GRA, GSBC, GSK, GT, GTY, GWW, GXP, GY, HAE, HAL, HAS, HBAN, HBHC, HCP, HD, HE, HES, HL, HLS, HMC, HNR, HNT, HNZ, HOG, HON, HP, HPQ, HRB, HRC, HRL, HRS, HSC, HSH, HST, HSY, HTCH, HTSI, HUM, HWAY, IBM, IDA, IDCC, IDTI, IDXX, IFF, IGT, IHC, IMGN, IMMU, INT, INTC, IO, IP, IPAR, IPG, IR, IRF, ISH, ITIC, ITW, IVC, JBHT, JCI, JCP, JCS, JEC, JKHY, JNJ, JNY, JPM, JWN, K, KAMN, KBH, KELYA, KEY, KIM, KLAC, KMB, KMPR, KMT, KO, KR, KSU, KSWS, KWR, KYO, L, LANC, LAWS, LCUT, LEG, LEN, LG, LH, LLTC, LLY, LM, LMT, LNC, LNCE, LNT, LOW, LPX, LRCX, LSCC, LSI, LTD, LTXC, LUB, LUK, LUV, LYTS, LZB, MAG, MAN, MAS, MAT, MBI, MCD, MCRS, MCY, MDC, MDP, MDT, MDU, MEI, MENT, MERC, MGA, MGEE, MGM, MGRC, MHP, MKC, MKTAY, MLHR, MLI, MMC, MMM, MNR, MO, MOD, MOLX, MPR, MRK, MRO, MSA, MSB, MSEX, MSFG, MSFT, MSI, MTB, MTG, MTR, MU, MUR, MWV, MXIM, MXWL, MYL, NAV, NAVG, NBBC, NBL, NBR, NC, NE, NEE, NEM, NEU, NFG, NHTB, NI, NKE, NL, NNN, NOC, NPBC, NPK, NRT, NSC, NSEC, NTRS, NTSC, NU, NUE, NVE, NWL, NWS, NX, NYT, OCR, ODC, ODP, OGE, OI, OII, OKE, OLN, OMC, OMX, ONB, ORCL, ORI, OXM, OXY, PAYX, PBI, PBT, PBY, PC, PCAR, PCG, PCH, PCL, PCP, PENX, PEP, PFE, PG, PGR, PH, PHG, PHI, PHM, PKD, PKE, PL, PLAB, PLL, PMCS, PMFG, PMTC, PNC, PNM, PNR, PNRA, PNW, PNY, POM, POPE, PPG, PPL, PRGO, PRK, PSA, PTSI, PVA, PVH, QCOM, R, RAD, RDC, REGN, RELL, REX, REXI, RF, RGEN, RHP, RJF, RLI, ROL, ROST, RPM, RRD, RSH, RT, RWC, RYL, S, SAFM, SAN, SBCF, SCG, SCHW, SCI, SCX, SEE, SF, SFD, SHLM, SHW, SIAL, SIGM, SJI, SJT, SKY, SLB, SLM, SNA, SNE, SNV, SO, SON, SPAN, SPAR, SPF, SPLS, SPW, SR, SSP, STC, STFC, STI, STJ, STR, STT, SUP, SUSQ, SVNT, SVU, SWK, SWKS, SWX, SWY, SYK, SYMC, SYY, T, TAP, TCB, TDS, TDW, TE, TECD, TECUB, TEF, TEG, TEN, TER, TEVA, TFX, TGT, THC, THO, TIF, TJX, TKR, TLAB, TMK, TMO, TMP, TOL, TOT, TR, TRN, TRP, TRST, TRV, TSN, TTC, TTEK, TWIN, TXI, TXN, TXT, TYC, UBSI, UDR, UFCS, UFI, UGI, UHS, UIL, UIS, UL, UMBF, UNAM, UNF, UNH, UNP, UNS, USB, USG, USLM, UTX, UVV, VGR, VGZ, VHI, VICR, VLGEA, VMC, VMI, VNO, VVC, VZ, WAG, WDFC, WEYS, WFC, WGL, WHR, WMT, WOR, WPPGY, WRB, WRI, WSB, WSCI, WSM, WST, WTR, WTS, X, XEL, XL, XOM, XOMA, XRAY, XRX

NASDAQ 2002-2012 (2667 stocks):

A, AA, AAME, AAN, AAON, AAPL, AB, ABAX, ABC, ABCB, ABCO, ABFS, ABIO, ABM, ABMD, ABT, ABTL, ABV, ABX, ACAT, ACCL, ACET, ACFN, ACGL, ACHC, ACI, ACIW, ACLS, ACNB, ACO, ACPW, ACT, ACU, ACUR, ACXM, ACY, ADAT, ADBE, ADC, ADEP, ADI, ADM, ADP, ADSK, ADTN, ADVS, ADY, AE, AEC, AEE, AEG, AEGN, AEHR, AEIS, AEM, AEO, AEP, AEPI, AES, AET, AEZS, AF, AFAM, AFCE, AFFX, AFG, AFL, AFOP, AGCO, AGEN, AGM, AGN, AGU, AGX, AGYS, AHPI, AI, AIG, AIM, AIN, AIQ, AIR, AIRM, AIRT, AIT, AIV, AJG, AKAM, AKR, AKS, ALB, ALCO, ALCS, ALE, ALG, ALGN, ALK, ALKS, ALL, ALLB, ALOG, ALOT, ALR, ALRN, ALSK, ALTE, ALTR, ALTV, ALU, ALV, ALVR, ALX, ALXN, AM, AMAG, AMAT, AMBT, AMCC, AMD, AMED, AMG, AMGN, AMIC, AMKR, AMNB, AMOT, AMOV, AMRB, AMRI, AMRN, AMS, AMSC, AMSG, AMSWA, AMT, AMTD, AMWD, AMZN, AN, ANAD, ANAT, ANDE, ANEN, ANF, ANH, ANIK, ANLY, ANN, ANNB, ANSS, ANTP, AOI, AON, AOS, AP, APA, APAGF, APC, APD, APFC, APH, API, APL, APOG, APOL, APRI, APT, APU, AQQ, ARCI, ARCW, ARDNA, ARE, ARG, ARIA, ARKR, ARL, ARLP, ARMH, ARNA, AROW, ARQL, ARRS, ARRY, ARTC, ARTNA, ARTW, ARTX, ARW, ASBC, ASBI, ASCA, ASEI, ASFI, ASGN, ASH, ASI, ASIA, ASMI, ASML, ASNA, ASRV, ASRVP, ASTC, ASTE, ASTM, ASTX, ASUR, ATAX, ATEA, ATK, ATLC, ATMI, ATML, ATNI, ATO, ATR, ATRI, ATRM, ATRO, ATRS, ATVI, ATW, ATX, AU, AUBN, AUDC, AVA, AVB, AVCA, AVD, AVID, AVNR, AVP, AVT, AVX, AVY, AWC, AWRE, AWX, AXAS, AXDX, AXE, AXL, AXLL, AXP, AXR, AXTI, AZN, AZO, AZPN, AZZ, B, BA, BABY, BAC, BAK, BAM, BAMM, BANF, BANR, BAP, BASI, BAX, BBBY, BBCN, BBGI, BBRY, BBSI, BBT, BBVA, BBX, BBY, BC, BCE, BCO, BCOR, BCPC, BCR, BCRX, BCS, BCSB, BDC, BDE, BDGE, BDL, BDMS, BDN, BDR, BDX, BEAM, BEAV, BEBE, BELFA, BELFB, BEN, BERK, BFLY, BFR, BGC, BGCP, BGG, BH, BHB, BHE, BHI, BHLB, BHP, BID, BIG, BIIB, BIOL, BIOS, BIRT, BJRI, BK, BKE, BKH, BKI, BKMU, BKR, BKSC, BLDP, BLL, BLX, BMC, BMI, BMO, BMRC, BMRN, BMS, BMTC, BMY, BNSO, BOBE, BOH, BOKF, BOLT, BONT, BOOM, BOSC, BOTA, BP, BPAX, BPFH, BPHX, BPL, BPO, BPOP, BPT, BRC, BRCD, BRCM, BRE, BREW, BRID, BRKL, BRKR, BRKS, BRLI, BRN, BRO, BRS, BRT, BRY, BSAC, BSDM, BSET, BSI, BSQR, BSRR, BSTC, BSX, BT, BTH, BTI, BTUI, BTX, BUSE, BVN, BVSN, BVX, BWINA, BWINB, BWS, BXG, BXP, BXS, BYD, BYFC, BZH, C, CA, CAC, CACB, CACC, CACH, CACI, CAFI, CAH, CAKE, CALM, CAM, CAMP, CAMT, CARV, CAS, CASC, CASH, CASM, CASS, CASY, CAT, CATO, CATY, CAW, CB, CBAN, CBB, CBD, CBI, CBIN, CBK, CBL, CBM, CBR, CBRL, CBRX, CBSH, CBST, CBT, CBU, CBZ, CCBG, CCC, CCE, CCF, CCI, CCJ, CCK, CCL, CCMP, CCNE, CCRN, CCU, CCUR, CCZ, CDE, CDI, CDNS, CDR, CDTI, CDZI, CEA, CEB, CEC, CECE, CECO, CEDC, CELG, CENT, CENX, CERN, CERS, CETV, CFBK, CFFI, CFFN, CFI, CFNB, CFNL, CFR, CGEN, CGG, CGI, CGNX, CGX, CHCO, CHD, CHDN, CHDX, CHE, CHFC, CHG, CHH, CHK, CHKE, CHKP, CHL, CHNR, CHS, CHU, CI, CIA, CIB, CIEN, CIG, CIMT, CINF, CIR, CITZ, CIX, CIZN, CKEC, CKH, CKP, CKSW, CL, CLB, CLC, CLCT, CLDX, CLF, CLFD, CLGX, CLH, CLI, CLRO, CLRX, CLS, CLSN, CLWT, CLX, CM, CMA, CMC, CMCO, CMCSA, CMCSK, CMI, CMN, CMO, CMS, CMTL, CNA, CNBC, CNBKA, CNH, CNI, CNL, CNMD, CNP, CNQR, CNR, CNTY, CNW, CNX, COBR, COBZ, COCO, COF, COG, COH, COHR, COHU, COKE, COLB, COLM, COO, COP, COST, COT, CP, CPB, CPE, CPF, CPHD, CPK, CPRT, CPSS, CPST, CPT, CPTS, CPWR, CQB, CR, CRAI, CRAY, CRBC, CRC, CRDS, CRESY, CRH, CRIS, CRK, CRMT, CRNT, CRR, CRRB, CRRC, CRS, CRT, CRUS, CRV, CRVL, CRVP, CRWN, CRZO, CS, CSC, CSCO, CSFL, CSGP, CSGS, CSH, CSL, CSPI, CSS, CSTR, CSU, CSV, CSX, CT, CTAS, CTB, CTBI, CTCH, CTGX, CTHR, CTL, CTO, CTS, CTSH, CTWS, CTXS, CUB, CUZ, CVA, CVBF, CVC, CVD, CVG, CVH, CVLY, CVM, CVO, CVR, CVS, CVTI, CVU, CVV, CVX, CW, CWBC, CWCO, CWEI, CWH, CWST, CWT, CWTR, CXPO, CXW, CY, CYAN, CYBE, CYD, CYMI, CYN, CYT, CYTR, CYTX, D, DAEG, DAIO, DAKT, DAR, DARA, DAVE, DB, DBD, DBLE, DCI, DCO, DCOM, DD, DDS, DDT, DE, DECK, DEL, DELL, DENN, DEO, DEPO, DEST, DFZ, DGAS, DGICB, DGII, DGIT, DGSE, DGX, DHI, DHIL, DHR, DIN, DIS, DISH, DIT, DJCO, DLA, DLHC, DLTR, DLX, DNB, DNDN, DNR, DO, DOM, DORM, DOV, DOW, DOX, DPW, DRAM, DRCO, DRD, DRE, DRI, DRIV, DRL, DRQ, DRRX, DSCI, DSCO, DSGX, DSPG, DSS, DST, DSWL, DTE, DTLK, DUK, DV, DVA, DVD, DVN, DW, DWCH, DWSN, DX, DXLG, DXPE, DXR, DXYN, DY, DYAX, EA, EAT, EBAY, EBF, EBIX, ECBE, ECL, ECOL, ECTE, ED, EDAC, EDAP, EDE, EDGW, EDUC, EE, EEFT, EEI, EEP, EFII, EFX, EGAN, EGAS, EGBN, EGHT, EGN, EGOV, EGP, EGY, EIX, EL, ELGX, ELN, ELNK, ELON, ELP, ELRC, ELS, ELSE, ELTK, ELX, ELY, EMAN, EMC, EMCI, EME, EMITF, EMKR, EML, EMMS, EMMSP, EMN, EMR, ENB, ENDP, ENG, ENI, ENMD, ENTG, ENZ, ENZN, EOC, EOG, EONC, EPAY, EPD, EPHC, EPIQ, EPM, EPR, EQIX, EQR, EQT, EQU, EQY, ERB, ERF, ERIC, ERIE, ESBF, ESBK, ESC, ESCA, ESE, ESGR, ESI, ESIO, ESL, ESLT, ESMC, ESP, ESRX, ESS, ESV, ESYS, ETFC, ETH, ETM, ETP, ETR, EV, EVBS, EVI, EVOL, EWBC, EXAC, EXAR, EXAS, EXC, EXE, EXEL, EXM, EXP, EXPD, EXPO, EXTR, EZCH, EZPW, F, FAC, FALC, FARM, FARO, FAST, FBMI, FBN, FBNC, FBP, FBSS, FC, FCAP, FCBC, FCCY, FCEL, FCF, FCFC, FCFS, FCH, FCN, FCNCA, FCX, FCZA, FDEF, FDO, FDP, FDS, FDX, FE, FEIC, FEIM, FELE, FFBC, FFBH, FFCH, FFEX, FFG, FFIC, FFIN, FFIV, FFKT, FFKY, FGP, FHCO, FHN, FICO, FII, FINL, FISI, FISV, FITB, FIX, FIZZ, FL, FLEX, FLIC, FLIR, FLL, FLML, FLO, FLOW, FLS, FLWS, FLXS, FMBI, FMC, FMER, FMFC, FMNB, FMS, FMX, FNB, FNBN, FNHC, FNLC, FNP, FNSR, FOE, FONR, FORD, FORR, FORTY, FOSL, FR, FRBK, FRD, FRED, FRM, FRME, FRS, FRT, FRX, FSBK, FSCI, FSI, FSRV, FSS, FST, FSTR, FSYS, FTE, FTEK, FTR, FUL, FULT, FUN, FUNC, FUR, FWLT, FWRD, FWV, FXEN, GABC, GAI, GAIA, GAS, GBCI, GBL, GBR, GBX, GCBC, GCFB, GCI, GCO, GCOM, GD, GDI, GDP, GE, GEF, GEL, GEO, GEOS, GERN, GES, GFED, GFF, GFI, GG, GGAL, GGB, GGG, GGR, GHM, GIB, GIFI, GIGA, GIGM, GIII, GIL, GILD, GILT, GIS, GIVN, GK, GKNT, GLCH, GLDC, GLF, GLOW, GLT, GLW, GMCR, GMK, GMT, GMXR, GNCMA, GNI, GNTX, GNVC, GPC, GPI, GPIC, GPK, GPS, GPX, GRA, GRC, GRIF, GRMN, GROW, GRT, GS, GSBC, GSH, GSIG, GSK, GSOL, GSS, GSX, GT, GTI, GTIM, GTIV, GTY, GV, GVA, GVP, GWR, GWW, GXP, GY, GYRO, HA, HAE, HAFC, HAIN, HAL, HALL, HAR, HAS, HAST, HAUP, HBAN, HBHC, HBIO, HCBK, HCC, HCKT, HCN, HCP, HCSG, HD, HDNG, HDSN, HDY, HE, HEB, HEI, HELE, HES, HFBC, HFC, HFFC, HFWA, HGR, HGT, HH, HHS, HIBB, HIG, HIHO, HILL, HITK, HIW, HKTV, HL, HLIT, HLS, HLX, HMA, HMC, HME, HMG, HMN, HMNF, HMNY, HMSY, HMY, HNI, HNP, HNR, HNT, HNZ, HOG, HOLL, HOLX, HON, HOT, HOTT, HOV, HP, HPOL, HPQ, HPT, HR, HRB, HRC, HRG, HRL, HRS, HRT, HSC, HSH, HSIC, HSII, HSKA, HST, HSTM, HSY, HT, HTBK, HTCH, HTCO, HTLD, HTSI, HUBG, HUM, HURC, HVT, HW, HWAY, HWD, HWG, HWKN, HXL, HYGS, HZO, IACI, IART, IBA, IBCA, IBKC, IBM, ICA, ICAD, ICCC, ICGE, ICH, ICLR, ICON,

ICUI, IDA, IDCC, IDN, IDRA, IDSA, IDSY, IDTI, IDXX, IEC, IEP, IEX, IFF, IG, IGLD, IGT, IGTE, IHC, IHT, IIIN, IIJI, IIN, IIT, IIVI, IKNX, ILMN, IM, IMAX, IMCB, IMGN, IMH, IMKTA, IMMR, IMMU, IMN, IMO, IN, INAP, INCY, INDB, INFA, INFI, INFY, ING, INGR, ININ, INO, INOC, INOD, INPH, INS, INT, INTC, INTG, INTL, INTT, INTU, INVE, IO, IOSP, IOT, IP, IPAR, IPG, IPT, IR, IRE, IRET, IRF, IRIX, IRM, IRS, ISCA, ISH, ISIG, ISIL, ISIS, ISLE, ISNS, ISRG, ISRL, ISSC, ISSI, IT, ITI, ITIC, ITMN, ITRI, ITT, ITW, IVAC, IVAN, IVC, IVZ, IX, IXYS, JACK, JAH, JAKK, JBHT, JBL, JBSS, JCI, JCOM, JCP, JCS, JCTCF, JDSU, JEC, JJSF, JKHY, JLL, JNJ, JNPR, JNS, JNY, JOB, JOE, JOEZ, JOSB, JOUT, JOY, JPM, JST, JWN, K, KAI, KAMN, KBALB, KBH, KCG, KCLI, KDN, KEG, KELYA, KELYB, KEM, KEP, KEQU, KERX, KEX, KEY, KEYN, KFRC, KFY, KGC, KGJI, KID, KIM, KKD, KLAC, KLIC, KMB, KMG, KMP, KMPR, KMR, KMT, KMX, KNX, KO, KOOL, KOPN, KOSS, KR, KRC, KSS, KSU, KSWS, KT, KTCC, KTEC, KTOS, KTP, KUB, KVHI, KWK, KWR, KYO, L, LABL, LACO, LAD, LAKE, LAMR, LANC, LARK, LAWS, LAYN, LBAI, LBIX, LBY, LCI, LCUT, LDL, LDR, LECO, LEE, LEG, LEN, LFL, LFUS, LG, LGF, LGL, LGND, LH, LHO, LIFE, LII, LIME, LION, LIOX, LKFN, LLL, LLTC, LLY, LM, LMIA, LMNX, LMT, LNBB, LNC, LNCE, LNDC, LNN, LNT, LOAN, LOGI, LOJN, LOOK, LOW, LPHI, LPNT, LPSN, LPTH, LPX, LRAD, LRCX, LRY, LSBI, LSCC, LSI, LSTR, LTC, LTD, LTRE, LTRX, LTS, LTXC, LUB, LUFK, LUK, LUV, LUX, LVB, LVLT, LWAY, LXK, LXP, LXRX, LXU, LYG, LYTS, LZB, M, MAA, MAC, MAG, MAGS, MAN, MANH, MAR, MARPS, MAS, MASC, MAT, MATR, MATW, MAXY, MAYS, MBFI, MBI, MBRG, MBTF, MBVT, MBWM, MCBC, MCBI, MCD, MCF, MCHP, MCK, MCRI, MCRL, MCRS, MCS, MCY, MCZ, MD, MDC, MDCA, MDCI, MDCO, MDM, MDP, MDR, MDRX, MDT, MDU, MEAD, MEAS, MED, MEG, MEI, MENT, MEOH, MERC, METR, MFA, MFI, MFLR, MFNC, MFRI, MFSF, MGA, MGAM, MGEE, MGIC, MGM, MGPI, MGRC, MGT, MHK, MHO, MHP, MIDD, MIG, MIL, MIND, MINI, MITK, MKC, MKL, MKSI, MKTAY, MLAB, MLHR, MLI, MLM, MLNK, MLP, MLR, MMC, MMM, MMR, MMS, MMSI, MMUS, MNDO, MNI, MNR, MNRO, MNST, MNTG, MO, MOC, MOCO, MOD, MOLX, MOLXA, MON, MOSY, MOV, MOVE, MPAA, MPB, MPET, MPR, MPX, MRCY, MRGE, MRK, MRO, MRTN, MRVL, MS, MSA, MSB, MSCC, MSEX, MSFG, MSFT, MSI, MSL, MSLI, MSM, MSN, MSON, MSTR, MT, MTB, MTD, MTEX, MTG, MTH, MTN, MTOR, MTR, MTRN, MTRX, MTSC, MTSL, MTSN, MTW, MTX, MTZ, MU, MUR, MUX, MVIS, MW, MWV, MWW, MXIM, MXWL, MYE, MYGN, MYL, NAFC, NAII, NANO, NASB, NAT, NATH, NATI, NAV, NAVB, NAVG, NAVR, NBBC, NBIX, NBL, NBR, NBS, NBTB, NC, NCI, NCR, NCS, NDSN, NDZ, NE, NEE, NEM, NEN, NEOG, NEON, NETC, NEU, NEWP, NEWT, NFG, NFX, NGT, NHC, NHI, NHTB, NI, NICE, NICK, NJR, NKE, NKSH, NKTR, NL, NLS, NLY, NMRX, NNBR, NNN, NOC, NOK, NOV, NOVB, NPBC, NPK, NPSP, NR, NRCI, NRGY, NRIM, NRT, NSC, NSEC, NSIT, NSP, NSSC, NSYS, NTAP, NTCT, NTE, NTIC, NTL, NTN, NTRS, NTSC, NTT, NTWK, NTZ, NU, NUAN, NUE, NUS, NUTR, NVDA, NVE, NVEC, NVGN, NVMI, NVO, NVR, NVS, NVTL, NWBI, NWFL, NWL, NWLI, NWN, NWPX, NWS, NWSA, NX, NYCB, NYMX, NYNY, NYT, O, OBAS, OBCI, OBT, OCC, OCFC, OCLR, OCN, OCR, ODC, ODFL, ODP, OFC, OFG, OFIX, OGE, OGXI, OHI, OI, OII, OIIM, OKE, OKSB, OLN, OLP, OMC, OMCL, OME, OMEX, OMG, OMX, ONB, ONCY, ONFC, ONNN, ONTY, ONVI, ONXX, OPAY, OPK, OPLK, OPOF, OPY, ORB, ORBK, ORBT, ORCL, ORI, ORLY, ORRF, OSBC, OSIS, OSK, OSUR, OTEX, OTTR, OVBC, OVRL, OVTI, OXGN, OXM, OXY, OZRK, PAA, PAAS, PACW, PAG, PAL, PANL, PAR, PATK, PATR, PAYX, PB, PBCT, PBHC, PBI, PBNY, PBT, PBY, PC, PCAR, PCBK, PCC, PCCC, PCG, PCH, PCL, PCLN, PCMI, PCP, PCTI, PCYC, PCYO, PDCE, PDCO, PDEX, PDFS, PDII, PDLI, PDS, PEBK, PEBO, PEGA, PEI, PENN, PENX, PEP, PERF, PERY, PESI, PETM, PETS, PFBI, PFE, PFH, PFIN, PFSW, PG, PGC, PGI, PGNX, PGR, PH, PHG, PHI, PHII, PHIIK, PHM, PHMD, PHX, PICO, PII, PIR, PKD, PKE, PKI, PKOH, PKX, PKY, PL, PLAB, PLCC, PLCE, PLCM, PLD, PLL, PLM, PLNR, PLPC, PLT, PLUG, PLUS, PLXS, PLXT, PMBC, PMCS, PMD, PMFG, PMTC, PMTI, PNBK, PNC, PNFP, PNK, PNM, PNR, PNRA, PNRG, PNTR, PNW, PNY, POM, POOL, POPE, POT, POWI, POWL, POWR, POZN, PPBI, PPG, PPHM, PPL, PPS, PQ, PRCP, PRE, PRFT, PRGO, PRGS, PRGX, PRK, PRKR, PRLS, PROV, PRPH, PRWT, PRXL, PSA, PSB, PSEM, PSMT, PSUN, PT, PTEN, PTIE, PTIX, PTN, PTNR, PTNT, PTRY, PTSI, PTSX, PTX, PULB, PULS, PURE, PVA, PVD, PVFC, PVH, PVSW, PVTB, PW, PWER, PWOD, PWR, PWX, PX, PXD, PXLW, PZZA, PZZI, QADB, QBAK, QCOM, QCOR, QCRH, QDEL, QGEN, QLGC, QLTI, QSII, QUIK, R, RAD, RADA, RAI, RAS, RAVN, RBA, RBC, RBCAA, RBNF, RBPAA, RCI, RCII, RCKY, RCL, RCMT, RDC, RDCM, RDEN, RDI, RDN, RDNT, RDWR, RE, RECN, REDF, REFR, REG, REGN, REIS, RELL, RELV, RENT, RES, REV, REX, REXI, RF, RFIL, RFMD, RGCO, RGEN, RGLD, RGR, RGS, RHI, RHP, RHT, RIC, RICK, RIG, RIGL, RIMG, RIO, RITT, RIVR, RJF, RKT, RL, RLH, RLI, RMBS, RMCF, RMD, RMKR, RMTI, RNR, RNST, RNWK, ROCK, ROCM, ROG, ROIA, ROIAK, ROK, ROL, ROP, ROST, ROVI, ROYL, RPI, RPM, RPRX, RPT, RPTP, RRC, RRD, RS, RSG, RSH, RSTI, RSYS, RT, RTEC, RTI, RTIX, RTK, RUK, RUSHB, RVLT, RVP, RVSB, RWC, RWT, RY, RYAAY, RYL, RYN, S, SABA, SAFM, SAH, SAL, SALM, SAM, SAN, SANM, SAP, SAPE, SASR, SBAC, SBBX, SBCF, SBGI, SBR, SBSA, SBSI, SBUX, SCBT, SCCO, SCG, SCHL, SCHN, SCHW, SCI, SCL, SCLN, SCOK, SCS, SCSC, SCSS, SCVL, SCX, SDIX, SEAC, SEB, SED, SEE, SEIC, SENEA, SENEB, SEV, SF, SFD, SFE, SFG, SFI, SFNC, SFY, SGA, SGB, SGC, SGEN, SGK, SGMA, SGMO, SGMS, SGRP, SGU, SGY, SHBI, SHFL, SHI, SHLM, SHLO, SHOO, SHPG, SHS, SHW, SIAL, SIEB, SIF, SIFY, SIG, SIGA, SIGI, SIGM, SILC, SIM, SIMG, SIVB, SJI, SJR, SJT, SJW, SKM, SKS, SKT, SKX, SKY, SKYW, SLAB, SLB, SLG, SLGN, SLI, SLM, SLP, SLTC, SLXP, SM, SMBC, SMG, SMIT, SMP, SMRT, SMSI, SMTC, SMTX, SNA, SNAK, SNBC, SNDK, SNE, SNFCA, SNHY, SNPS, SNV, SO, SOFO, SOHU, SON, SONC, SONS, SPA, SPAN, SPAR, SPCHB, SPEX, SPF, SPG, SPH, SPIL, SPIR, SPLS, SPNC, SPNS, SPP, SPPI, SPPR, SPRT, SPTN, SPW, SQNM, SR, SRCE, SRCL, SRDX, SRE, SRI, SRPT, SRT, SSD, SSL, SSP, SSRI, SSS, SSY, SSYS, STAA, STBA, STC, STE, STEC, STEI, STEL, STEM, STFC, STI, STJ, STKL, STL, STLD, STLY, STM, STMP, STNR, STR, STRA, STRM, STRS, STRT, STS, STSA, STSI, STT, SU, SUBK, SUI, SUP, SUPX, SUSQ, SVBL, SVNT, SVT, SVU, SWC, SWHC, SWIR, SWK, SWKS, SWM, SWN, SWS, SWX, SWY, SXI, SXT, SYBT, SYK, SYKE, SYMC, SYMM, SYNL, SYNM, SYNT, SYPR, SYX, SYY, T, TACT, TAIT, TAP, TARO, TASR, TATT, TAXI, TAYD, TBAC, TBI, TCB, TCBK, TCCO, TCI, TCO, TCP, TCX, TD, TDS, TDW, TE, TECD, TECH, TECUA, TECUB, TEF, TEG, TELK, TEN, TEO, TER, TESO, TESS, TEVA, TEX, TFCO, TFX, TG, TGA, TGB, TGC, TGI, TGS, TGT, TGX, THC, THFF, THG, THO, THOR, THRD, THRM, TIBX, TIF, TIGR, TIK, TILE, TINY, TISA, TISI, TIVO, TJX, TK, TKR, TLAB, TLF, TLK, TLM, TM, TMK, TMNG, TMO, TMP, TNC, TNH, TOF, TOL, TORM, TOT, TPC, TPL, TQNT, TR, TRC, TREX, TRIB, TRK, TRMB, TRMK, TRN, TRNS, TROW, TRP, TRR, TRST, TRT, TRV, TSBK, TSCO, TSEM, TSH, TSM, TSN, TSO, TSRI, TSS, TST, TSU, TSYS, TTC, TTEC, TTEK, TTI, TTMI, TTWO, TUC, TUES, TUP, TV, TVC, TVE, TWI, TWIN, TWMC, TWTC, TWX, TXCC, TXI, TXN, TXT, TYC, TYL, UAM, UAMY, UBA, UBCP, UBFO, UBOH, UBP, UBSH, UBSI, UCFC, UDR, UEIC, UFCS, UFI, UFPI, UFPT, UG, UGI, UHAL, UHS, UHT, UIL, UIS, UL, ULBI, ULGX, ULTI, UMBF, UMH, UMPQ, UN, UNAM, UNB, UNF, UNFI, UNH, UNM, UNP, UNS, UNT, UNTD, UNTY, UPIP, UPL, UQM, URBN, URI, URS, USAK, USAP, USAT, USB, USBI, USEG, USG, USLM, USM, USNA, USPH, USTR, USU, UTEK, UTHR, UTIW, UTL, UTMD, UTSI, UTX, UUU, UVSP, UVV, VAL, VALU, VAR, VASC, VBFC, VCBI, VCI, VCLK, VCO, VDSI, VECO, VFC, VGR, VGZ, VHC, VHI, VICL, VICR, VIDE, VIFL, VII, VIRC, VIVO, VLCCF, VLGEA, VLO, VLY, VMC, VMI, VMO, VNO, VOD, VOXX, VPHM, VPV, VRML, VRNM, VRSN, VRTX, VRX, VSAT, VSCI, VSEC, VSR, VTNC, VTNR, VTR, VTSS, VVC, VVTV, VVUS, VZ, WAB, WABC, WAC, WACLY, WAFD, WAG, WASH, WAT, WAVX, WAYN, WBCO, WBK, WBS, WBSN, WCBO, WCC, WCN, WDC, WDFC, WDR, WEBM, WEC, WEN, WERN, WETF, WEX, WEYS, WFC, WFM, WFR, WFT, WG, WGA, WGL, WGO, WHR, WIBC, WILC, WINA, WIRE, WLB, WLFC, WLT, WM, WMAR, WMB, WMGI, WMK, WMS, WMT, WNC, WOOF, WOR, WPC, WPO, WPP, WPPGY, WR, WRB, WRI, WRLD, WRLS, WSB, WSBC, WSCI, WSFS, WSM, WSO, WST, WSTG, WSTL, WTFC, WTM, WTR, WTS, WTSL, WTT, WVFC, WVVI, WWD, WWE, WWW, WY, WYY, X, XEL, XL, XLNX, XOM, XOMA, XOXO, XRAY, XRSC, XRX, XXIA, Y, YAVY, YHOO, YORW, YPF, YUM, YZC, ZAZA, ZBRA, ZEUS, ZIGO, ZION, ZIXI, ZLC, ZNH, ZOLT, ZOOM, ZQK

Appendix C

Moments

We use the following definition

$$\Phi(x) = \frac{1}{2} + \frac{1}{2}\,\mathrm{erf}\left(\frac{x}{\sqrt{2}}\right) \tag{C.1}$$

with the error function

$$\mathrm{erf}(y) = \frac{2}{\sqrt{\pi}} \int_0^y \mathrm{d}\tau \mathrm{e}^{-\tau^2} \tag{C.2}$$

to express the moments.

Zeroth moment

$$\begin{aligned} m_0(u) =& \int_{-\infty}^{\hat{F}} d\hat{V} \sqrt{\frac{N}{2\pi T(1-c)\rho^2}} \exp\left(-\frac{(\hat{V}+\sqrt{cT}u\rho)^2}{2T(1-c)\rho^2/N}\right) \\ =& \Phi\left(\frac{\hat{F}+\sqrt{cT}u\rho}{\sqrt{T(1-c)\rho^2/N}}\right) \end{aligned} \tag{C.3}$$

First moment

$$\begin{aligned} m_1(z,u) =& m_0(u) - \frac{V_0}{F} \int_{-\infty}^{\hat{F}} d\hat{V} \sqrt{\frac{N}{2\pi T(1-c)\rho^2}} \\ & \times \exp\left(\sqrt{z}\hat{V} + (\mu - \frac{\rho^2}{2})T\right) \exp\left(-\frac{(\hat{V}+\sqrt{cT}u\rho)^2}{2T(1-c)\rho^2/N}\right) \\ =& m_0(z,u) - \frac{V_0}{F} \exp\left((\mu - \frac{\rho^2}{2})T - \sqrt{cTz}u\rho + T(1-c)\frac{\rho^2 z}{2N}\right) \\ & \times \Phi\left(\frac{\hat{F} - T(1-c)\rho^2\sqrt{z}/N + \sqrt{cT}u\rho}{\sqrt{T(1-c)\rho^2/N}}\right) \end{aligned} \tag{C.4}$$

Second moment

$$
\begin{aligned}
m_2(z,u) &= -m_0(u) + 2m_1(z,u) + \frac{V_0^2}{F^2} \int_{-\infty}^{\hat{F}} d\hat{V} \sqrt{\frac{N}{2\pi T(1-c)\rho^2}} \\
&\qquad \times \exp\left(2\sqrt{z}\hat{V} + 2\mu T - \rho^2 T\right) \exp\left(-\frac{(\hat{V} + \sqrt{cT}u\rho)^2}{2T(1-c)\rho^2/N}\right) \\
&= -m_0(z,u) + 2m_1(z,u) + \frac{V_0^2}{F^2} \\
&\qquad \times \exp\left(2\mu T - \rho^2 T - 2\sqrt{cTz}u\rho - 2T(1-c)\frac{\rho^2 z}{N}\right) \\
&\qquad \times \Phi\left(\frac{\hat{F} + \sqrt{cT}u\rho - 2T(1-c)\rho^2\sqrt{z}/N}{\sqrt{T(1-c)\rho^2/N}}\right) \qquad \text{(C.5)}
\end{aligned}
$$

Appendix D

Rotated and scaled returns

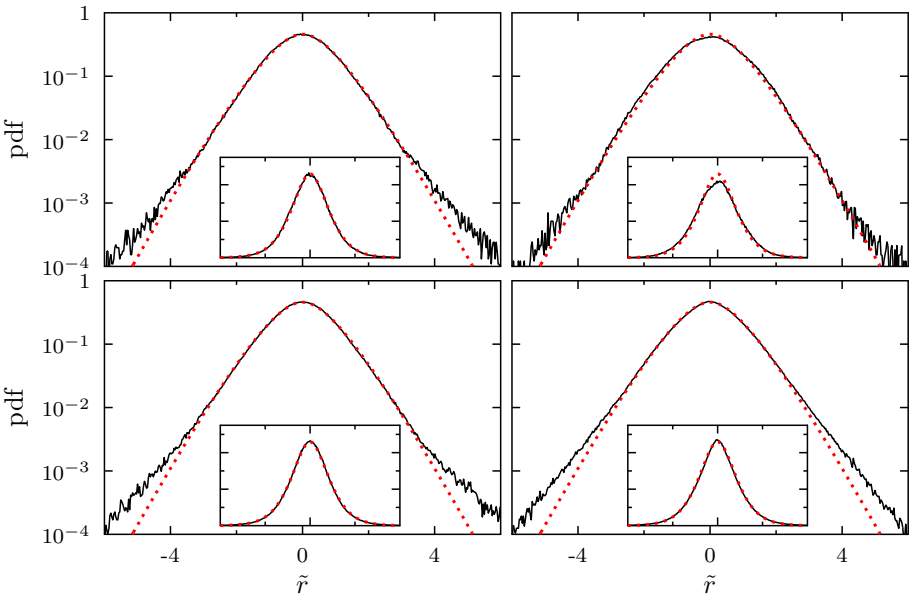

Figure D.1: Aggregated distributions for the rotated and scaled yearly returns using the covariance matrix $\hat{\Sigma}$ with homogeneous correlation structure. The empirical distribution is shown in black and the theoretical result is red and dotted. The S&P 500 and the NASDAQ data use $N = 6$. Top left/right: S&P 500 (1992-2012) / (2002-2012), bottom left/right: NASDAQ (1992-2012) / (2002-2012). The average correlation levels are $c = 0.28, 0.42, 0.23$ and $c = 0.31$, respectively.

Figure D.1 shows the distributions for the rotated and scaled yearly returns for the covariance matrix with homogeneous correlation structure.

List of Figures

List of Tables

Bibliography

[1] T. A. Schmitt, D. Chetalova, R. Schäfer, and T. Guhr. "Non-Stationarity in Financial Time Series and Generic Features". In: *Europhysics Letters* 103 (2013), p. 58003.

[2] T. A. Schmitt, D. Chetalova, R. Schäfer, and T. Guhr. "Credit risk and the instability of the financial system: An ensemble approach". In: *Europhysics Letters* 105 (2014), p. 38004.

[3] D. Chetalova, T. A. Schmitt, R. Schäfer, and T. Guhr. "Portfolio return distributions: Sample statistics with non-stationary correlations". In: *ArXiv: 1308.3961* (2013). arXiv: `1308.3961`.

[4] T. A. Schmitt, R. Schäfer, D. Wied, and T. Guhr. "Spatial Dependence in Stock Returns-Local Normalization and VAR Forecasts". In: *SSRN.com/abstract=2320675* (2013).

[5] T. A. Schmitt, R. Schäfer, and T. Guhr. "Credit risk: Taking fluctuating asset correlations into account". In: *in preparation* (2014).

[6] T. A. Schmitt, R. Schäfer, T. Guhr, and H. Dette. "Quantile correlations: Uncovering temporal dependencies in financial time series". In: *submitted to International Journal of Theoretical and Applied Finance* (2014).

[7] T. A. Schmitt, R. Schäfer, M. C. Münnix, and T. Guhr. "Microscopic understanding of heavy-tailed return distributions in an agent-based model". In: *Europhysics Letters* 100 (2012), p. 38005.

[8] D. Wagner, T. A. Schmitt, R. Schäfer, T. Guhr, and D. Wolf. "Analysis of a decision model in the context of equilibrium pricing and order book pricing". In: *ArXiv: 1404.7356* (2014).

[9] H. E. Stanley, V. Afanasyev, L. Amaral, S. Buldyrev, A. Goldberger, S. Havlin, H. Leschhorn, P. Maass, R. N. Mantegna, C. Peng, P. Prince, M. Salinger, M. Stanley, and G. Viswanathan. "Anomalous fluctuations in the dynamics of complex systems: from DNA and physiology to econophysics". In: *Physica A* 224 (1996), pp. 302–321.

[10] D. Bernoulli. *Hydrodynamica*. 1738.

[11] H. Levy and M. Sarnat. *Portfolio and investment selection: Theory and practice*. Prentice Hall, 1984, p. 110.

[12] J. C. Cox, V. Sadiraj, and B. Vogt. "On the empirical relevance of St. Petersburg lotteries". In: *Economics Bulletin* 29.1 (2009), pp. 221–227.

[13] D. Bernoulli. "Exposition of a New Theory on the Measurement of Risk". In: *Econometrica* 22.1 (1954), pp. 23–36.

[14] P. A. Samuelson. "The St. Petersburg Paradox as a Divergent Double Limit". In: *International Economic Review* 1.1 (1960), pp. 31–37.

[15] O. Peters. "The time resolution of the St. Petersburg paradox." In: *Philosophical Transactions of the Royal Society A* 369 (2011), pp. 4913–31.

[16] A. Einstein. "Über die von der molekularkinetischen Theorie der Wärme geforderte Bewegumg von in ruhenden Flüssigkeiten suspendierten Teilchen". In: *Annalen der Physik* 322.8 (1905), pp. 549–560.

[17] R. Brown. "A brief account of microscopical observations made in the months of June, July and August, 1827, on the particles contained in the pollen of plants; and on the general existence of active molecules in organic and inorganic bodies". In: *The miscellaneous botanical works of Robert Brown* 1 (1866).

[18] L. Bachelier. "Théorie de la spéculation". In: *Annales Scientifiques de l'École Normale Supérieure* 3.17 (1900), pp. 21–86.

[19] B. Mandelbrot. "The variation of certain speculative prices". In: *The Journal of Business* 36.4 (1963), pp. 394–419.

[20] B. Mandelbrot. *The Fractal Geometry of Nature*. W. H. Freeman and Company, 1982.

[21] F. Black and M. Scholes. "The Pricing of Options and Corporate Liabilities". In: *The Journal of Political Economy* 81.3 (1973), pp. 637–654.

[22] B. Eichengreen, A. Mody, M. Nedeljkovic, and L. Sarno. "How the Subprime Crisis went global: Evidence from bank credit default swap spreads". In: *Journal of International Money and Finance* 31.5 (2012), pp. 1299–1318.

[23] European Commission. *Unemployment rate by sex and age groups - monthly average [une_rt_m]*. 2014. URL: `http://appsso.eurostat.ec.europa.eu/nui/show.do?dataset=une%5C_rt%5C_m%5C&lang=en`.

[24] F. S. Mishkin. *The economics of money, banking, and financial markets*. 7th. Addison-Wesley, 2007.

[25] M. Bensasson and M. Petrakis. *Biggest Greek Bondholders Will Forgive More Than Half Debt in Aid Accord*. 2012. URL: `http://www.bloomberg.com/news/2012-02-21/greece-s-creditors-agree-to-forgive-more-than-half-debt.html`.

[26] M. Phillips and E. Bartha. *German Yields South of Zero*. 2012. URL: http://on.wsj.com/wXuEKc.

[27] N. Wilkinson and M. Klaes. *An Introduction to Behavioral Economics*. 2nd ed. Palgrave Macmillan, 2012.

[28] B. J. Alder and T. E. Wainwright. "Studies in Molecular Dynamics. I. General Method". In: *The Journal of Chemical Physics* 31.2 (1959), pp. 459–466.

[29] A. Rahman. "Correlations in the Motion of Atoms in Liquid Argon". In: *Physical Review* 136.2A (1964), A405–A411.

[30] J. M. Haile. *Molecular Dynamics Simulation: Elementary Methods*. 1st ed. Wiley-Interscience, 1997.

[31] R. C. Merton. "Theory of Rational Option Pricing". In: *The Bell Journal of Economics and Management Science* 4.1 (1973), pp. 141–183.

[32] J. C. Hull. *Options, Futures and Other Derivatives*. 7th ed. Prentice Hall, 2008.

[33] D. Friedman and J. Rust. *The Double Auction Market*. The Advanced Book Program, 1993.

[34] B. Johnson. *Algorithmic Trading & DMA*. 4Myeloma Press, 2010.

[35] *Standard & Poor's 500 data from Yahoo! Finance*. 2013. URL: http://finance.yahoo.com.

[36] W. C. Mitchell. "The Making and Using of Index Numbers". In: *Bulletin of the U.S. Bureau of Labor Statistics* 173 (1915).

[37] M. Oliver. "Les Nombres indices de la variation des prix". PhD thesis. Paris, 1926.

[38] F. C. Mills. *The Behavior of Prices*. New York: National Bureau of Economic Research, Inc., 1927.

[39] P. K. Clark. "A Subordinated Stochastic Process Model with Finite Variance for Speculative Prices". In: *The Econometric Society* 41.1 (1973), pp. 135–155.

[40] W. B. Arthur, J. H. Holland, B. LeBaron, R. Palmer, and P. Tayler. "Asset Pricing Under Endogenous Expectations in an Artificial Stock Market". In: *The Economy as an Evolving Complex System II*. Ed. by W. B. Arthur, S. N. Durlauf, and D. H. Lane. Vol. 1001. Addison-Wesley, 1996, pp. 15–44.

[41] B. Mandelbrot. *Fractals and Scaling in Finance*. Springer, 1997.

[42] D. Sornette. "Multiplicative processes and power laws". In: *Physical Review E* 57.4 (1998), pp. 4811–4813.

[43] T. Lux and M. Marchesi. “Scaling and criticality in a stochastic multi-agent model of a financial market”. In: *Nature* 397 (1999), pp. 498–500.

[44] R. Cont. “Herd behavior and aggregate fluctuations in financial markets”. In: *Macroeconomic Dynamics* 4 (2000), pp. 170–196.

[45] D. Challet, A. Chessa, M. Marsili, and Y.-C. Zhang. “From Minority Games to real markets”. In: *Quantitative Finance* 1.1 (2001), pp. 168–176.

[46] X. Gabaix, P. Gopikrishnan, and V. Plerou. “A theory of power-law distributions in financial market fluctuations”. In: *Nature* 423 (2003), pp. 267–270.

[47] J. D. Farmer and F. Lillo. “On the origin of power-law tails in price fluctuations”. In: *Quantitative Finance* 4.1 (2004), pp. C7–C11.

[48] E. F. Fama. “The Behavior of Stock-Market Prices”. In: *The Journal of Business* 38.1 (1965), pp. 34–105.

[49] K. G. Koedijk. “The tail index of exchange rate returns”. In: *Journal of International Economics* 29.1990 (1990), pp. 93–108.

[50] F. M. Longin. “The Asymptotic Distribution of Extreme Stock Market Returns”. In: *The Journal of Business* 69.3 (1996), pp. 383–408.

[51] T. Lux. “The stable Paretian hypothesis and the frequency of large returns: an examination of major German stocks”. In: *Applied Financial Economics* 6.6 (1996), pp. 463–475.

[52] R. N. Mantegna and H. E. Stanley. “Scaling behaviour in the dynamics of an economic index”. In: *Nature* 376.6535 (1995), pp. 46–49.

[53] V. Plerou, P. Gopikrishnan, L. A. Nunes Amaral, M. Meyer, and H. E. Stanley. “Scaling of the distribution of price fluctuations of individual companies.” In: *Physical Review E* 60.6 (1999), pp. 6519–29.

[54] P. Gopikrishnan, V. Plerou, L. A. Nunes Amaral, M. Meyer, and H. E. Stanley. “Scaling of the distribution of fluctuations of financial market indices.” In: *Physical Review E* 60.5 (1999), pp. 5305–16.

[55] Y. Malevergne, V. Pisarenko, and D. Sornette. “Empirical Distributions of Log-Returns: between the Stretched Exponential and the Power Law?” In: *Quantitative Finance* 5.4 (2005), pp. 379–401.

[56] C. C. Ying. “Stock Market Prices and Volumes of Sales”. In: *Econometrica* 34.3 (1966), pp. 676–685.

[57] T. W. Epps and M. L. Epps. “The Stochastic Dependence of Security Price Changes and Transaction Volumes: Implications for the Mixture-of-Distributions Hypothesis”. In: *Econometrica* 44.2 (1976), pp. 305–321.

[58] R. J. Rogalski. "The Dependence of Prices and Volume". In: *The Review of Econometrics and Statistics* 60.2 (1978), pp. 268–274.

[59] J. D. Farmer, L. Gillemot, F. Lillo, S. Mike, and A. Sen. "What really causes large price changes?" In: *Quantitative Finance* 4.4 (2004), pp. 383–397.

[60] F. Black. "Studies of stock price volatility changes". In: *Proceedings of the 1976 Meetings of the American Statistical Association, Business and Economics Statistics Section*. 1976, pp. 177–181.

[61] G. W. Schwert. "Why Does Stock Market Volatility Change Over Time?" In: *The Journal of Finance* 44.5 (1989), pp. 1115–1153.

[62] Z. Ding, C. W. Granger, and R. F. Engle. "A long memory property of stock market returns and a new model". In: *Journal of Empirical Finance* 1.1 (1993), pp. 83–106.

[63] P. Jorion. *Value at Risk*. 3rd ed. McGraw-Hill, 2007.

[64] *Squeezing the accelerator*. 2008. URL: `http://www.economist.com/node/12501847`.

[65] H. Markowitz. "Portfolio Selection". In: *The Journal of Finance* 7.1 (1952), pp. 77–91.

[66] N. N. Taleb, D. G. Goldstein, and M. W. Spitznagel. "The Six Mistakes Executives Make in Risk Management". In: *Harvard Business Review* (2009).

[67] Basel Committee on Banking Supervision. *International Convergence of Capital Measurement and Capital Standards*. 2006.

[68] Basel Committee on Banking Supervision. *Basel III: A global regulatory framework for more resilient banks and banking systems*. 2010.

[69] L. Laloux, P. Cizeau, J. Bouchaud, and M. Potters. "Noise Dressing of Financial Correlation Matrices". In: *Physical Review Letters* 83.7 (1999), pp. 1467–1470.

[70] P. Gopikrishnan, B. Rosenow, V. Plerou, and H. E. Stanley. "Quantifying and interpreting collective behavior in financial markets". In: *Physical Review E* 64.3 (2001), p. 035106.

[71] L. Giada and M. Marsili. "Data clustering and noise undressing of correlation matrices". In: *Physical Review E* 63.6 (2001), p. 061101.

[72] E. J. Elton, M. J. Gruber, S. J. Brown, and W. N. Goetzmann. *Modern Portfolio Theory and Investment Analysis*. 7th ed. Wiley, 2006, p. 752.

[73] F. M. Longin and B. Solnik. "Is the correlation in international equity returns constant: 1960–1990?" In: *Journal of International Money and Finance* 14 (1995), pp. 3–26.

[74] G. Bekaert and C. R. Harvey. “Time-varying world market integration”. In: *The Journal of Finance* L.2 (1995), pp. 403–44.

[75] M. C. Münnix, T. Shimada, R. Schäfer, F. Leyvraz, T. H. Seligman, T. Guhr, and H. E. Stanley. “Identifying states of a financial market.” In: *Scientific reports* 2 (2012), p. 644.

[76] Y. Demyanyk and O. Van Hemert. “Understanding the Subprime Mortgage Crisis”. In: *Review of Financial Studies* 24.6 (2009), pp. 1848–1880.

[77] J. K. Brueckner, P. S. Calem, and L. I. Nakamura. “Subprime mortgages and the housing bubble”. In: *Journal of Urban Economics* 71.2 (2012), pp. 230–243.

[78] J. Bouchaud and M. Potters. *Theory of Financial Risk and Derivative Pricing: From Statistical Physics to Risk Management*. 2nd ed. Cambridge University Press, 2009.

[79] V. Plerou, P. Gopikrishnan, X. Gabaix, and H. E. Stanley. “Quantifying stock-price response to demand fluctuations”. In: *Physical Review E* 66 (2002), p. 027104.

[80] S. Pafka and I. Kondor. “Noisy covariance matrices and portfolio optimization”. In: *The European Physical Journal B* 27.2 (2002), pp. 277–280.

[81] S. Pafka and I. Kondor. “Noisy covariance matrices and portfolio optimization II”. In: *Physica A* 319 (2003), pp. 487–494.

[82] T. Guhr and B. Kälber. “A new method to estimate the noise in financial correlation matrices”. In: *Journal of Physics A* 36.12 (2003), pp. 3009–3032.

[83] R. Schäfer, N. F. Nilsson, and T. Guhr. “Power mapping with dynamical adjustment for improved portfolio optimization”. In: *Quantitative Finance* 10.1 (2010), pp. 107–119.

[84] E. Pantaleo, M. Tumminello, F. Lillo, and R. N. Mantegna. “When do improved covariance matrix estimators enhance portfolio optimization? An empirical comparative study of nine estimators”. In: *Quantitative Finance* 11.7 (2011), pp. 1067–1080.

[85] W. F. Sharpe. “A simplified model for portfolio analysis”. In: *Management science* 9.2 (1963), pp. 277–293.

[86] M. Arnold, S. Stahlberg, and D. Wied. “Modeling different kinds of spatial dependence in stock returns”. In: *Empirical Economics* 44.2 (2011), pp. 761–774.

[87] R. Schäfer and T. Guhr. “Local normalization: Uncovering correlations in non-stationary financial time series”. In: *Physica A* 389.18 (2010), pp. 3856–3865.

[88] T. Bollerslev. “Generalized Autoregressive Conditional Heteroskedasticity”. In: *Journal of Econometrics* 31 (1986), pp. 307–327.

[89] T. Bollerslev, R. F. Engle, and J. M. Wooldridge. “A Capital Asset Pricing Model with Time-Varying Covariances”. In: *The Journal of Political Economy* 96.1 (1988), pp. 116–131.

[90] R. F. Engle. “Autoregressive Conditional Heteroscedasticity with Estimates of the Variance of United Kingdom Inflation”. In: *Econometrica* 50.4 (1982), pp. 987–1007.

[91] P. R. Hansen and A. Lunde. “A forecast comparison of volatility models: does anything beat a GARCH(1,1)?” In: *Journal of Applied Econometrics* 20.7 (2005), pp. 873–889.

[92] A. A. P. Santos, F. J. Nogales, and E. Ruiz. “Comparing Univariate and Multivariate Models to Forecast Portfolio Value-at-Risk”. In: *Journal of Financial Econometrics* 11.2 (2012), pp. 400–441.

[93] L. Anselin. *Spatial econometrics: methods and models*. Studies in Operational Regional Science. Springer, 1988.

[94] N. Cressie. *Statistics for spatial data*. Wiley series in probability and mathematical statistics: Applied probability and statistics. J. Wiley, 1993.

[95] J. LeSage and R. Pace. *Introduction to Spatial Econometrics*. Statistics: a Series of Textbooks and Monographs. CRC PressINC, 2009.

[96] L.-f. Lee and X. Liu. “Efficient GMM Estimation of High Order Spatial Autoregressive Models With Autoregressive Disturbances”. In: *Econometric Theory* 26.01 (2009), pp. 187–230.

[97] X. Lin and L.-f. Lee. “GMM estimation of spatial autoregressive models with unknown heteroskedasticity”. In: *Journal of Econometrics* 157.1 (2010), pp. 34–52.

[98] T. Kuen and T. Hoong. “Forecasting volatility in the Singapore stock market”. In: *Asia Pacific Journal of Management* 9.1 (1992), pp. 1–13.

[99] D. M. Walsh and G. Y.-G. Tsou. “Forecasting index volatility: sampling interval and non-trading effects”. In: *Applied Financial Economics* 8.5 (1998), pp. 477–485.

[100] S.-H. Poon and C. W. Granger. “Forecasting volatility in financial markets: A review”. In: *Journal of Economic Literature* XLI (2003), pp. 478–539.

[101] H. Markowitz. *Portfolio Selection: Efficient Diversification of Investment*. Yale University Press, 1959.

[102] M. Yang. “Normal Log-normal Mixture: Leptokurtosis, Skewness and Applications”. In: *Econometric Society 2004 Australasian Meetings* (2004).

[103] T. Bollerslev. “Glossary to ARCH (GARCH)”. In: *CREATES Research Paper* 49 (2008).

[104] A. Pagan. “The econometrics of financial markets”. In: *Journal of Empirical Finance* 3.1 (1996), pp. 15–102.

[105] P. Cizeau, Y. Liu, M. Meyer, C.-K. Peng, and H. E. Stanley. “Volatility distribution in the S&P500 stock index”. In: *Physica A* 245 (1997), pp. 441–445.

[106] Y. Liu, P. Cizeau, M. Meyer, C.-K. Peng, and H. E. Stanley. “Correlations in economic time series”. In: *Physica A* 245 (1997), pp. 437–440.

[107] S. Figlewski and X. Wang. “Is the "Leverage Effect" a Leverage Effect?” In: *Finance Working Papers* (2000). URL: `http://hdl.handle.net/2451/26702`.

[108] A. C. Aydemir, M. Gallmeyer, and B. Hollifield. “Financial leverage does not cause the leverage effect”. In: *AFA 2007 Chicago Meetings Paper* (2006).

[109] Y. Aït-Sahalia, J. Fan, and Y. Li. “The leverage effect puzzle: Disentangling sources of bias at high frequency”. In: *Journal of Financial Economics* 109.1 (2013), pp. 224–249.

[110] T.-H. Li. “Laplace Periodogram for Time Series Analysis”. In: *Journal of the American Statistical Association* 103.482 (2008), pp. 757–768.

[111] R. Koenker. *Quantile Regression*. Econometric Society Monographs. Cambridge University Press, 2005.

[112] T.-H. Li. “Quantile Periodograms”. In: *Journal of the American Statistical Association* 107.498 (2012), pp. 765–776.

[113] B. Kedem. “Binary Time Series”. In: *Lecture Notes in Pure and Applied Mathematics* 52 (1980).

[114] H. Dette, M. Hallin, T. Kley, and S. Volgushev. “Of Copulas, Quantiles, Ranks and Spectra an L1-approach to spectral analysis”. In: *arXiv:1111.7205v1, to appear in: Bernoulli* (2011). arXiv: `arXiv:1111.7205v1`.

[115] D. B. Nelson. “Conditional Heteroskedasticity in Asset Returns: A New Approach”. In: *Econometrica* 59.2 (1991), pp. 347–370.

[116] L. R. Glosten, R. Jagannathan, and D. E. Runkle. “On the relation between the expected value and the volatility of the nominal excess return on stocks”. In: *The Journal of Finance* 48.5 (1993), pp. 1779–1801.

[117] P.-A. Reigneron, R. Allez, and J. Bouchaud. "Principal regression analysis and the index leverage effect". In: *Physica A* 390.17 (2011), pp. 3026–3035.

[118] A. Ghalanos. *rugarch: Univariate GARCH models.* R package version 1.3-1. 2014.

[119] C. P. Kindleberger and R. Z. Aliber. *Manias, Panics and Crashes; A History of Financial Crises.* Palgrave Macmillan, 2005.

[120] T. Frank. "The Financial Crisis of 33 A.D." In: *American Journal of Philology* 56.4 (1935), pp. 336–341.

[121] O. Hekster. *Rome and its Empire, AD 193-284.* Edinburgh University Press, 2008.

[122] T. Guhr, A. Müller-Groeling, and H. Weidenmüller. "Random-matrix theories in quantum physics: common concepts". In: *Physics Reports* 299 (1998).

[123] J. Wishart. "The Generalised Product Moment Distribution in Samples from a Normal Multivariate Population". In: *Biometrika* 20A.1/2 (1928), pp. 32–52.

[124] S. D. Dubey. "Compound gamma, beta and F distributions". In: *Metrika* 16.1 (1970), pp. 27–31.

[125] O. Barndorff-Nielsen, J. Kent, and M. Sørensen. "Normal Variance-Mean Mixtures and z Distributions". In: *International Statistical Review* 50.2 (1982), pp. 145–159.

[126] A. P. Doulgeris and T. Eltoft. "Scale Mixture of Gaussian Modelling of Polarimetric SAR Data". In: *EURASIP Journal on Advances in Signal Processing* 2010.2 (2010).

[127] M. Brookes. *The Matrix Reference Manual.* 2011.

[128] A. G. Akritas, E. K. Akritas, and G. I. Malaschonok. "Various proofs of Sylvester's (determinant) identity". In: *Mathematics and Computers in Simulation* 42 (1996), pp. 585–593.

[129] F. W. J. Olver, D. W. Lozier, R. F. Boisvert, and C. W. Clark. *NIST Handbook of Mathematical Functions.* Cambridge University Press, 2010.

[130] R. Höhmann, U. Kuhl, H.-J. Stöckmann, L. Kaplan, and E. J. Heller. "Freak Waves in the Linear Regime: A Microwave Study". In: *Physical Review Letters* 104.9 (2010), p. 093901.

[131] J. C. Hull. "The credit crunch of 2007: What went wrong? Why? What lessons can be learned?" In: *The Journal of Credit Risk* 5.2 (2009), pp. 3–18.

[132] M. Crouhy, D. Galai, and R. Mark. “A comparative analysis of current credit risk models”. In: *Journal of Banking & Finance* 24.1-2 (2000), pp. 59–117.

[133] T. R. Bielecki and M. Rutkowski. *Credit Risk: Modeling, Valuation and Hedging*. Springer, 2004.

[134] C. Bluhm, L. Overbeck, and C. Wagner. *An Introduction to Credit Risk Modeling*. Chapman & Hall/CRC, 2003.

[135] D. Duffie and K. J. Singleton. “Modeling Term Structures of Defaultable Bonds”. In: *Review of Financial Studies* 12.4 (1999), pp. 687–720.

[136] R. Ibragimov and J. Walden. “The limits of diversification when losses may be large”. In: *Journal of Banking & Finance* 31.8 (2007), pp. 2551–2569.

[137] D. Lando. *Credit Risk Modeling: Theory and Applications*. Princeton University Press, 2008.

[138] A. J. McNeil, R. Frey, and P. Embrechts. *Quantitative Risk Management: Concepts, Techniques, and Tools*. Princeton University Press, 2005.

[139] E. Heitfield, S. Burton, and S. Chomsisengphet. “Systematic and idiosyncratic risk in syndicated loan portfolios”. In: *Journal of Credit Risk* 2.3 (2006), pp. 3–31.

[140] P. Glasserman and J. Ruiz-Mata. “Computing the credit loss distribution in the Gaussian copula model: a comparison of methods”. In: *Journal of Credit Risk* 2.4 (2006), pp. 33–66.

[141] G. Mainik and P. Embrechts. “Diversification in heavy-tailed portfolios: properties and pitfalls”. In: *Annals of Actuarial Science* 7.1 (2013), pp. 26–45.

[142] P. J. Schönbucher. “Factor Models: Portfolio Credit Risks When Defaults are Correlated”. In: *The Journal of Risk Finance* 3.1 (2001), pp. 45–66.

[143] P. Glasserman. “Tail approximations for portfolio credit risk”. In: *The Journal of Derivatives* 12.2 (2004), pp. 24–42.

[144] R. Schäfer, M. Sjölin, A. Sundin, M. Wolanski, and T. Guhr. “Credit risk - A structural model with jumps and correlations”. In: *Physica A* 383.2 (2007), pp. 533–569.

[145] A. F. R. Koivusalo and R. Schäfer. “Calibration of structural and reduced-form recovery models”. In: *Journal of Credit Risk* 8.4 (2012), pp. 31–51.

[146] M. C. Münnix, R. Schäfer, and T. Guhr. “A Random Matrix Approach on Credit Risk”. In: *PLOS ONE* 9.5 (2014).

[147] K. Giesecke. *Credit risk models and management*. Ed. by D. Shimko. Risk Books, 2004, pp. 487–525.

[148] R. C. Merton. "On the pricing of corporate debt: the risk structure of interest rates". In: *The Journal of Finance* 29.2 (1974), pp. 449–470.

[149] K. Itô. "Stochastic integral". In: *Proceedings of the Imperial Academy* 20.8 (1944), pp. 519–524.

[150] New York Stock Exchange. *TAQ 3 User's Guide*. 2008, pp. 1–47.